Durham E-Theses

Incorporation of pigment producing cells into novel 3D skin equivalents to study the role of the dermal compartment upon pigmentation in skin equivalents

MEAD, HUGH,DAVID

How to cite:

MEAD, HUGH,DAVID (2022) *Incorporation of pigment producing cells into novel 3D skin equivalents to study the role of the dermal compartment upon pigmentation in skin equivalents*, Durham theses, Durham University. Available at Durham E-Theses Online: http://etheses.dur.ac.uk/14575/

Use policy

Abstract

Hugh Mead - Incorporation of pigment producing cells into novel 3D skin equivalents to study the effects of ageing and environmental stressors on skin tone.

Recent generations of skin equivalents have started to become more complex and dynamic, which more closely capitulate the intricate workings of human skin. The importance of this research, since moving away from animal models, should not be understated. It is imperative to mimic the structure and hence the function of skin to ensure chemicals that are tested on this model system yield accurate results. As these models become more complex with inclusion of pigmentation, neurons or hair follicles, it is important to know how different models interact. Therefore, this thesis aims to understand the role of the dermal compartment and how it may influence the viability and efficacy of melanocytes within skin equivalents. The results showed that there is an important role for the dermis in providing support to the epidermis for the production of melanin and the transfer to HEKn cells in the *Stratum Basale*. Furthermore, there is proof of concept for the protocol and technology used to produce this pigmented skin equivalent.

Incorporation of pigment producing cells into novel 3D skin equivalents to study the role of the dermal compartment upon pigmentation in skin equivalents

Hugh David Mead

MRes

Bioscience

Durham University

2021

Contents

1. Introduction

the skin plays an essential role in maintaining an internal environment and interacting with the external one. At the heart of this interaction, keratinocytes act as protective barrier allowing the skin to be strong yet dynamic and malleable. However, the role of skin is not limited to acting as a barrier. The skin is involved in regulation of water loss, temperature control, reacting to external stimuli, appearance and social interaction. To fulfill this diverse set of functions: immune cells, fibroblasts, nerve cells, melanocytes and many other cell types work together to make the skin the complex organ it is.
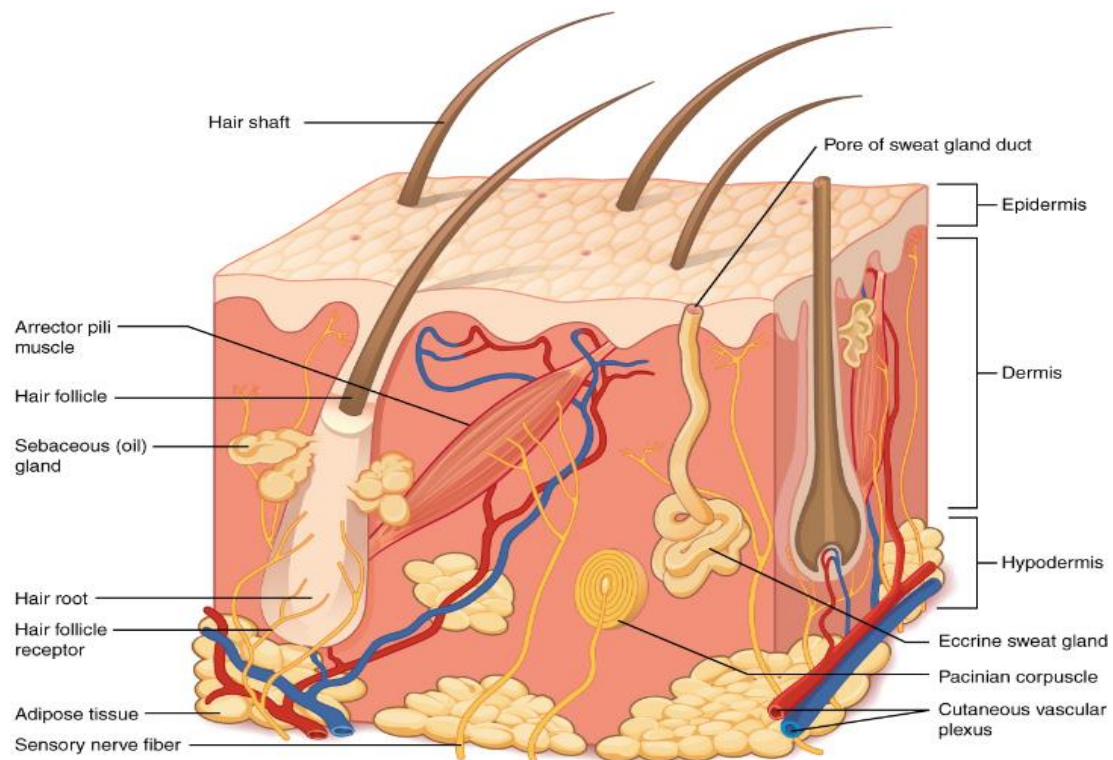
Figure 1. An image showing the structure of skin, with its appendages, vascularisation, lymphatic tissue and the different layers. At the top exist the epidermis, providing a barrier for the organism. Next the dermis, where most of the appendages orginate from, here we can see vascularisation to feed the epidermis. Finally, the hypodermis, a fatty layer where major arteries and veins pass through. Chapter 5.1 OpenStax, Anatomy & Physiology. OpenStax CNX. Feb 26, 2016

The skin is divided into three distinct layers (Figure 1): the epidermis, the dermis and the hypodermis. The epidermis which comprises predominantly of keratinocytes that provide the skin its protective barrier properties. Keratinocytes exist in four morphological stages which help to make the four layers of the epidermis: *Stratum Basale, Stratum Spinosum, Stratum Granulosum, Stratum Corneum.* In the stratum basal keratinocytes are columnar in shape, show a distinct polarised morphology and are highly proliferative. As they move through the four layers, they specialise into flattened cells packed with keratin filaments, without a nucleus. They form tight junctions and start to form a brick-wall like structure that acts as a water-proof barrier. Also, in the epidermis are melanocytes, these are dendritic type cells that reside in the

Stratum Basale. These often-overlooked cells play an important protective role, transferring melanin to neighbouring keratinocytes to protect them from ultraviolet radiation (UVR).

The dermis is located below the epidermis and begins at the dermal-epidermal junction. This is the point where cells in the basal layer come into contact and share signals with the epidermis and vice versa. The most prevalent cell type found in the dermis are fibroblast cells. Fibroblasts are well renowned as the cell that provides structural support to tissues by producing an array of proteins including collagen, elastins, fibronectin, laminins and proteoglycans (Theocharidis et al 2016) that make up the extracellular matrix (ECM). The ECM allows other cells populations to adhere to it and provide mechanical support within tissues. In addition to a range of protein macromolecules, a network of blood vessels and lymphatic tissue make up 90% of the dermal layer which provide nutritional support to the skin. Furthermore, the dermis plays a crucial role in wound healing, hence, has a large population of immune cells to aid wound healing. However, the immune cells are not just responsible for wound healing, they also maintain homeostasis of skin against a variety of invading organisms.

The hypodermis is located below the dermis and adjacent to underlying tissue, normally musculoskeletal. It consists mostly of adipose tissue and is the storage site for the majority of fat in the human body. Therefore, keratinocytes, melanocytes and fibroblasts are at the heart of the skin's ability to act as a barrier. Working together to provide the foundations for neurons, muscle and immune cells to perform their function in maintaining healthy skin and organism.

1.2 Skin Cell Types

1.2.1 Keratinocytes

Keratinocytes are the cell type known for providing the barrier function in human skin by becoming specialised corneocytes that form the outer layer of skin. Keratinocytes start out in the *Stratum Basale* of the epidermis, here they have a columnar morphology, are highly proliferative and express keratin 5 and 14 - these are strong markers of basal keratinocytes. This is the cell population that feeds the subsequent layers of the epidermis by proliferating, specialising and moving through the subsequent layers of the epidermis, the cells produce a differentiated and stratified tissue with barrier properties. Calcium signalling plays an important role in keratinocyte specialisation as they move through the four layers of the epidermis (Hennings et al 1983). The calcium gradient in the epidermis, increases from the *Stratum Basale* to the *Stratum corneum* and controls a number of intracellular signalling

pathways seen in Figure 2. The signalling cascade within keratinocytes starts with the full-length calcium sensing receptor (CaSR), a G-protein coupled receptor found on the cell surface that activates phospholipase C (Tu et al 2011, Tu et al 2005). In addition, Oda showed that only the full-length version of CaSR controls keratinocyte differentiation through calcium response (Oda et al 1998). In mutant mice lacking the full-length receptor, alternately spliced receptors were seen on the surface, however, keratinocyte differentiation was hindered in these mutant mice. Furthermore, in CaSR knockout mice caused a significant decrease in post-CaSR differentiation markers (Tu et al 2012).

Once the extracellular calcium increases, the intracellular increases in two phases, an acute phase and a sustained phase (Tu et al 2013). The acute phase comes from the release of intracellular calcium in response to CaSR activation on the cell surface. CaSR activation recruits PlyC to the plasma membrane and catalyses a release of IP3 into the cytoplasm. IP3 acts on IP3R which in turn rapidly releases intracellular calcium from the endoplasmic
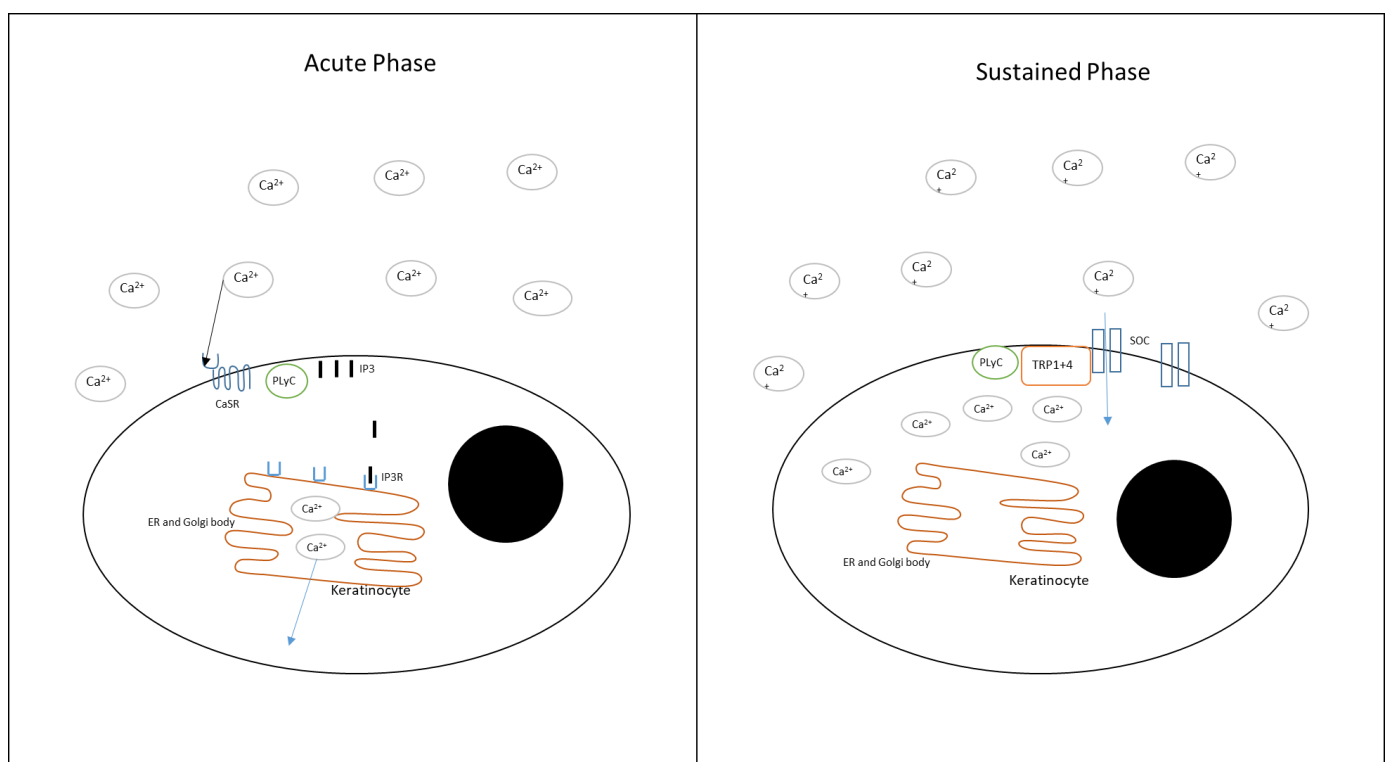
Figure 2. The method of keratinocyte specialisation caused by a high calcium gradient that is found in the upper levels of the epidermis. The acute phase, the external calcium is sensed by CaSR and activates an internal cascade to release intracellular calcium. The increase in IP3 and calcium depletion activates the sustained phase. During the sustained phase PLyC activates SOC which transport external calcium and maintain the high levels of intracellular calcium. Along with other pathways, this activates genes involved in cornification.

reticulum (ER) and golgi body (Calautti et al 2005). However, the acute phase of intracellular

calcium increase is not enough to induce keratinocyte differentiation which is shown when intracellular calcium is increased through ATP (Pillai et al 1992). Therefore, maintaining this high level of intracellular calcium is the driver for the sustained phase (Xie et al 1999, Tu et al 2005). With the depletion of calcium stores and an increase in IP3R activation, keratinocytes activate store-operated channels (SOC). Transient receptor potential channels 1 and 4 (TRP1 and 4) interact with SOC after activation of PLCy1, since inhibition of PLCy1 blocks calcium dependent keratinocyte differentiation (Xie et al 1999). TRP1 and 4 located on the plasma membrane and transfer calcium into the cell which creates the consistently high level of intracellular calcium attributed to the sustained phase.

Once keratinocytes leave the *Stratum Basale*, their morphology changes. As keratinocytes move through the four layers, they encounter the extracellular calcium gradient. The gradient is low in the *Stratum Basale* and increases through to the *Stratum Granulosum*. At the stratum corneum however, the calcium concentration is at its lowest point (Celli et al 2010). Since keratinocytes have already terminally specialised by this point, it is unlikely they require further signalling. The morphological changes that calcium induces are required for the skins permeability function and allow keratinocytes to carry this out. A change in calcium concentration leads to E-cadherins expression to form tight junctions with their counterparts (Tinkle et al 2004). This in turn recruits PI3K to the complex and initiates calcium release through SOC channels. Downstream of PI3K, Akt acts to promote differentiation and keratinocyte survival (Calautti et al 2005). In addition to PI3K, Rho-GTPases are recruited to the complex following an increase in calcium (Tu et al 2011). The Rho-GTPases act via the Fyn/SRC family of kinases to control E-cadherin junctions (Calautti et al 2002). This function allows the keratinocytes to tightly pack together as they move up through the *Stratum spinosum* and *Stratum Granulosum.*

In order for keratinocytes to complete their journey and become corneocytes that provide a vital function to the body as a barrier they must first undergo distinct changes. This process of cornification takes keratinocytes through a process similar to programmed cell death. However, keratinocytes avoid completing the process and do not undergo phagocytosis. They are, however, continually removed from the *Stratum Corneum* through desquamation, the process of shedding corneocytes so they are replaced with new differentiating keratinocytes. Even though at a macro level, the process of differentiation is understood, the drivers behind regulating this complicated process remain a mystery. To undergo this cornification cells must firstly remove the nucleus and degrade DNA. Nuclei found in the

Stratum Corneum is often a sign of impaired barrier function and paraketosis (Katagiri et al 2010). Caspase 14 is thought to be the main driver behind DNA degradation in differentiating keratinocytes. Yamato-Tanaka showed that keratinocytes expressing Caspase-14 had a positive TUNEL value, suggesting that these cells have removed their nucleus and have improved barrier function (Yamato-Tanaka et al 2014). With Caspase-14 potentially being an upstream regulator, the search for methods of action downstream to breakdown DNA also remains a mystery. In hair and nails DNase1L2 has been shown to play an active role in DNA degradation. In DNase1L2 knock-outs there is nuclear retention in the *Stratum Corneum* which in turn affects the viability of these cells as corneocytes (Fischer et al 2011).

In addition to DNA degradation, cells must undergo a process similar to autophagy to breakdown intracellular material. The intracellular organelles are broken down however, unlike apoptosis, cells are not phagocytosed, leaving behind a cell densely packed with keratin filaments that provides flexibility under mechanical stress. It is thought that autophagy-related 7 (AR7) a protein involved in regulating this process in keratinocytes (Jaeger et al 2019). However, even though protein expression changed in AR7 knockouts and some morphological changes were witnessed, few conclusions about the intricacies of this process could be drawn. Due to the importance of apoptotic proteins for organism survival, it is difficult to study these processes in knockout organisms. Once keratinocytes have removed the majority of intracellular material, one of the most important aspects of their transition to corneocytes occurs. Transglutaminases are central to building cross-linked intermediate filaments with the cytoskeleton and allow for proper *Stratum Corneum* development (Matsuki et al 1998). Finally, corneocytes are packed between an ECM rich in lipids that compose lamellar bodies. Rich in extremely hydrophobic lipids, this helps the skin as a barrier and remain hydrated (Schmuth et al 2008). Mutations in encoding genes leads to pathological problems in lamellar bodies leading to Ichthyoses, a disease characterised by dry, thickened, scaly skin (Crumrine et al 2019).

1.2.2 Dermal Fibroblast

Fibroblasts can be found throughout the body, they are the primary cell type found in connective tissue, produce ECM and play a crucial role in basement membrane formation. Skin is no different with the dermal fibroblasts providing underlying support to the epidermis. However, the role of dermal fibroblast cells should not be reduced down to simply supporting the epidermis. This cell type has a crucial part to play in maintaining healthy skin which can react to

an external environment. Dermal fibroblasts have been implicated in having a role in wound healing, ageing, cancer, protection from stress and mechanical strength of the skin.

As previously stated, one of the main roles of fibroblasts is to produce and remodel ECM to provide a foundation for the epidermis. The ECM consists of collagens, proteoglycans/glycosaminoglycans, elastin, fibronectin, laminins, and several other glycoproteins. This range of proteins allows cells to not only adhere to but receive various signals dependent on exact biochemical composition of ECM throughout the body (Theocharis et al 2016). The skin is no different, with the epidermis residing and interacting with the ECM, receiving nutrients and growth factors. The dermal fibroblasts are responsible for building and remodelling the ECM by producing the aforementioned components of ECM, particularly collagen. Collagen is synthesised as procollagen containing N- and C-propeptides at each end of a triple helical domain. This synthesis requires specific post-translational enzymes, including intracellular lysine modifications, glycosylation, extracellular cleavage by a procollagen N-proteinases and the C-proteinases, lysine modifications to form a complex series of cross-links (Nystrom et al 2018, Uzawa et al 1998). Fibroblasts are also responsible for breaking down the ECM through the secretion of matrix metalloproteinases (MMPs). These are particularly prevalent in cancers and are attributed to enabling the process of metastasis. Furthermore, this remodelling of the ECM has been attributed to play a part in the ageing process.

The epidermis functions as an impressive barrier, preventing a variety of external factors from entering the body, however, this barrier is not perfect and compared other forms of protection in the animal kingdom it falls short. Therefore, the skin must be able to respond to breakages in barrier and heal the wound. Wound repair can be split into overlapping sections: inflammatory response, granulation tissue formation and matrix remodelling (Figure 3). Fibroblasts are most active during the granulation phase, their activation comes during the inflammatory response by the release of various factors that promote proliferation and growth (Katz et al 1991). Along with the production of new blood vessels during wound-healing two populations of fibroblasts exist, fibroblasts and myofibroblasts. The myofibroblasts are able to provide mechanical force, similar to smooth muscle cells to aid in closing the wound. This allows fibroblasts to produce new ECM to heal the wound. Furthermore, when fibroblasts are damaged, wound healing time increases (El Ghalbzouri et al 2004). This ability to produce and remodel ECM makes fibroblasts a key player when it comes to wound-healing.

Melanocytes are derived from the neural crest cells, which migrate out of the neural tube during development. They are found in a range of organs throughout the body such as: eyes, ears, hair follicles, brain, heart (Plonka et al 2009) and for the purpose of this review, the skin. One of the main roles for melanocytes within the skin is producing pigment to protect the organism from UV damage. They exist in the bottom layer of the epidermis – the *Basale Stratum* – where the epidermis and the dermis interact. This allows them to carry out their function most efficiently, with their dendritic projections reaching between 30 and 40 keratinocytes. To protect the skin from UV damage, melanocytes produce a molecule, called melanin, inside a special lysosomal like structure called a melanosome. These are transferred to the keratinocytes along the dendritic projections. The melanin is degraded as the keratinocytes move up through the layers of the epidermis and by the *Stratum Spinosum* the melanin has degraded.
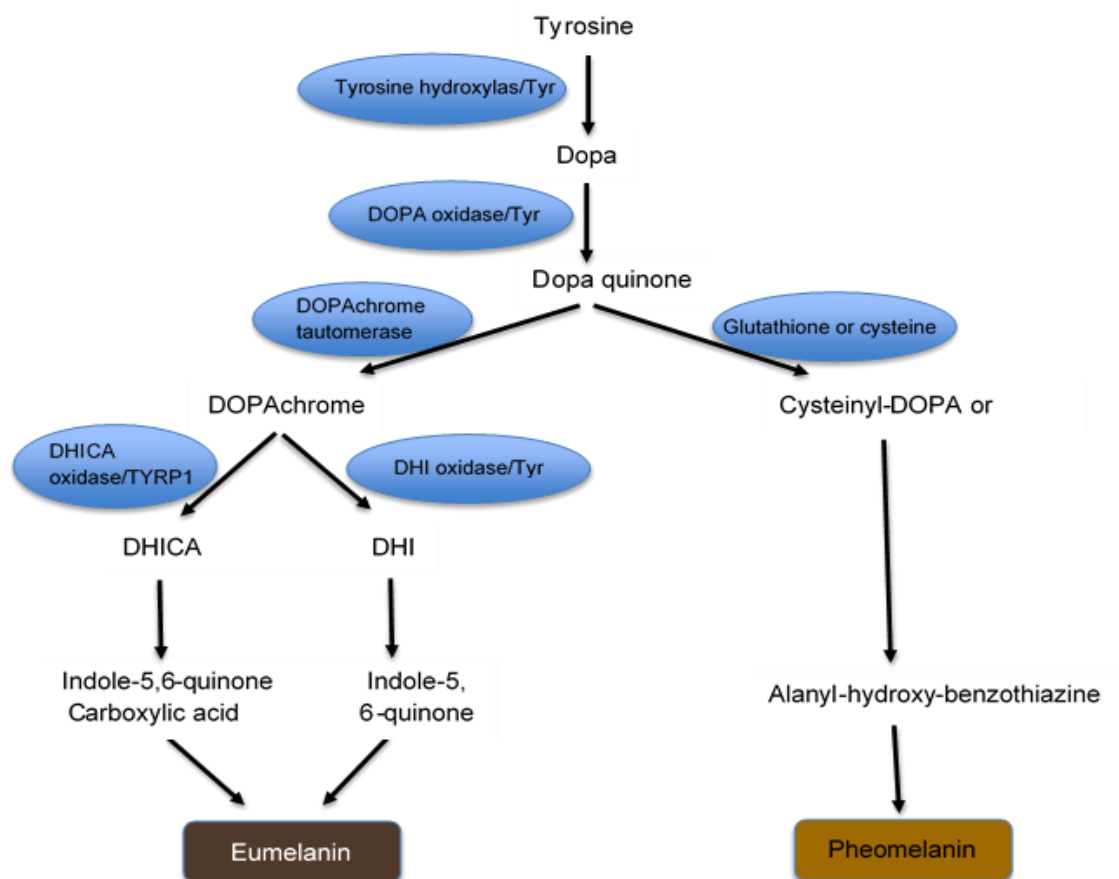
Figure 4. The pathway to produce Eumelanin and Pheomelanin from tyrosine and the enzymes involved in the process. The decision to produce Pheomelanin or Eumelanin is influenced by the availability of Glutathione/Cysteine and requires fewer enzymes than Eumelanin. Other factors influencing this decision are genetics and the environment.

There are two types of melanin, pheomelanin, which is a yellow red colour and eumelanin, which is a brown/black colour. Amongst other factors, the quantity of each type of melanin produced is a strong indicator of skin tone. Both types of melanin are under the control of Tyrosinase, the rate-limiting step in the synthesis reaction, when tyrosine hydroxylation occurs to produce L-3,4-dihydroxyphenylalanine (DOPA) (Figure 4). In the presence of cysteine, at a weakly acidic pH, pheomelanin is produced (Wakamatsu et al 2017), However, Eumelanin requires two more Tyrosinase related proteins – Tyrosinase related protein 1 and 2 (TRP1 and 2). TRP1 and TRP2 are required for the final two steps to produce eumelanin. (Seiji et al 1961).

The decision for a melanocyte to produce either pheomelanin or eumelanin is influenced internally. However, one of the main factors influencing the gene regulation of melanin is UV, an external factor, more commonly known as 'tanning' (Hennessy et al 2005). In response to UV damage, melanocytes have to been shown to modulate melanin production appropriately by producing factors to influence melanin production as seen in Figure 5. The main receptor controlling melanin production is melanocortin 1 receptor (MCR1) and mutations in this gene are responsible for pale skin and ginger hair. MCR1 is activated by a-MSH and Adrenocorticotrophic hormone (ACTH) and inhibited Agouti Signalling Protein (ASP) (Patel et al 2017). However, the control of melanin production is a complicated process. Inhibition of MCR-1 leads to a downregulation of eumelanin production, by inhibiting tyrosinase activity, which leads to a preferential reduction in eumelanin but not pheomelanin. (Le Pape et al 2008). It is likely that melanocytes produce pheomelanin at rest, whereas upon receiving a signal, production switches to eumelanin. Other factors that have been implicated in the regulation of melanin are prostaglandins, nitric oxide, histamine and it is likely there are more to be uncovered (Nordlund et al 1986, Lassale et al 2003).
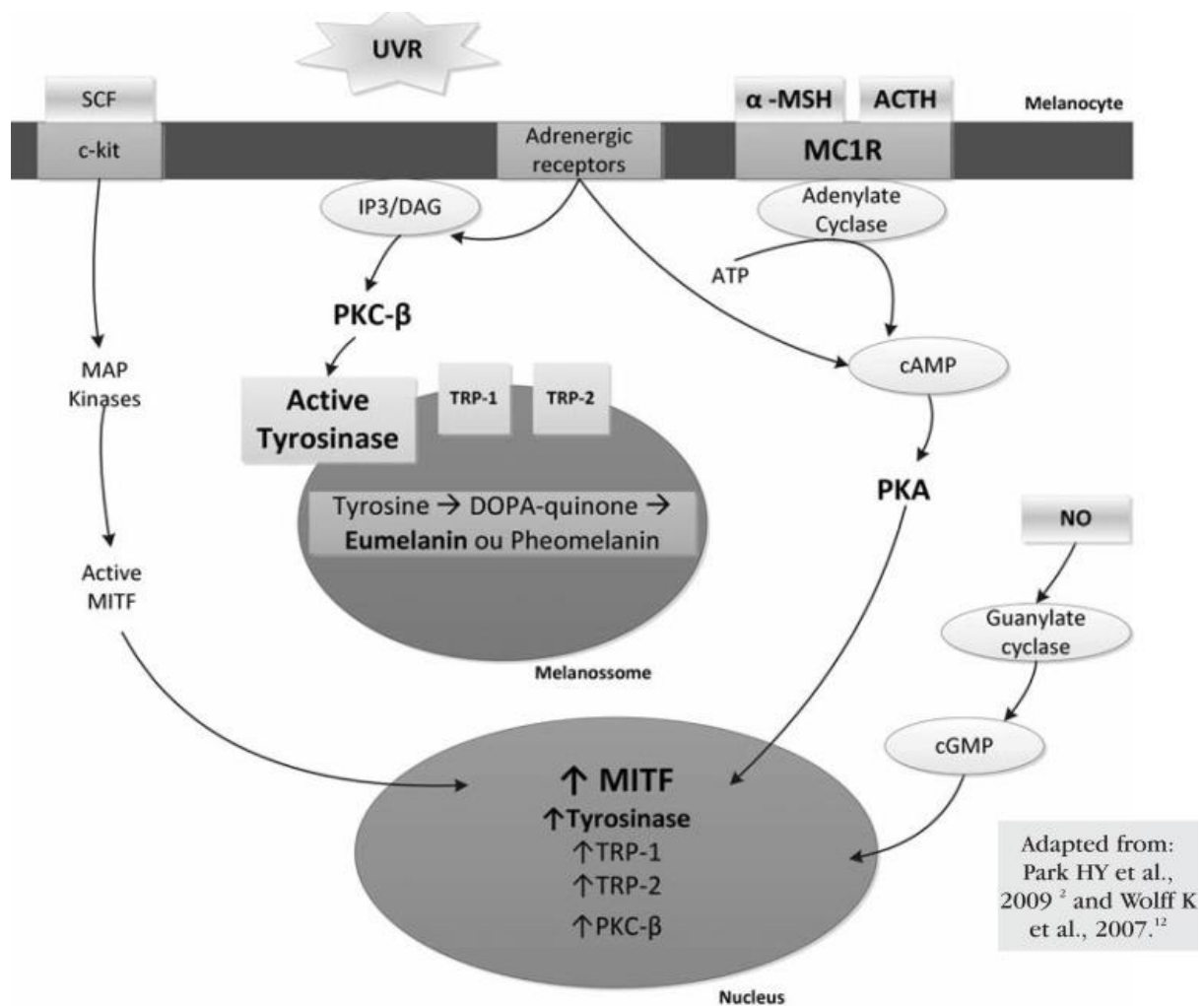
Figure 5. The process of Melanogenesis.

Two pathways exist to upregulate genes associated with melanogenesis. The first and best understood exists through a-MSH binding to MC1R on the cell surface and starting a signalling cascade within the melanocyte via cAMP and PKA to increase transcription. The other route comes from activation of c-kit receptors by the SCF protein complex. This activates a cascade of MAP kinases that results in an active version of MITF. In order to increase melanogenesis, adrenergic receptors can activate tyrosinase, the rate limiting step in melanin production. Videira et al 2013

Downstream of MCR-1 is a transcription factor – microphthalmia-associated transcription factor (MITF) - that regulate proteins involved in melanogenesis. More specifically, it is the MITF-M motif that acts as a promoter for melanogenesis related genes and is the main motif expressed in melanocytes. MCR-1 activation increases intracellular cAMP, which activates protein kinase A (PKA). Englaro et al 1995 showed that an increase in melanin synthesis in B-16 melanoma cells prompted an increase in cAMP. PKA phosphorylates cAMP response element (CREB), which is a transcription factor for, amongst other proteins, MITF (Busca et al 2000). After MITF is transcribed, it is also dependent on

phosphorylation from kinases of mitogen activated protein (MAP). MAP relies on a keratinocyte produced SCF, which binds c-kit receptor tyrosine and promotes MITF phosphorylation. Another pathway for MITF activation is via Wnt-3a. Activation of the Wnt-3a pathway leads to an increase in MITF-M mRNA in mouse melanocyte cells. MITF expression occurs via B-catenin transcription factor, by binding to the LEF-1/TCF motif (Takeda et al 2000).

After melanin has been synthesised and packaged inside of the melanosome, it must mature and transport along the melanocyte's dendritic projections. It is somewhat debated about which method of intracellular movement melanosomes use. There is strong evidence to suggest that myosin/actin is the predominant method of melanosome transport (Evans et al 2014). However, it has been shown in Myosin V knockout mice that melanosomes can be transported along microtubules (Robinson et al 2017). Furthermore, the movement of bidirectional movement of microtubules along the cell body is shown to be microtubule dependent (Wu et al 1998). In addition to showing that melanosome transport was microtubule dependent, Wu's research supports a role for both actin and microtubules in melanosome location. Microtubules have the ability to transport melanosomes throughout the body of the melanocyte, However, they were unable to accumulate in the periphery. The periphery of each dendrite was shown to be actin rich and may be responsible for finer movement of melanosomes. Although melanocytes are an integral cell type in modulating skin tone and pigmentation, they do not do this alone and communication amongst the cells of the epidermis is crucial in responding to external stimuli such as UVR.

1.4 Cell-cell interactions

1.4.1 Melanin transfer and uptake

One of the core interactions in the skin and especially for the purpose this topic is between melanocytes and keratinocytes. As outlined in previous sections, melanocytes are responsible for producing and maturing melanin within the cell. However, the function of melanin goes beyond melanocytes and mainly protects the genetic material in keratinocytes. Once melanin is produced it must enter keratinocytes and position itself above

the nucleus, polarised towards the sun. Little is known about the processes following melanogenesis, with the process of melanosome uptake being a controversial topic. There are currently four proposed mechanisms of melanosome transfer between melanocytes and keratinocytes visualised in Figure 6: Cytophagocytosis, membrane fusion, shedding phagocytosis and endocytosis/exocytosis (Wu X et al 2012). In recent years the two former methods have not received much attention, however, evidence is growing for the latter methods. Two main studies showed strong evidence for shedding phagocytosis. (Wu X et al 2012), generated transgenic 'Holly skin' mice, whereby, the membranes of melanocytes and keratinocytes were fluorescent for red and green proteins respectively. They showed that Melanosomes can be found in the

Figure 6. A visualisation of four proposed methods of melanin transfer from melanocytes to keratinocytes. Evidence points to methods three and four as the most likely methods of melanin transfer. However, there is still some debate which it is. Wu X et al 2012

extracellular space and inside keratinocytes with membranes from both cell types. Furthermore, Ando *et al* showed that electron microscopy (EM) images of melanocytes found melanosome 'globules' on the surface of the melanocytes. However, these are only still EM images and offer little in the way of dynamic evidence for shedding phagocytosis. Strong evidence for endocytosis/exocytosis comes from (Tarafder et al 2014), who showed EM images of melanin cores exocytosed into the extracellular space between melanocytes and keratinocytes. However, again EM images are limited as they do not show any dynamic processes. Further evidence for endo/exocytosis comes from (Moreiras et al 2020), they showed that silenced of suggested machinery involved in exocytosis, impairs melanin transfer to keratinocytes.

Regardless of the actual mechanisms, some light has been shed on proteins involved in the uptake in keratinocytes. Correia et al (2018) showed that PAR2 and Rab proteins are heavily involved in the uptake of melanosomes. PAR2 is a membrane receptor, when silenced by siRNA's significantly impairs the uptake of melanocores. In addition, the rab family of proteins, which are known to be involved in membrane trafficking, are shown to have a role in melanosomes uptake. Along with PAR2, Correia et al 2018 investigated the role of Rab proteins. Rab5 silencing was shown to have a similar effect on melanocores as PAR2.
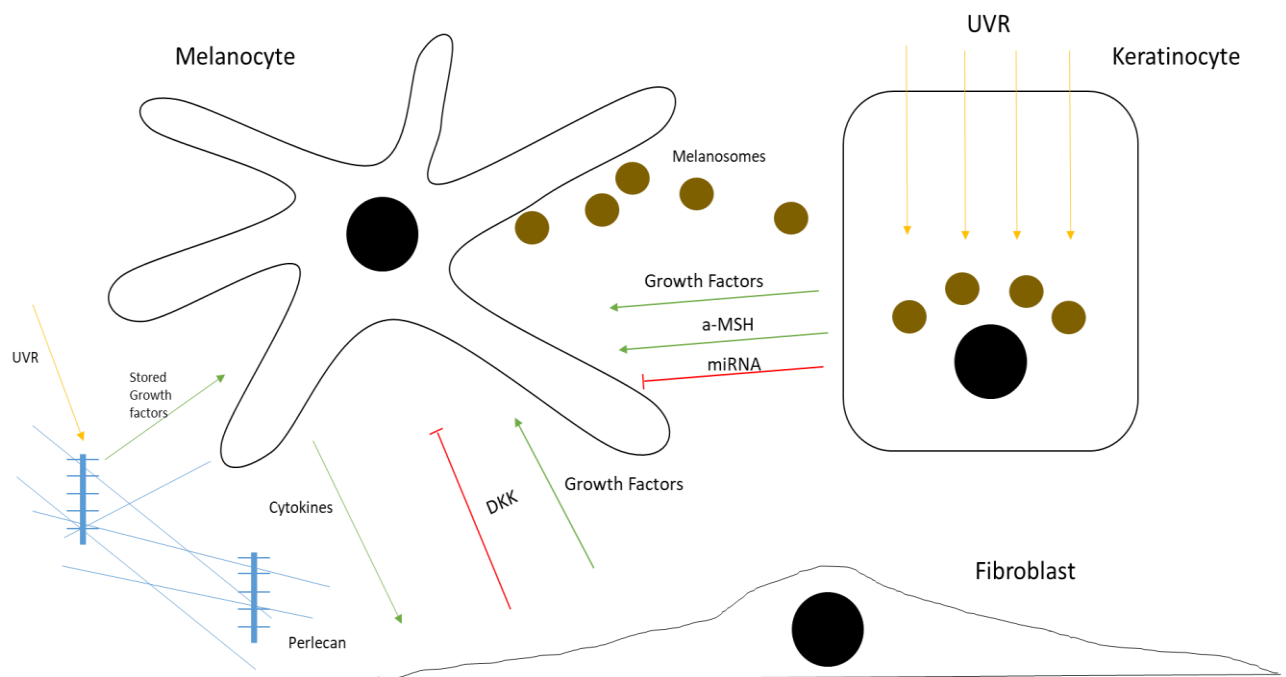
Figure 7. The crosstalk that occurs between melanocytes, keratinocytes and fibroblasts. In response to UVR keratinocytes release factors to increase production of melanin which are transferred via melanosomes to keratinocytes. The factors released by fibroblasts have both an inhibitory and excitatory method of action upon melanocytes. Finally, the response of ECM to UVR results in a release of growth factors from perlecan that stimulate melanocytes growth. All these pathways result in a system that can respond to UVR and protect the organism.

Once the melanosome has been absorbed by the keratinocyte, by one of the four proposed mechanisms, the melanosomes must avoid degradation and position correctly around the nucleus. Following treatment by UV or IBMX - 3-isobutyl-1-methylxanthine which is known to increase intracellular cAMP - keratinocytes are shown to have increased supranuclear cap formation in skin equivalents (Gibbs et al 2000). However, little is known about the driving forces behind the formation of this structure. Similar to the transport of melanosomes within melanocytes, keratinocytes have been shown to use the microtubule network to deliver melanosomes to their desired location (Byers et al 2003). Keratinocytes

are shown to express cytoplasmic dynein and it co-localises with the melanosomes in human skin. It would make sense that a similar machinery drives melanosomes transport in both melanocytes and keratinocytes. Further to this, organisation of melanocores are reliant on keratinocyte specific signals. When keratinocytes from donors of different ethnic origin are cultured with melanocytes of different ethnic origins. Regardless of the origin of melanocytes, the keratinocytes organise the melanocores differently after uptake. Dark skin keratinocytes organise melanocores individually, whereas light-skinned keratinocytes organise them in clusters (Minwalla et al 2001). However, this data doesn't help understand the mechanisms that polarise melanosomes to the top of the nucleus, which remain elusive.

1.4.2 Regulation of Melanogenesis

Keratinocytes have a tightly linked relationship with melanocytes so it is unsurprising that there is a host of interactions between the two cell types, as seen in Figure 6. Following UVR we see an increase in vesicle transfer from melanocytes (Waster et al 2016). Upon excessive stimulation by UVR, the tumour suppressor protein p53 becomes stable in keratinocytes. In other cell types, p53 works by acting as a cell cycle and DNA repair regulator, however, in keratinocytes it causes an upregulation in the production of a-MSH.

Furthermore, new research has implicated miRNAs into the process of melanin regulation. MiRNA's are short non-coding RNA molecules designed to regulate protein synthesis at the post-transcriptional level. The RNA interference pathway, of which miRNA's are a member, are highly conserved and seem to regulate a variety of critical processes (Friedman et al 2009, Lewis et al 2005). These miRNAs are likely transferred through vesicles from keratinocytes along with other regulatory factors (Lo Cicero et al 2015) Therefore, it is unsurprising that miRNA's have a role in melanogenesis. MIR-330-5p when overexpressed it was found in exosomal vesicles that were transferred to melanocytes. This which had an inhibitory effect on the production of melanin (Liu et al 2019). in B16 melanoma cells, miRNA-183 overexpression and knockout's decreased and increased, respectively, mRNA and protein levels in genes involved in melanogenesis. Liu also saw the same effects on genes involved in proliferation and migration. However, with these cells being melanoma cells, it might not be representative of melanocytes proliferative capacity.

Whilst important, cross-talk between keratinocytes and melanocytes is only one of many cell-cell interactions that occur in human skin. Dermal fibroblasts were outline as the supportive cell type of the skin and in the case of melanocytes, this is no different. Observing

18

the level of pigmentation found in the palmoplantar region (palms of hands and soles of feet) shows a distinct physiological difference. The melanocyte density is significantly decreased and evidence shows the dermal fibroblasts are responsible for this regulation. Fibroblasts in this region express high levels of dickkopf1 (DKK1). DKK1 is a wnt antagonist, inhibiting melanin production through this signalling pathway (Yamaguchi et al 2004). Furthermore, reduced expression of Wnt-1 inhbiting factor (WIF-1) expression was attributed for skin hyperpigmentation (Kim et al 2013). Certain growth factors have also been shown to play a part in regulation of melanogenesis. Hirobe et al showed KGF stimulated melanocytes to differentiate, proliferate and produce melanin in culture. KGF is produced by both fibroblast and keratinocytes in order to increase melanogenesis and melanin transfer (Cardinali et al 2007), most likely in times of UV stress.

Fibroblasts may also have an indirect method of action upon melanocytes. Keratinocytes and fibroblasts have a role in ECM production and through this ECM manipulation they are able to regulate melanogenesis. Nakazawa showed that melanocytes cultured on ECM derived from keratinocytes, dendrite formation was increased. Interestingly, in keratinocyte ECM cultured from cells exposed to UVB radiation resulted in a 219% increase in melanocyte dendrite formation. Even though this does not show an increase in actual melanogenesis (Nakazawa et al 1995). The role of dendrites for melanin transfer is extremely important and an interesting role for ECM. Fibroblasts are also able to influence melanocytes through ECM, with potentially greater influence than keratinocytes. Melanocytes interact with Perlecan, a member of the proteoglycan family with heparan sulphate chains. These chains have been shown to store fibroblast produced growth factors, which, in the presence of UVR breakdown and release melanocyte growth factors (Migliorini et al 2015, Jung et al 2012)

Finally, Melanocytes have been implicated in a wider role than melanin production. In times of an immunological response, melanocytes have been shown to produce cytokines that have an inflammatory response. Part of this is tied to sunburn, as when the skin is damaged by UV, we see the release of cytokines and stereotypical burn response. However, it is also potential that melanocytes can aid in repair as a result of wound healing. Releasing cytokines and growth factors in response to immune cells being recruited to an area of damage (Muthusamy et al 2013). Furthermore, this release of cytokines will further recruit immune cells to the site of damage and help to prevent further infection. Although, the factors which initiate melanocyte to produce cytokines has only been studied in the context of UVR. There may be wider role in immune responses that has yet to be studied.
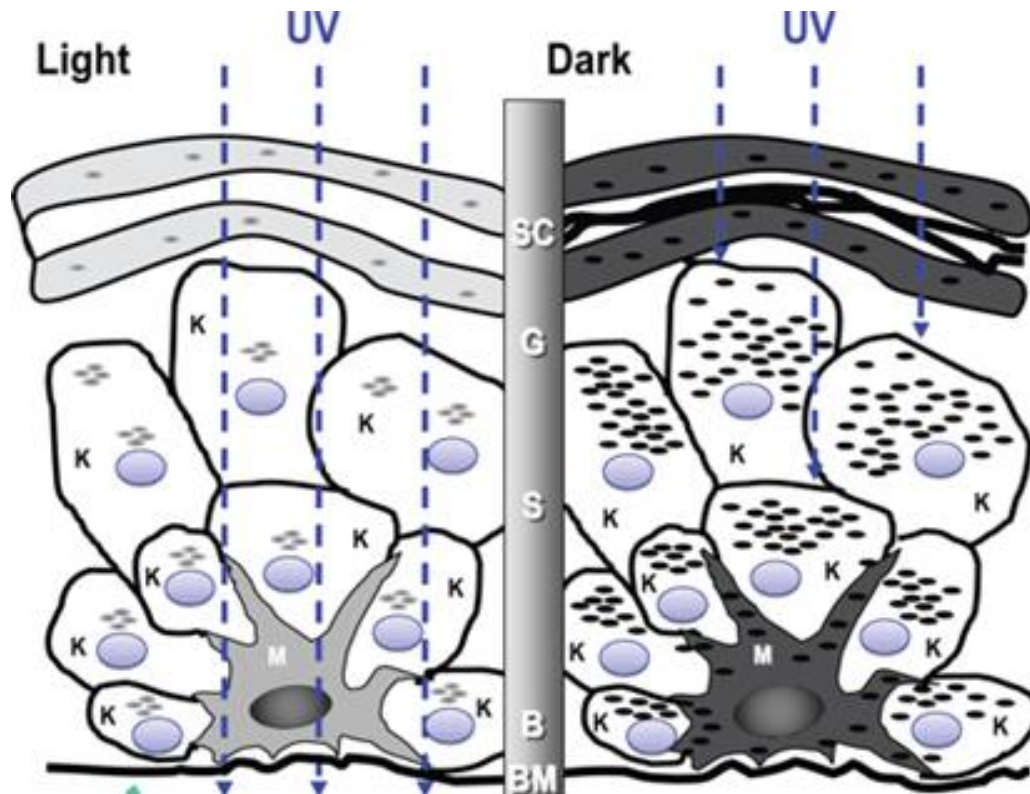
Figure 8. Shows the localisation of melanin in side keratinocytes forming supranuclear caps in dark and light skin tones.

For melanin to carry out its function of protecting DNA from UV damage inside keratinocytes, it must localise to the topside of the cell. This Figure shows melanosomes localising around the top of the nucleus. There is a larger population of melanosomes in side the dark skin tone individual, with a higher proportion of that melanin being Eumelanin. Yamaguchi et al 2007

Melanin and UV protection

Melanocytes have an important role in counteracting the effects of UVR. Their production of melanin in the form of melanosomes, is transferred to neighbouring keratinocytes – each melanocyte serves about 30-40 keratinocytes (Abdel Naser 2016 et al, Thingnes et al 2012). These melanosomes then form a supranuclear cap towards the external environment, to act as a barrier to protect the nucleus from UVR (Figure 8 and 9). The formation of this supranuclear cap is not clearly understood however, dynein has been implicated in the process. Actin have been shown to be the chosen method of transport for melanin inside melanocytes and it is likely to do the same in keratinocytes. Byers et al showed co-localization of dynein chains with melanin pigmentation in human skin (Byers et al 2003). However, if this localization of melanin is the default or if occurs in response to UVR it is poorly understood. Interestingly, iPSC derived cells (Gledhill et al 2015) derived melanocytes and keratinocytes in 2D culture, melanin forms around the nucleus but without any polarisation there is not localisation to one particular side of the nucleus. This suggests

that localisation of melanosomes around the nucleus might be innate but requires signals to determine which side UVR is coming from. Therefore, whether polarisation is innate, potentially from basal keratinocytes *in vivo* that have a distinct top and bottom or whether it is UV that signals to keratinocytes where to localise melanin is unknown and requires further research.
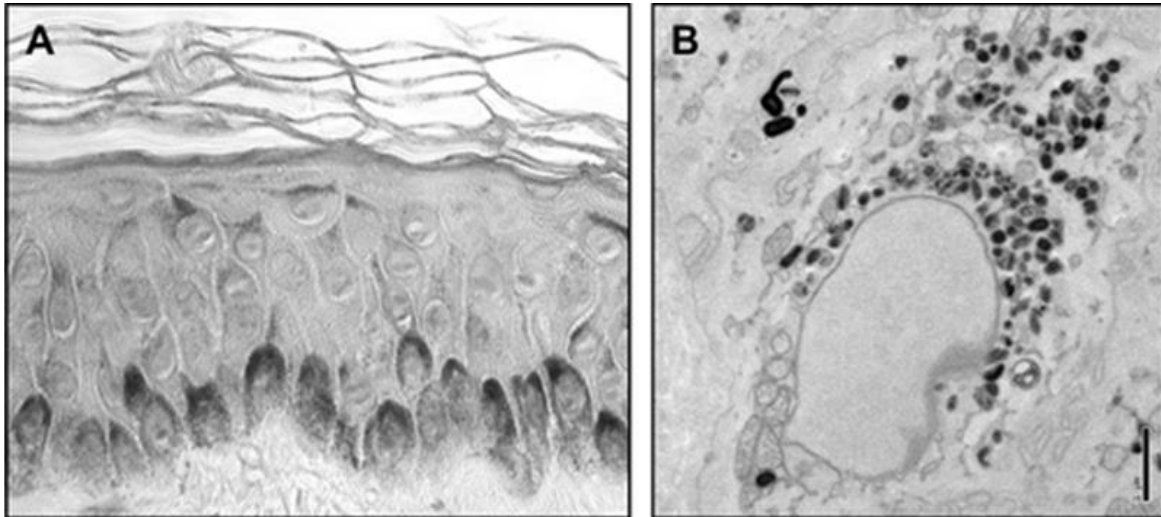
Figure 9. Melanosome localisation and organisation within a human epidermis and keratinocyte.

These images show Transmission electrion microscopy of a human skin biopsy which highlights the formation of supranuclear caps inside human skin. This function helps melanosomes to protect keratinocyte DNA from harmful UV radiation. Serre et al 2018

The response of human skin to UVR and its method of action has been studied greatly. UVR is defined as a specific wavelength of the electromagnetic spectrum between visible light and x-rays. It is sub-divided into three different types – UVA, UVB and UVC. UVC is almost entirely filtered out by the atmosphere, therefore research has focused on the effects of UVA and UVB on the skin. UVA only penetrates into the epidermis, however UVB has the potential to affect the proteins and cells of the dermis.

Research into UVR effects on skin has led to the development of a variety of compounds to help prevent UVR damage to skin and other methods of prevention. UVR produces DNA damage in the form of pyrimidine dimers by direct action of UVR (Cooke et al 2003) and induction of reactive oxygen species (ROS) (Cooper et al 2009). The former is caused by radiation acting directly on DNA and causes mismatch pairing and kinks in the DNA strand. The latter causes an increase in ROS faster than the cell can dispose of them. This causes oxidative stress which damages DNA. Both of these pathways can lead in an array of cancers in the skin including melanoma, one of the most common forms of cancer.

UVR can also cause damage to the skin, not just at a cellular/molecular level but also at a physiological level. Known more commonly as sunburn, it is a combination of apoptosis of cells in the epidermis (Godar et al 1996), damage to the ECM (Watson et al 2014) and release of cytokines that create an inflammatory response (Faustin et al 2008, Feldmeyer et al 2007). Furthermore, in the previous section, proteoglycans were highlighted as a possible factor for the release of growth factors to control melanocytes and melanogenesis. It is likely this acts as reservoir in times of UVR stress to promote melanogenesis. However, in keratinocytes UVR also promotes the transcriptional activation of pro-opiomelanocortin (POMC) gene. P53 overexpression leads to a similar level of POMC transcription as UVR in murine keratinocytes (Cui et al 2007). Once POMC is transcribed, it is post-translationally processed by proconvertase 1 to generate ACTH, this is cleaved to form corticotrophin-like intermediate peptide and a-MSH. A-MSH is released by keratinocytes and acts on the receptor and initiates the cascade previously mentioned in section 1.2. potentially upstream of POMC is a protein called upstream stimulating factor-1 (USF1). In USF1 knockout mice we see a defective UV response and the inability to mount a tanning response to UV stress. This is mediated by p38 kinase (Corre, et al 2004, Galibert et al 2001). This method of melanin production might work independently of the first pathway; however, it is more likely to run alongside the p53 pathway, promoting melanin production through a number of pathways.

1.6 Pigmentation disorders

When the process of melanogenesis and pigmentation is disrupted, it can lead to disorders of pigmentation. There are a wide variety of pigmentation disorders ranging from hyperpigmentation, hypopigmentation and uneven pigmentation. Such disorders can have negative societal impacts both physically and mentally for an individual, for this reason it is important to expand research in these areas to better understand the underlying cellular mechanisms and develop subsequent interventions

1.6.1 Hypopigmentation

Like most organs and tissues, the skin and in particular pigmentation has cases where normal function fails and we see altered skin function that can result in a pathological condition. Two of the most widely known pigmentations disease are albinism and vitiligo due to a recent societal shift towards body positivity, sufferers of these diseases have been empowered to showcase their visible physiological changes. A vitiligo sufferer is shown in Figure 10. Both albinism and vitiligo are examples of hypopigmentation, a lack of pigmentation in areas or in the case of albinism, entirely missing (Graier et al 2020, Zhang et al 2016). Whilst not life-threatening, the resulting stress caused by physiological changes to one's appearance causes a reduction in the quality of life (Onganae et al 2005). However, there is an emerging understanding of the effect that Vitiligo has on other aspects of the body. Melanocytes, although important in the skin are not solely found in this organ. They can be found throughout the body carrying out crucial functions. A link between Vitiligo and hearing loss has been drawn and may be the first of a number of other unknown effects of this disease (Akay et al 2010).

Figure 10. An example of a vitiligo sufferer. This image shows the potential for psychological stress from the disease as it can showcase in areas that can be tough to cover, leading to body issues. In this case, the patient suffers from a lack of pigmentation in the facial region. However, in recent years a push towards body positivity has led sufferers from the disease to speak out and raise awareness of the issue.

The two strongest hypotheses for Vitiligo are genetic and autoimmune causes. Whilst there does seem to be a single inherited factor, there is evidence to suggest that vitiligo has an element of its pathology in genetics (Kim et al 1998, Silva de Castro et al 2010). However, it might be more likely to have genetic variants that cause a susceptibility to the disease making patients more likely to develop an autoimmune destruction of melanocytes. There is evidence from research that points to an autoimmune cause for vitilgio, however, like genetic factors, conflicting results have been found. Evidence for shows a prominence of other autoimmune diseases in vitiligo sufferers (Alkhateeb et al 2003) and the detection of melanocyte specific antibodies in serum of patients (Cui et al 1989). There are a number of other working hypothesis out there for the aetiology of vitiligo, however, due to the complexity of pin pointing a single cause, evidence suggests it is multi-factoral which includes various cell types.

Figure 11. An example of albino version of a humpback whale. The genes for melanin are highly conserved and numerous examples of animals in the animal kingdown displaying a form of Oculotaneous Albinism. The disease potentially has different epidemiology in different species but the similarity is a lack of pigmentation throughout the body.

Oculotaneous albinism (OCA) is a group of disorders characterized by a genetic defect in melanin producing genes, that result in an lack of pigmentation throughout the organism. Examples of this disease have been seen throughout the animal kingdom, with examples of rare albino animals (Figure 11). Unlike Vitiligo, OCA has been well studied and the epidemiology is well understood. Some genes involved in melanogenesis are named after their discovery to do with OCA. The OCA family of genes (OCA1-4) are the most common genetic defects seen in OCA and the proteins they encode for. The lack of pigmentation is not just noticed in skin, both the hair and the iris are affected and can often lead to visual impairment in sufferers (Creel et al 1978). Due to the inherited nature of OCA, one or both parents are carriers of OCA genes and therefore, follows mendellian genetics which gives a minimum of 25% chance to occur in offspring. OCA is offered as part of prenatal testing however, it is often unlikely that parents request prenatal testing, most likely due to the quality of life that OCA sufferers are still able to experience (Fassihi et al 2006). This level of

prenatal testing also mirrors the lack of a cure; however, treatment often manages any symptoms that arise instead of needing to treat the disease.

1.6.2 Hyperpigmentation

The previously examples of pigmentation disease are examples of hypopigmentation, where not enough or no pigmentation is produced. In the opposite scenario, one of the most common is melanoma. Melanoma is malignant growth of melanocytes, often brought about by excessive UVR, leading to DNA damage. Since melanin is required for protection from UV and light-skinned ethnicities have lower melanin content/melanocytes, there is a disproportionate incidence of melanoma in fair skinned individuals (Brenner et al 2008). Over the last century, rates of incidence and mortality of melanoma has been increasing (Guy et al 2015, Whiteman et al 2016). Therefore, governments often implement policies to educate the general public. Since the damage that UVR does to skin is well researched and understood and to reduce the risk a number of simple prevention methods – sunscreen, clothes, reducing midday sun exposure – can drastically reduce melanoma cases.

In addition to melanoma, age spots are a natural progression throughout life towards hyperpigmentation. Age spots develop in chronically UV-exposed skin and display an area of darker pigmentation with an elongated like appearance. Whilst age spots don't pose any adverse effects on a person's health, understanding the mechanisms behind the formation of age spots may shed light on other pathological disorders. However, the mechanisms behind their development is poorly undetrsood. Some studies have pointed to the role of paracrine growth factors such as KGF, HGF, Stem cell factor or endothilin (Chen et al 2010, Kovacs et al 2010). Whilst other studies suggest a role for inflammation and an immune response (Goyarts et al 2007). Although a fairly recent paper pointed to a build up of melanosomes in the *Stratum Basale* due to a lack of melanin breakdown in keratinocytes (Choi et al 2017).

Understanding the mechanisms behind melanin production is important because irregularities in these pathways lead to the aforementioned pigmentation disorders and others. Creating bioengineered skin models *in vitro* will allow us to study these molecular mechanisms that underpin skin pigmentation and ultimately screen compounds that regulate pigmentation and could have potential medical and cosmetic beneficial effects. [pigment conditions in a laboratory setting allow us to generate and test compounds. These compounds help people to have an improved quality of life that might otherwise not have been possible.

1.7 *In vitro* tissue culture

The history of tissue culture began with a controversial decision to culture an immortalised cell line from the patient Henrietta Lacks in the 1950's. Henrietta Lacks was suffering from a cervical tumour when she was admitted to John's Hopkins hospitals. Biopsies from this tumour were taken and cultured and eventually became HeLa cells, the oldest and most commonly used cell line. However, Henrietta never granted permission for the use of her cells and to this day these cells are still controversially used throughout scientific research. Following from the culture of the first immortal cell line, there was an explosion of various different immortal cell lines from different organs in the body. This led to a variety of research in different tissue types and experimentation to try and recreate human organs in culture. Cell culture started in 2D but later transcended into 3D structures and skin is no different. The first models were simple 2D cultures of one or more cell types. These models are good for simple experiments and at the time, it was the extent of the technology that was available. Nowadays, these 2D cultures are cheap and quick to produce, making them simpe and easy models for drug testing (Matei et al 2019, Gibbs et al 2013). However, the simplicity that makes these models attractive is the reason more complex models are required. Structure and function go hand in hand, to achieve appropriate function of a model, structure of the organ must be mimicked as closely as possible.

The desire for a more complex model brought about culturing cells in 3D. This has developed into multi-cellular models which closely resemble the desired organ. There are number of factors that influence how cells respond to their

Figure 12. An image to show microenvironmental factors influencing the cell.

These range of external factors that a cell comes into contact with in its microenvironment influence the genotype and phenotype of a cell. Bao et al 2018

external microenvironment and these are not present in 2D cultures. A pioneer in the cell microenvironment is Mina Bissell, she showcased the importance of cell interactions in 3D
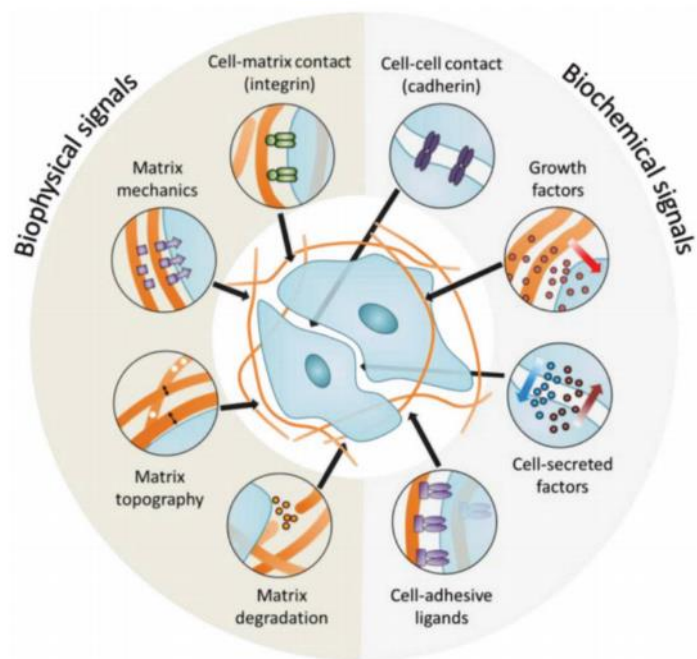
culture in the context of breast tumours (Han et al 2010, Inman et al 2010). The microenvironment is the localised environment that the cell exists in within the tissue. This environment includes oxygen availability, ECM interaction, nutrients and waste which all contribute to how a cell may act in culture (Huh et al 2011). These range of factors influence the morphology and gene expression of cells in culture. The influence of this microenvironment should not be understated and for the validity of experiments using cells grown in culture, it is important to try and recreate this environment as closely as possible. Figure 24 shows the range of external factors from the microenvironment influencing internal cell signalling.

The benefits of culturing cells in 3D became clear which led to the development of a range of techniques to recreate the environment of the body. Firstly, in order to provide a structure for cells to grow on, solid scaffolds became a popular choice for 3D cell culture. These scaffolds tend to be biologically inert materials – such as polystyrene - provide a cross-linked structure that acts as a base structure for cells to grow on. Over time the cells will grow and, with the correct media, starts to represent the desired tissue. Hydrogels also offer a similar method of action. These gel-like substances provide a meshwork of ECM molecules to provide the anchorage for cells to begin to grow on. Hydrogels provide the structural support of solid scaffolds but may provide more in the way of biological signals, since they are often made from ECM proteins (Breslin et al 2013). Another important 3D method of cell culture are spheroids. Only recently were these applied to skin and specifically melanocytes (Zurina et al 2020), however they have been a popular technique to provide a more native environment by giving cells a 3D environment to grow in and can contain more than one cell type.

In 2013, the ability to test cosmetic products on animals was made illegal (EU act reference). This gave cosmetic companies and university laboratories the financial motivation to further develop an alternative to replace animal testing. There has since been an explosion of skin models to market.

1.8 Bioengineered Skin Models

1.8.1 De-epidermised Dermis (DED)

One of the first types of skin models involved removing the cells from a skin biopsy, leaving a decellularised dermis or DED. Previously, a skin biopsy has to be treated with a number steps in order to achieve a DED – dehydration, sterilization and removing the epidermis – before it can be used to seed a skin equivalent (Ghosh et al 1997). The process for cell removal was often harsh and can lead to damage of the proteins in the decellularised scaffold. This may

lead to large variability between models and give unpredictable results. However, more recent studies have shown the ease in which a DED can be produced by incubation with 100% ethanol (Brancato et al 2018). This ease of production is starting to bring DED back into popularity, especially due to their ability to recapitulate a specific environment, making it a good candidate for generating disease models from patients own skin. Regardless of the method used, what remains is native ECM which has biochemically relevant signals. In the last 10-20 years, cancer research has shown the affects the environment of the tumour has on cell proliferation. Therefore, it is important to produce a model to study cancer that can mimic this. This specific environment is an attractive trait for cancer research, which leads to DED being used heavily in melanoma research (Haridas et al 2017, Commandeur et al 2014).

1.8.2 Plastic membrane

Another method of producing skin equivalents relies on a porous plastic membrane incubated with collagen. The collagen coated plastic mimics the basement membrane to allow keratinocytes to adhere to it and form an epidermis. This type of model is popular due to its ease of generation and normally takes around two weeks to grow. After an incubation period submerged in media, the model is raised to the air-liquid interface to mimic the interaction of skin between the inside and outside of the body. Unlike a DED, it doesn't require the use of human tissue, due to the human tissue act, human tissue can be difficult and time consuming to work with. Therefore, generating human skin equivalents without human tissue is a more favourable process. Whilst these models have shown great promise in mimicking the function of skin and are a replacement for animals in cosmetic testing, the models are still lacking complexity. In this introduction, the importance of the dermis on normal function of the skin and to mimic function of an organ, structure is important. Therefore, it would seem that these models, whilst a good start, lack the complexity of skin to effectively replicate the function of skin.

1.8.3 Collagen gel

The simplicity of the plastic membranes doesn't appropriately recreate the complexity that the ECM has and the effect this has on the surrounding cells. Therefore, the addition of collagen gels to inert plastic membranes provides a more biologically relevant basement membrane. (Li et al 2011, Szymański et al 2020). Both these protocols require the use of animal collagen - rat and bovine collagen – which still experience shrinkage and may affect the validity of the experiments using animal collagen. Szymański counter collagen shrinkage by inclusion

of genipin – a compound known for its cross-linking ability – which reduces collagen shrinkage by 25%. However, it still occurs and with the use of exogenous collagen, it is difficult to monitor changes in the ECM. Furthermore, collagen gel has also been shown to shrink (Shi et al 2003) and the collagen is often derived from animals – commonly rat-tail collagen – which may cause cells and models to respond differently in culture.

1.8.4 Collagen Matrix

More recently, these epidermal models have become more complex. In this review we have discussed the importance of communication between the epidermal and dermal compartments of skin, which has a profound effect on the function of the tissue. It is therefore important to re-create the cellular environment *in vitro* by adopting a full thickness approach to model both compartments simultaneous. Collagen matrixes provide the ability to populate a collagen-based gel with dermal fibroblasts. In this model type, fibroblasts are free to produce endogenous ECM on top of the collagen gel, providing a similar basement membrane to that of human skin (Lee et al 2000). Once this basement membrane has developed and the fibroblasts have produced and remodelled the ECM, keratinocytes are free to be seeded on top, generating an epidermis. This model provides the interaction between the epidermal layer and a constructed dermis that more close resembles the physiology of the human dermis than a collagen gel. The collagen matrix provides the ability to generate a full thickness skin model that that not only has a basement membrane but it has a basement membrane containing fibroblasts that have the opportunity to influence and remodel the proteins that are crucial to the function of the dermis.

1.8.5 Bioprinting

An emerging technique is the ability to print cells onto biological scaffolds using 3D printing techniques. Since 3D printing has revolutionised various fields, it is understandable that it will influence biology. The ability to print cells onto a scaffold is new and exciting field, reducing labour and the time for tissue generation (Won et al 2019). Cells are added to a polymer based 'bioink' and then subsequently printing in layers in order to build up the tissue sequentially. In the case of skin, a simple model is produced by printing keratinocytes onto a basement membrane and allowing it to develop. Ultimately, the aim of this technology is to generate a simple and reproducible way to create tissues and organs with minimal human interaction. The technology certainly shows enough promise to do this and is being researched for use in a wide array of tissue and organ types. However, the technology is in its infancy and

requires further time and research before it becomes a commercially viable method of producing 3D models.

1.8.6 Melanospheres

Finally, a recent study has shown that melanocytes cultured in '3D melanospheres' have great promise for a model for drug testing (Zurina et al 2020). Melanocytes cultured on a agarose plate which aggregate and form 3D spheres. The process for creating these melanocyte spheroid cultures is fairly simple, once placed in agarose plates, the spheroid forms without intervention. Zurina used fuxocanthin to study the efficacy of these 3D monocultures and there response to pigment altering compounds. The results showed that the melanospheres had a stronger response to fuxocanthin showed by an increase in immunofluorescence of GP100 and an upregulation of gene expression of MC1R and Tyrosinase. Whilst this model shows promise the lack of co-cultures or inclusion of other cell types is definitely a drawback. Although, as a simple model for analysing the effects of drugs on melanocytes shows promise. It is likely that this model should be used in conjuncture with other model systems to ensure the most accurate results.

1.9 Developing the platform technology

The Przyborski lab at Durham University have generated a new model, using neonatal human dermal fibroblasts (HDFn) seeded onto a polystyrene membrane called Alvetex® (Roger et al 2019). These fibroblasts produce an endogenous ECM that closely resembles human skin. This provides the keratinocytes the chance to grow on an ECM with structure much closer to what is found *in vivo*. The Alvetex® insert is the main focus of why this model can outperform other models. Alvetex® is porous polystyrene scaffold with interconnecting windows that allows cells to move and adhere to, providing crucial structural support for tissue development. The strength of Alvetex® can be seen in its ability to be used to model different organs. It has acted as the base for to study liver cells, intestinal cells, stem cells and bone tissue. This diversity shows the value of Alvetex® and the importance a technology like this has in tissue culture. The polystyrene membrane comes in three sizes and consists of cross-linked polystyrenes with gaps of different sizes between the three models.

The fibroblasts are then able to invade into the membrane and after a month incubation, the ECM produced is similar to that of human skin (Roger et al 2019). The fibroblasts produce collagen 1,3 and 4 along with other ECM proteins fibronectin and elastin. Therefore, the increased complexity in the ECM, compared to epidermal models that have a polystyrene insert

coated in collagen 1, provides more support to the epidermal section. Furthermore, the fibroblasts can be seen producing integrins at the dermal-epidermal junction to provide structural integrity to the model. After the month incubation, the dermal section has developed and is ready for keratinocytes to be seeded on top, however, at this point the model can be used as a dermal equivalent. These dermal equivalents represent the human dermis and can provide a scaffold for the full thickness model or can used as a model to study the human dermal compartment.

Once the ECM is produced, there is the potential to use this as a dermal equivalent or continue to a full thickness model and seed keratinocytes on top. After seeding keratinocytes, the model is raised to the ALI after two days and incubated for another two weeks. After this time period the model shows the four distinct layers of skin, with columnar keratinocytes in the basal layer, a stratified top layer of corneocytes. Furthermore, the paper shows that fibroblasts are producing a number of proteins consistent with ECM *in vivo*. The ECM addresses one major issue of other models, and provides the keratinocytes with a wider range of signals than is seen in an epidermal equivalent. Since the structure and function go hand in hand in organisms, this model provides a base to start to create more complex skin models.
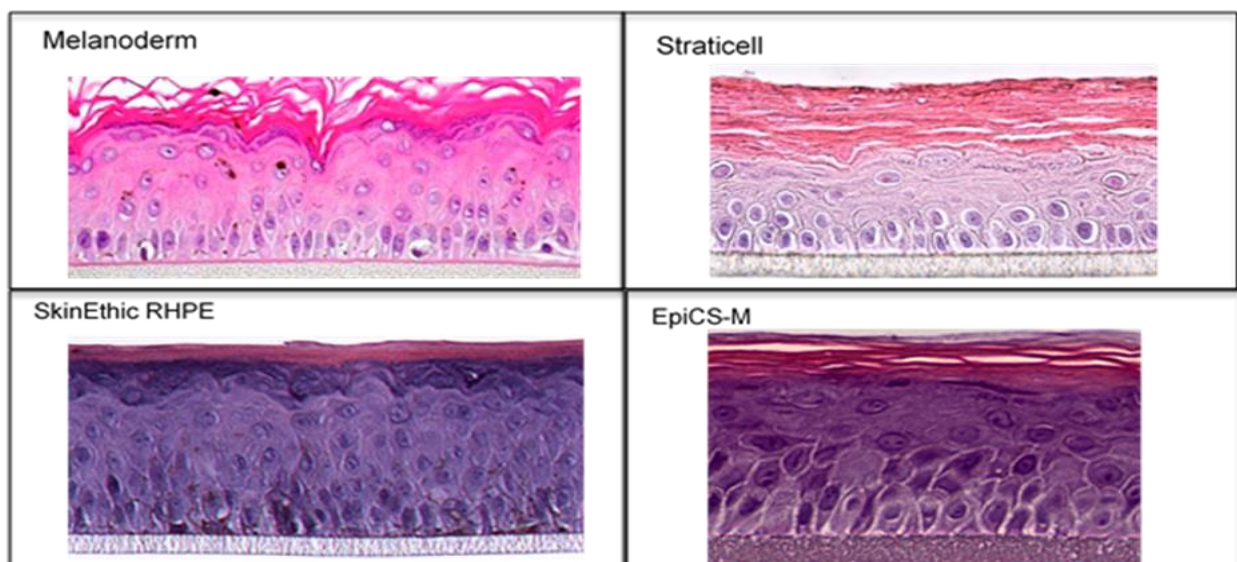
Figure 13. Four examples of available competitor skin equivalents. They are all epidermal equivalents lacking a dermis, with a plastic insert as the basement membrane. All the models show strong epidermal morphology with four distinct layers of specialised keratinocytes and, in some cases, melanocytes are recognisable in melanoderm and SkinEthic.

1.10 Current skin models

Once the platform technology for generating a full thickness model using fibroblasts to produce endogenous ECM was in place. The ability to improve the complexity of the model presented

itself. Whilst the model showed good promise, in terms of comparison to human skin, it is lacking a number of key elements, namely pigmentation. There a number of pigmented skin equivalents on the market, the main four being: Melanoderm, Straticell, SkinEthic and EpiCS-M, of these four models (Figure 10), Melanoderm seems to be the market leader. Melanoderm is the most transparent in terms of information about their product which shows a confidence that other skin models might not have. Melanoderm is advertised as a model system used for cosmetic and UV testing, however, the pigmentation in their model is inconsistent, it shown to darken over time, without any external influence. There is the expectation that a model will respond to natural light and darken, however, the extent to the pigmentation change is surprising. This is an issue for a pigmented skin equivalent because they are used for testing pigment altering compounds, if the model has excessive natural darkening, the validity of the compounds being tested is thrown into question. Whether or not the compound is causing the darkening or if the efficacy of this compound over/understated.

Interestingly, all these models are epidermal only models, grown on a polystyrene insert often with the addition of animal collagen. In Yoon et al 2003, Melanoderm showcase a full thickness model through a third-party paper. Information on this model is sparse and the function of the model needs further characterisation. A large amount of evidence shows the importance of the dermis for proper epidermal maintenance in human skin. Therefore, Whilst these epidermal models showcase the four epidermal layers and proper specialisation of keratinocytes into corneocytes, there is little evidence into the difference between the epidermal equivalents and full thickness models.

2 Aims and Objectives

The main aim for this research was to develop a novel, pigmented skin equivalent for use in industrial applications. We also investigated the influence of the dermis on melanogenesis and ultimately the transfer of melanosomes to keratinocytes in this model system. Currently, the standard practice for cosmetic testing is to use epidermal equivalents. However, since the structure and function of a tissue go hand in hand, it is hypothesised that these epidermal models fall short of the function of human skin and that a model that has a dermal compartment will perform favourably. In order to create a model that functions as closely to the tissue it is trying to recreate, all parts of the organ should be included, therefore, since epidermal only models are lacking a dermis, it is potentially lacking a large part of its functionality. Research into human skin shows that the dermis has a supportive role to play in maintaining appropriate skin homeostasis. The hypothesis for this thesis is: pigmented skin

equivalents cultured with neonatal human dermal fibroblasts in a dermal compartment will perform favourably compared to an epidermal only model and support

The first aim of this project was to incorporate melanocytes into the simplistic epidermal model. epidermal models are quick and simple to generate, therefore, this provides an excellent system to show proof of concept for the melanocytes into a skin equivalent. Once melanocytes had been successfully introduced into an epidermal model, it provided a foundation to introduce melanocytes into the more complex full thickness skin equivalent. Melanocytes were incorporated into the model at a 1:10 ratio with keratinocytes. Whilst a range of seeding ratios exist in the literature, melanocytes exist at this ratio in human skin, therefore, we chose to use the ratio that exists *in vivo.*

The next aim was to investigate the link between the dermis and melanocyte function with skin equivalents. Once the melanocytes are successfully introduced into the full thickness model, melanocyte function can be examined and compared to the epidermal model. Furthermore, it was important to compare this to human skin as a benchmark of melanocyte function. Therefore, models were grown under the normal conditions and then examined with H&E, Fontana Masson, immunohistochemistry and electron microscopy. The images acquired will be compared against human skin with the same stains in order to understand how the models compared against each other and human skin. In addition, to qualitative methods showing the structure of the models under a variety of stains, quantification of melanocyte function was applied alongside the images to add validity to any conclusions drawn.

In order to show the strength of the Alvetex model compared to current models on the market, it is important to show that this model had consistent pigmentation. This required measuring pigmentation at a number of time points within the standard incubation period. Models were raised to the air-liquid interface then harvested at three time points. The amount of pigmentation was observed through Fontana Masson staining of the models to highlight melanin. Although the general structure of the models was observed through H&E staining. It is hypothesised that the models will have period of melanin production early on, however, this remained consistent after a certain point.

A crucial element of pigmented skin models is application of the model using pigment altering compounds. In order to be sure, the model functions the same as native skin, the pigmentation has to respond and alter its pigmentation. Furthermore, this model is to be intended for commercial and academic use, therefore, application of function is important. The

model will be incubated with a-MSH and Kojic acid, two well-known and widely used pigment altering compounds. The expectation here is that the models respond appropriately to the respective compound and either increase or reduce the level of melanin in the models. Immunofluorescence will be used to examine to change in the strength of pigmentation in both 2D and 3D cultures. The objectives for this thesis are as follows:

- Incorporate melanocytes into the simplistic epidermal equivalent
- Incorporate melanocytes into the more complex full thickness skin equivalent
- Comparison of melanocyte function in full thickness, epidermal and human skin
- Characterisation of the full thickness skin equivalent
- Stability of pigmentation over a time course
- Addition of a-MSH and Kojic acid

3 Materials and methods

3.1 Cell Culture

3.1.1 Cell Line Maintenance

3.1.1.1 Primary Keratinocytes

Human neonatal epidermal keratinocytes (HEKn) (ThermoFisher Scientific, city, UK were cultured in a T175 flask (Greiner Bio-one, city, country) with 24 mL of Epilife® media with Human Keratinocyte Growth Supplement (HKGS) (Life Technologies), further referred to as complete Epilife. Lot number for cell lines: #888, 926. Each T175 flask was seeded at a density of 0.5×10^6 cells. HEKn were grown to 80 % confluency before being seeded into skin models at 0.5×10^6 cells. Media was changed three times per week and cultured at 37 °C with 5 % CO_2 in a humidified environment

3.1.1.2 Primary Dermal Fibroblasts

Human Dermal Fibroblast (HDFn) (Life Technologies) were cultured in a T175 flask (Greiner Bio-one) with 24 mL of Medium 106 (M106) (Life Technologies) with Low Serum Growth Supplement (LSGS) (Life Technologies), further referred to as complete M106. Lot number for cell lines: #356 Each T175 flask was seeded with 0.5×10^6 cells. HDFn were grown to 80-90% confluence before being seeded into the Alvetex at 0.25×10^6. 3D Medium was changed three times per week and cells were incubated at 37°C with 5 % CO_2 in a humidified environment

3.1.1.3 Primary Melanocytes

Darkly Pigmented Human Neonatal Epidermal Melanocytes (HEMn-DP) (Life Technologies) were cultured in a T75 flask (Greiner Bio-one) with 24 mL of Medium 254 (M254) (Life Technologies) with Human Melanocyte Growth Supplement (HMGS) (Life Technologies), further referred to as complete M254. Lot number for cell lines: #650, #107. Each T75 flask was seeded with 0.05×10^6 cells. HEMn were grown to 90 % confluency before using them in the epidermal or full thickness skin models at 0.5×10^5. Medium was changed three times per week and cells were incubated at 37°C with 5 % CO_2 in a humidified environment

3.1.2 Cell Revival

Cell populations were revived between passage two-seven from -150 °C frozen cell stocks. Frozen cells were stored in synthafreeze (Paisley, Fisher Scientific, UK) and were thawed by placing the bottom half of the cryovial (Fisher Scientific UK, Winsford, UK) into a water bath at 37 °C. Once only a small ice crystal remained in the cryovial (Fisher Scientific), cells were transferred to cell culture cabinet. Cells were resuspended with a 1 mL pipette to ensure even distribution. Next, cells were pipetted from the cryovial (Fisher Scientific) into a flask (Greiner Bio-one, Stonehouse, UK). Once the cells were seeded into a flask (Greiner Bio-one), they were placed into an incubator at 37 °C with 5 % CO_2 and 95 % relative humidity. Medium was changed 24 hours following revival to remove any remaining cryopreservative.

3.1.3 Cryopreservation

Remaining cells from seeding models were counted as part of the model generation process and were frozen down for future use. Once the number of cells were determined, cells were centrifuged at 1000 rpm for 5 minutes to form a pellet. Cells were diluted in an appropriate volume of Synthafreeze (Fisher scientific UK) – usually 1 mL – and placed into a Mr Frosty

Media A	Stock solution concentration	Final concentration	Dilution
KGF	10ug/ml	5ng/ml	2000X
CaCl2	2M	140uM	14300X
Ascorbic Acid	10mg/ml	50ug/ml	200X

Table 1. A table outlining the concentrations of required additives to media for culturing epidermal models before raising them to the air-liquid interface

in a -80°C freezer overnight for slow freezing at a rate of -1 degree per minute. The following day, the cells were moved to the -150°C cell bank for long term storage.

3.1.4 Generation of Epidermal Equivalents

Firstly, the media was aspirated from a flask of HEKn at 80 % confluence or HEMn at 100 % confluence and cells were washed in DPBS (Lonza, Basek, Switzerland). The flask was gently rocked from side to side to wash the cells thoroughly, then the DPBS was aspirated. 5 mL of Trypsin EDTA (Life Technologies) was added to the flask, which was incubated for 5 minutes at 37°C. Twice the volume of Trypsin neutraliser (Life Technologies) was added to the flask. The cells were then centrifuged for 5 minutes at 1000 rpm and the supernatant was removed. The cells were resuspended in 1 mL of Medium A. Cells were counted using a trypan blue (Sigma Aldrich, Dorset, UK) exclusion assay by diluting cell suspension to 1:10, using a hematocytometer to determine total number of cells in the 1 ml of media. 500,000 keratinocytes and 50,000 melanocytes in 500 uL total volume per model were seeded onto a Millicell insert (Merck Millipore Watforwad, UK) coated in human recombinant collagen coating matrix – Millicell inserts were incubated with collagen coating matrix (ThermoFisher) 30 minutes prior to setup. A deep-dish petri dish (VWR International, Pennsylvania, US) was filled with 35 mL of media containing KGF (Sigma Aldrich), CaCl2 (Sigma Aldrich) and ascorbic acid (Sigma Aldrich) at dilutions found in table 1 (Media A), maximum 6 models per petri dish. Finally, Millicell inserts were checked for air bubbles between the insert and the stand and placed into an incubator.

Media B	Stock solution concentration	Final concentration	Dilution
KGF	10ug/ml	5ng/ml	2000X
CaCl2	2M	1.64mM	1219X
Ascorbic Acid	10mg/ml	50ug/ml	200X

Table 2. A table showing the concentrations of the required additives to the media for culturing epidermal models after raising it to the air-liquid interface

After 2 days of incubation models were raised to the Air-Liquid interface (ALI), the media was removed from the dish itself and the apical chamber of the insert and 25 mL of complete Epilife

with supplements from table 2 (Media B) with high calcium concentration to induce keratinocyte differentiation. Once raised to the ALI, the models required 3 media changes per week. Models were used in experiments at 10 days ALI and following desired treatment conditions were harvested by removal of the membrane from the culture insert using a scalpel. Once removed, the membrane was added to the desired fixative for further analysis.

Table 3 Media C	Stock solution concentration	Final Concentration	Dilution
TGF β	10ug/ml	5ng/ml	2000X
Ascorbic acid	10mg/ml	100ug/ml	100X

Table 3. A table showing the concentrations of the required additives to the media for culturing HDFn cells in the dermal equivalents.

3.1.5 Generation of Dermal Equivalent using Alvetex® Scaffold

Once 2D cultures of HDFn reached 80-90 % confluence, cells were used to seed dermal models. In preparation Alvetex® Scaffolds (12-well format) were treated with 70 % ethanol and washed in DPBS to render them hydrophilic prior to cell seeding. Cells were then prepared by aspirating the medium from the flask and cells were washed in DPBS. 5 mL of Trypsin EDTA (Life Technologies) was added to the flask which was then returned, to the incubator for 5 minutes. Twice the volume of Trypsin neutraliser (life Technologies) was added to the flask. The cells were centrifuged for 5 minutes at 1000 rpm and the supernatant was removed. Cells were resuspended in 1 mL of complete M106. Cells were counted using a trypan blue exclusion assay by diluting cell suspension to 1:10 and a haematocytometer was used to determine total number of cells in the 1 mL of media. 500,000 HDFn cells in 100 uL total volume per model were seeded onto a 12-well format Alvetex® insert (Reprocell Europe Ltd, Sedgefield, UK in a 6 well plate (Greiner Bio One). After 2hours 10 mL Media C (M106 with TGF B1 (PeproTech) and Ascorbic Acid (Sigma Aldrich) – Table 3) was added to each well and models were further incubated.

Dermal equivalents were cultured for 28 days at 37 °C, 5 % CO_2 in a humidified environment and required media changing twice a week. The 6 well plate containing the models was changed for a new one at the first media change and at 14 days in culture, as HDFns fall through and sit in the bottom of the well, which consume medium and may have paracrine

effects on the model. After 28 days the dermal compartment of the model is matured enough to have the epidermal compartment seeded.

Table 4 Media D	Stock solution concentration	Final Concentration	Dilution
KGF	10ug/ml	5ng/ml	1000X
CaCl2	2M	140 uM	14300X
Ascorbic acid	10mg/ml	100ug/ml	100X

Table 4. A table showing the concentrations of the required additives to the media for culturing full thickness models after seeding HEKn and HEMn cells before raising it to the air-liquid interface.

3.1.6 Generation of a Full Thickness Skin Equivalent

HEMn and HEKn are grown in 2D as previously described in section 3.1.1. After 7 days or when cells reach 80-100 % confluency, were seeded onto a 28-day matured dermal compartment to form the full thickness skin equivalent. Cells were trypsinised and centrifuged as previously described 3.1.4. Cells were resuspended in 1 mL of complete Medium D Table #4. Cells were counted using a trypan blue exclusion assay and haemocytometer as previously described in section 3.1.4 and 500,000 keratinocytes and 50,000 melanocytes were seeded in 150-300 uL total volume per model onto a dermal equivalent. The HEKn and HEMn were left to adhere to the scaffold in an incubator at 37 °C. Following a minimum of 2 hours incubation 10 mL of media D was added to the well with 1 mL of media D on top of the dermal equivalent, to ensure the model was completely submerged. The models were placed into an incubator and left to grow for 2 days in submerged culture.

After two days the full thickness models were ready to raise to the air-liquid interface. To raise models to the ALI, 36 mL of media E was made for every 1-3 models. Each model was transferred to a reinnervate deep dish (Reprocell) with Alvetex® stands using a pair of sterile forceps. Each deep dish held up to three models and models were placed at the medium height setting. 35 mL of media E with high calcium to induce keratinocyte differentiation was added to each reinnervate deep-dish petri dish with medium touching the underside of the Alvetex® membrane but the apical side exposed to the air. Any remaining media was aspirated carefully off the top of the model. The models were returned to the incubator, media changed twice per week and maintained until 14 days to fully establish the epidermis for use in downstream applications. models were then harvested using the following method: The arms of the Alvetex© model - that clip onto the stand – were unclipped. Next, the polystyrene membrane was removed from the plastic by pushing up on the membrane from the underside with a pair of sterile forceps and carefully washing it with DPBS. The membrane was then added to the required fixative e.g., 4% PFA for wax embedding.

Table 5 Media E	Stock solution concentration	Final Concentration	Dilution
KGF	10ug/ml	5ng/ml	1000X
CaCl2	2M	1.64 mM	1219X
Ascorbic acid	10mg/ml	100ug/ml	100X

Table 5. A table showing the concentrations of the required additives to the media for culturing full thickness models after raising it to the air-liquid interface.

3.2 Fixation, embedding and sectioning

Once a model has reached maturity, it needs to be harvested, fixed and embedded in wax for histological purposes. In order to fix the model in wax, a 4% formalin (40% formalin 1:10 in PBS) solution was made. Once the model was removed from cell culture it was washed in PBS for 5 minutes, then transferred to 4 % formalin for 2 hours at room temperature or overnight in a fridge at 4 °C.

Once the model was fixed, it was dehydrated by moving it through increasing concentrations of ethanol . Samples were incubated in 30 %, 50 %, 70 % ,80 %, 90 %, 95 % for 10 minutes each at room temperature. Finally, the samples were placed in 100 % ethanol for 30 minutes.

After the models were dehydrated, they were moved to a Histology cassette and placed in a glass beaker of Histoclear II Scientific Laboratory Supplies) for 30 minutes at room temperature. Next, paraffin wax (Sigma Aldrich) molten at 65 °C was added at a ratio of 1:1 to the Histoclear II. The sample was placed in the oven at 65°C for 30 minutes. The Histoclear II:wax mixture was removed and the sample was submerged in 100 % wax at 65 °C and placed back into the oven for 1 hour.

To embed the sample, it was placed in an embedding mould (Cell Path Ltd, Mochdre, Newtown, UK) containing molten wax.. The desired section (tranverse or longitudinal) will determine the orientation of the model in the mould. Multiple models were able to be embedded in the same mould. The rest of the mould was filled with molten wax and the corresponding cassette was placed on top of the mould. Once the wax had cooled, the mould was removed and the wax block remained attached to the cassette.

To stain the tissue, the block was first cut into 5 um sections and mounted on a Superfrost microscope slide (Fisher Scientific). To achieve this, a Leica RM2125RT microtome (Leica Biosystems, Newcastle upon Tyne, UK) was used. The block was mounted onto the chuck of the microtome, using a razor-sharp blade cutting blade (Lieca Biosystems). Once a section had been cut using the microtome, the section was moved to a water bath at 40°C and gently floated the section out onto the water using a pair of tweezers and carefully transferred onto the microscope slide. Sections were dried overnight.

3.3 Haematoxylin and Eosin Staining

To stain slides with Heamatoxylin and Eosin (H&E) the slides were first deparaffinised in Histoclear I for 5 minutes then transferred to 100 % ethanol for 2 minutes. The samples were further rehydrated in 95 % ethanol then 70 % ethanol then distilled water for 1 minute each. Mayer's Haematoxylin (Sigma Aldrich) was the first staining step for 5 minutes followed by a wash in distilled water for 30 seconds. The nuclei of cells were stained blue by alkaline alcohol incubated for 30 seconds and then dehydrated in 70 % ethanol followed by 90 % ethanol for 30 seconds each. The samples were then counterstained in Eosin (Sigma Aldrich) for 30 seconds. The tissue was further dehydrated in 95 % ethanol twice for 10 seconds each. Followed by two washes in 100 % ethanol for 15 and 30 seconds. Finally, the sections were cleared by washing in Histoclear I twice for 3 minutes each. Slides were then mounted using omnimount medium (Fisher Scientific) and a coverslip was added. The Omnimount was left to set overnight and then the slides were ready to image under a microscope.

3.4 Fontana Masson stain

The Slides were incubated in histoclear II to deparaffinize the sections then rehydryated by moving the slides through 70% ,95%, 100% EtOH for 1 minute followed by 1 minute in distilled water. Ammoniacal Silver was made by mixing silver nitrate solution in distilled water at a ratio of 3:1. Ammonium Hydroxide was added to the solution one drop at a time, swirling the liquid after each drop. Following the addition of Ammonium Hydroxide the mixture turned dark brown then a fine layer of sediment emerged. The Ammonium Hydroxide step was repeated until the fine layer of sediment disappeared. The Ammoniacal Silver was placed in a water bath at 58-60 °C and left to equilibrate.

Once the slides were rehydrated, 200ul of Ammoniacal Silver was added to each slide and incubated at room temperature for 30 minutes. The slides were rinsed in several changes of distilled water and then incubated with 200ul per slide of Gold Chloride solution (0.2%) at room temperature for 30 seconds. The slides were rinsed in several changes of distilled water and then incubated with 200ul per slide of Sodium Thiosulfater solution (5%) for 2 minutes. The slides were rinsed for 2 minutes in running tap water followed by 2 changes of distilled water. The slides were then incubated with 200ul of Nuclear Fast Red solution for 5 minutes at room temperature. Finally the slides were rinsed for 2 minutes in running tap water then 2 changes in distilled water. The slides were dehydrated quickly in 3 changes of fresh alcohol. Slides were cleared in histoclear II and mounted with omnimount synthetic resin.

3.5 Immunofluorescence

In order to stain samples with fluorescent markers, first the wax sections were deparaffinised in Histoclear II for 15 minutes and rehydrated by moving them through 100 %, 95 % and 70 % ethanols for 5 minutes each, then 5 minutes in PBS. The slides were transferred into citrate buffer and incubated for 20 minutes in a 95 °C water bath for antigen retrieval. Samples were then blocked in a buffer of: 20 % dilution of neonatal calf serum (NCS) (Sigma Aldrich) and 0.4 % Triton X-100 in 1 hour at room temperature. During this incubation, the primary antibody solution was made. Antibody concentrations are antibody specific and should be optimised or referred to manufacturer's direction. The primary antibody (Table 8) was diluted to appropriate concentrations in blocking buffer. The blocking buffer was removed by gently dabbing the long side of the slide onto tissue paper and 100 uL of primary antibody solution was added per slide, and samples were incubated overnight at 4 °C. The slides were washed 3 times in 1X PBS for 10 minutes and incubated in the secondary antibody (Life

Technologies) (table 9) solution diluted at a 1:10000 concentration in blocking buffer. 100 uL of secondary antibody solution was added to each slide and left for an hour at room temperature. If required, Hoescht (Fisher Scientific) nuclei stain was added at a concentration 1:10000 to secondary antibody solution. The sample was then washed 3 times in 1X PBS for 10 minutes each and mounted in 10 uL Vectashield (Vector Labs, Peterborough, UK) with a coverslip. Seal the coverslip using nail varnish and place the slide in the fridge until ready to be imaged.

3.6 2D Immunoflourescence

Coverslips in a 12 well plate were placed on ice, and permeabilised in 0.1% Triton-X-100 in PBS for 15 minutes. Permeabilisation solution was removed from the well using a Pasteur pipette, and coverslips were then blocked in a buffer consisting of 10% NGS in 0.1% Tween20 in PBS solution for 60 minutes. 50 µl of the desired antibody at the appropriate concentration was pipetted onto Parafilm (Fisher Scientific UK) in a plastic tray, coverslips were removed from the plate and placed on the Parafilm with the cells in contact with the antibody solution. Primary antibody incubation was for 60 minutes, and coverslips were washed in blocking buffer by moving onto 50 µl droplets of blocking buffer on the Parafilm for 10 minutes. This was repeated 3 times. Coverslips were then placed onto 50 µl droplets of the appropriate secondary antibody and Hoescht nuclear stain at the correct concentration for 60 minutes, before washing again as described. To mount, a small amount of Vectashield™ was placed on a SuperFrost™ Plus slide, excess PBS carefully blotted from the coverslip, and the coverslip placed onto the Vectashield™ on the slide. The coverslips were sealed with nail varnish, allowed to dry and stored at 4°C until imaging.

3.7 Immunohistochemistry

To carry out immunohistochemistry, first the slides were deparaffinised in histoclear for 15 minutes and rehydrated in a decreasing series of ethanols for 5 minutes each (100 %, 95 %, 70 % and dH$_2$O). Next, the slides were incubated in peroxidase block solution (3 % hydrogen peroxide in methanol) for 15 minutes. The slides were then transferred into citrate buffer for antigen retrieval and incubated for 20 minutes in a 95 °C water bath. The samples were blocked by adding 100 uL in 10 % neonatal calf serum in PBS/0.2 % Triton-x-100 for 1 hour at room temperature in a humidified slide chamber. During the blocking incubation, the primary antibody solution as made. Concentrations of primary antibody vary and was either optimised or manufacturer advice was followed. After blocking, 100 uL of primary antibody

solution was added to each slide and incubated for 1 hour at room temperature or overnight at 4 °C. The samples were washed 3 times in 1X PBS. In order to visualise antibody binding the ImmunoCruz ABC kit (Santa Cruz Biotechnology, Dallas, Texas, USA) was used and manufacturer's instructions followed. The slides were incubated with the biotin conjugated secondary antibody at a 1:1000 concentration. The ABC reagent was made up 30 minutes prior to use, then incubated with the slides for 30 minutes. The slides were washed 3 times in 1X PBS for 5 minutes each. In order to visualise the antibody ABC complex, DAB solution was made (Vector Laboratories Ltd, Orton Southgate, UK) following the manufacturer's instructions immediately t before use. The slides were incubated with DAB for 10 minutes and were regularly checked throughout the 10 minutes. Once 10 minutes was over or the staining had reached a desired dark brown/black colour the slides were washed in dH_2O and incubated in haematoxylin for 5 minutes to counterstain the sample. Then the slides were washed in dH_2O for 30 seconds and nuclei were blued in alkaline ethanol for 30 seconds. The slides were dehydrated in 70 %, 95 % then 100 % ethanol for 30 seconds each. Finally, the slides were cleared in Histoclear II twice for 5 minutes each Slides were mounted using Omnimount and a coverslip was added. The Omnimount was left to set overnight and then the slides were ready to image under a microscope.

3.8 Transmission Electron Microscopy

After the models were harvested for Electron Microscopy, were fixed in Karnovsky's fixative. In order to so, 8 % PFA was made by mixing 40 % paraformaldehyde with dH_2O. 90 mL dH_2O was added to a conical flask and placed on a heat block in a fume hood with a stirrer and set to 65 °C. next, 8 g PFA was added to the dH_2O and stirred the mixture for 15-20 minutes. Finally, NaOH was added in a dropwise manner until the solution becomes clear.

Material	Quantity
8% Paraformaldehyde	8g
dH_2O	90ml
5M NaOH	Until solution is clear

Table 6. A table to show the proportion of chemicals used to create Karnovskys fixative to fix tissue in preparation for embedding.

To make up Karnovsky, the materials in table 6 were added together and mixed well. The samples were incubated in Karnovsky's for 1 hour at room temperature, the time may vary dependent on the size of the sample. The sample was moved to a falcon tube and washed 3 times for 5 minutes each in 0.1 M Cacodylate Buffer. The 0.1 M cacodylate buffer was removed and the samples were further mixed into a 1:1 ratio of 2 % Osmium tetroxide and 0.2 M Cacodylate Buffer pH 7.4 for one hour at room temperature. Next, the sample was washed in 0.1 M Cacodylate pH 7.6, 3 times for 5 minutes each. At this point, the samples can be stored in the fridge after the final wash until required.

Resin Material	Weight (g)
Agar 100 (epoxy resin	24
DDSA (Hardener)	9
MNA (Hardener)	15
BDMA (Accelerator)	1.4

Table 7. A table to show the proportions of chemicals used to create the embedding resin for TEM

The next stage was to dehydrate the sample. The sample was washed in 50 %, 70 %, 95 % ethanol 3 times for 5 minutes each in ascending order, the EtOH was changed after each wash. Finally, the sample was washed 100 % ethanol 3 times for 10 minutes each. After the model was dehydrated, they need to be infiltrated by resin in preparation to be embedded. An Agar 100Resin kit (Agar Scientific, Stansted, UK) was used. The resin kit was left in the oven 15 minutes prior to use. First, each sample was placed into a glass vial– one sample per vial - with 100 % ethanol and Propylene oxide at a 1:1 ratio. The sample was placed onto a rotator and left for 15 minutes. During this incubation, the resin was prepared by mixing the resin materials shown in table 4 in a fume hood. Next, the sample was infiltrated with propylene oxide. The ethanol:propylene oxide was removed and 2ml propylene oxide added. The sample was returned to the rotator for 15 minutes. Once the resin was ready, the ethanol:propylene oxide was removed and a 1:1 mix of propylene oxide:resin was added to the sample then returned to the rotator for 15 minutes. The Propylene oxide:resin mix was removed and 2 mL of fresh resin was added to each sample and place on the rotator for 1 hour. This step was repeated 3 times. Next, the sample was placed flat in the embedding mould with the smallest point facing the top

and/or bottom of the mould – two samples can fit in one block. The rest of the sample was covered in resin to fill the mould and returned to the oven to set overnight at 65 °C.

Once the resin had set, the samples were removed from the mould and prepared for imaging. A Leica Ultratrim was used in accordance with manufacturer's instructions (Leica Biotechnologies) in order to trim the block down to an appropriate size. The size of the block is dependent on sample size and grid size/number of sections per grid. Once the block is trimmed to size, it was mounted onto a Leica UC6 Ultramicrotome. The manufacturer's instructions were followed and sections cut from the block. Once the sample was mounted onto copper grids coated in formvar, it was stained according to the following protocol in order to highlight the intracellular structures. Following staining and drying, samples were ready to be imaged under the H7600 Transmission Electron Microscope (TEM).

3.9 Melanocyte:keratinocyte ratio

Slides were stained against S100 (Abcam, Cambridge, UK) melanocyte marker and imaged as stated in immunohistochemistry section – a 1:1000 concentration of primary antibody was used. Once the slides had been stained, two images were taken randomly from each wax section of the model – totalling 10 images per condition - at 20x magnification. After selecting images of the models at random, all cell populations in the epidermal layer were counted manually in ImageJ. Melanocytes were distinguished by their dark brown/black staining and dendritic morphology in the *Basale* layer of the epidermis. Whilst keratinocytes were distinguished by a columnar morphology stained blue from the haematoxylin counter stain. After the cell populations were counted, the final ratio was determined by dividing keratinocyte and melanocyte numbers and finding an average.

3.10 Melanin quantification through ImageJ

The protocol for this analysis was taken from Billings et al 2015. Six Images per condition were uploaded into GIMP image – GNU image manipulation software. Once the images were open, the tool 'select by colour' was selected. This allows pixels matching the selected pixel in colour to be highlighted. Multiple pixel corresponding to shades of melanin stain were selected using shift + left click. Once all the stained pixels were highlighted, the resulting area was copied (control + C) and pasted into a new black image file (control + V) by selecting open and new from the drop-down menu. The new image was saved containing only the highlighted pixels that correspond to melanin staining. The new image was opened in ImageJ and analysed using the histogram tool. This will bring up a graph with two peaks. The melanin colouration peaked around 0-100 in pixel value. The sum of the number of pixels in this range was used as the way of quantifying the amount of melanin in each image.

Primary antibody	Supplier	Product code	Dilution	Species raised in	Technique
S100	Abcam	Ab14849	1:100	Mouse	IHC
GP100	Abcam	Ab137078	1:1000	Rabbit	IF

Table 8. A table to show primary antibodies used and information about the antibody

Secondary antibody	Supplier	Product code	Species	Conjugated
Anti-Mouse secondary	Fischer Scientific	31430	Donkey	HRP
Anti-Rabbit secondary	Fischer Scientific	A32766	Donkey	Alexa-fluor 488

Table 9. A table to show secondary antibodies used and information about the antibody
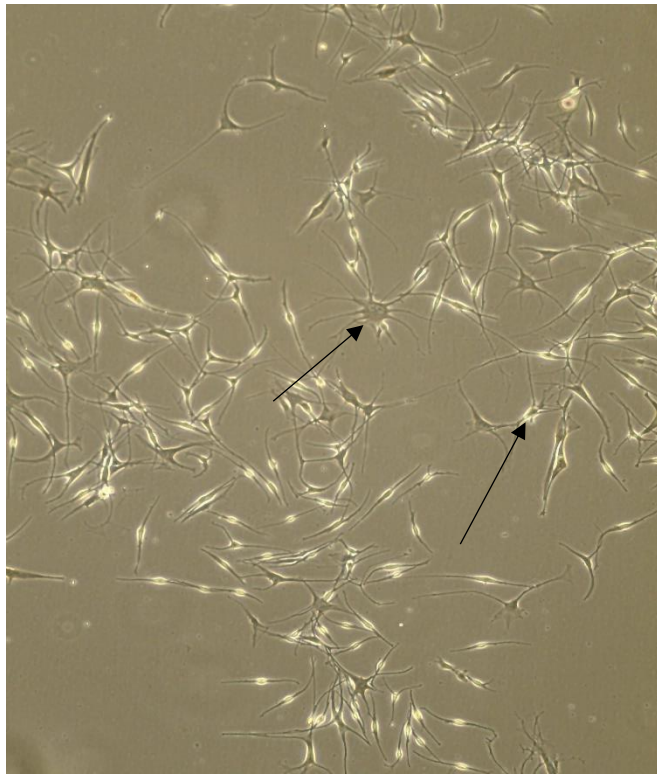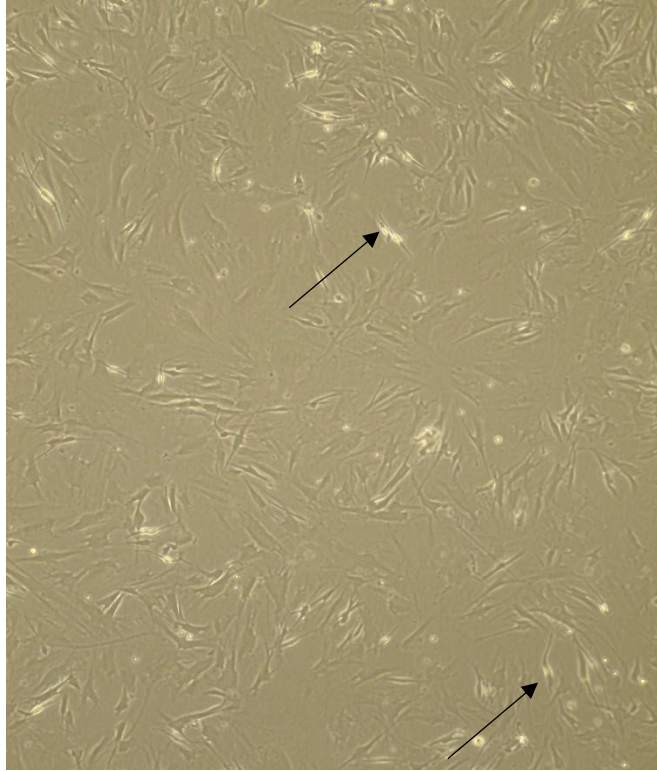
#650 #106

Figure 14. Characterisation of HEMn cells from different ethnic donors under the light microscope.

A comparison was drawn between HEMn cells #650 and #106 under the light microscope after 7 days in culture. A big visible difference using the light microscope was the amount of light that was passing through the HEMn cells. There is a visible outline around the body of the HEMn cell which is attributable to light not being able to pass through the melanin packed cell. Whilst the halo of light is visible in #106 condition, there are fewer and they are to a lesser intensity. The other difference is clear increase in the dendricity of the #650 melanocytes, which is highlighted by the arrows in the #650 image. This is possibly due to 2D culture conditions, however, the #650 HEMn cells seem to have an improved phenotype compared to #106
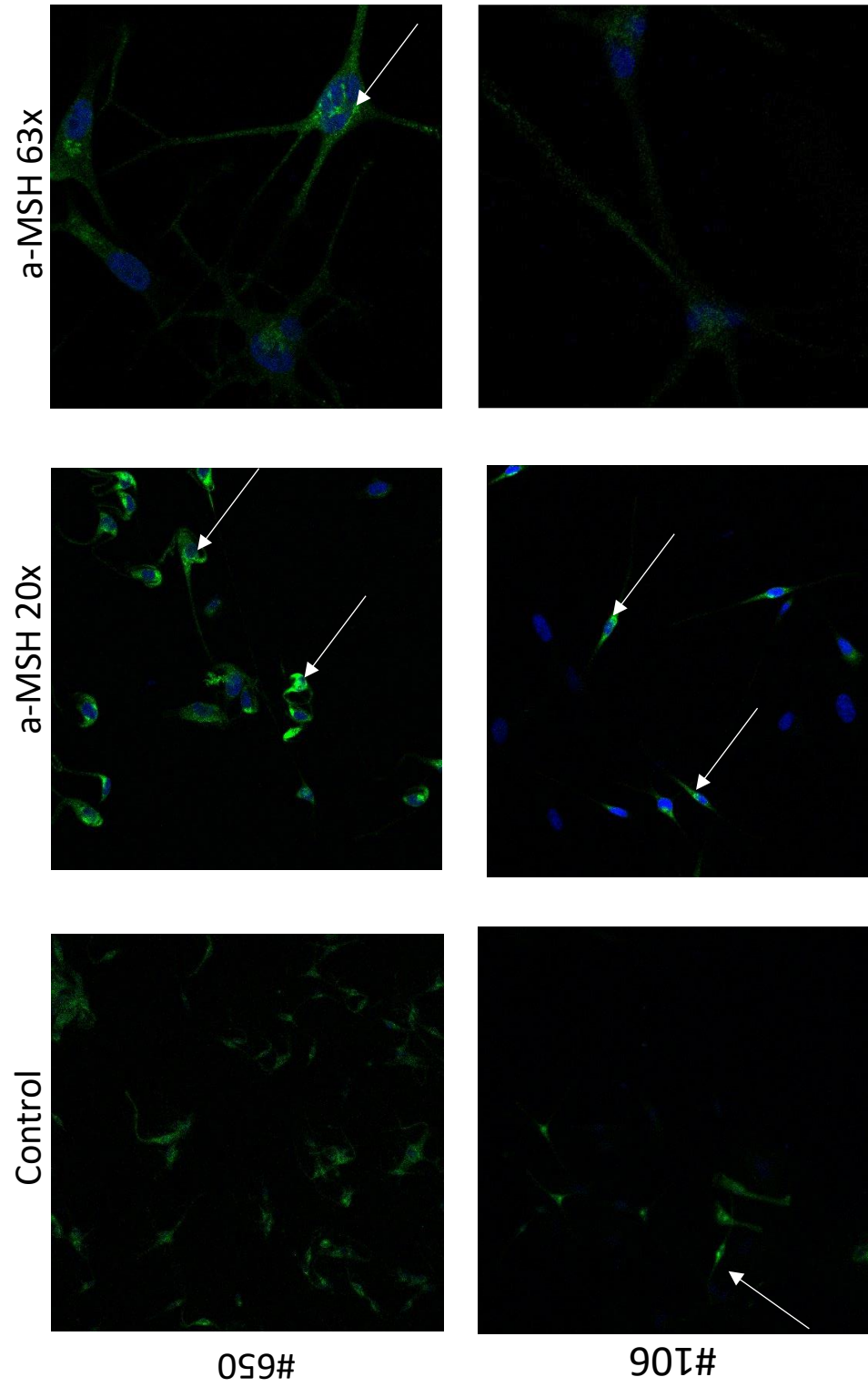
Figure 15 Immunofluorescence against GP100 for characterisation of HEMn cells cultured with a-MSH.

Cells were grown for seven days then incubated with a-MSH at 0.5ug/ml for 24 hours and stained using GP100 primary antibody, an early melanosome marker at 1:100 dilution. The control condition for both #650 and #106 show the base level of fluorescence from this antibody at this dilution level. There appears to be a slight difference in the number of cells in #106 cell type that have the same intensity of fluorescence as #650 cell type. The white arrow in the control #106 show the few HEMn cells that have the level of fluorescence seen in most of #650 HEMn cells. Once the HEMn cells are incubated with a-MSH for 24 hours, the intensity of the fluorescence significantly increase in both cell types. There is a
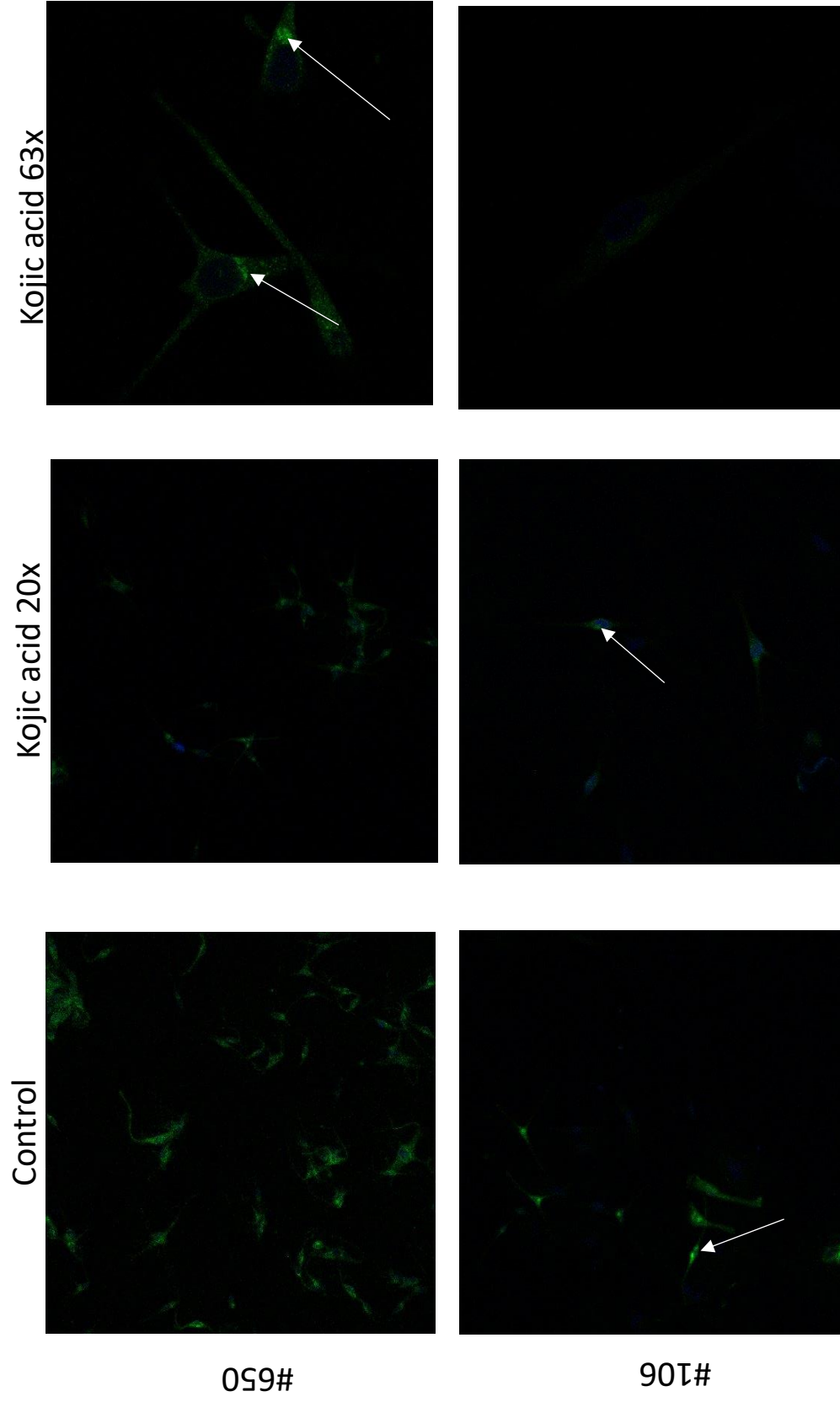
Figure 16 Immunofluorescence against GP100 for characterisation of HEMn cells cultured with Kojic acid.

Cells were grown for seven days then incubated with Kojic acid at 50ug/ml for 24 hours. Cells were stained against GP100, an early melanosome marker at 1:100 primary antibody dilution. Both donor HEMn cells show a response to Kojic acid, with a visible reduction in the strength of the fluorescence. It is clear from both the 20x and 63x magnification that #106 HEMn cells had the lowest fluorescent signal, after treatment with Kojic acid when compared to the control and #650 HEMn cells. In the 63x magnification of #650 HEMn cells a concentration of melanosomes near the nucleus, attributable to the location of endoplasmic reticulum where the process of melanosome synthesis begins in the. This is visible in the #107 HEMn cells to a lesser extent.

4. Results

The initial aim of this thesis was to develop a pigmented skin model with both an epidermal and full thickness model to be used for commercial and academic use. After noticing difference in pigmentation of the epidermal and full thickness models, it became obvious it was important to characterise the models and compare them to human skin. To characterise the models, human skin was used as a base comparison in order to examine how the generated skin equivalents performed. A number of stains were used to highlight structural similarities and differences. Furthermore, a number of analytical methods were used to look further into structural characteristics when compared with human skin. This allowed any observations seen in the images to be back up by quantifiable data. The first stain that was used was H&E stain, this is a non-specific stain that can highlight various structural aspects of skin without being melanocyte specific. Following the H&E staining, more specific melanin and melanocyte stains were used to examine the viability of HEMn cells within the model. Images collected from these stains were used to quantify different aspects the models against human skin. Furthermore, models were examined at a molecular level through transmission electron microscopy, which gave an in-depth view of the cells in the model compared to human skin.

4.1 Characterisation of neonatal human melanocytes

To identify and characterise differences between HEMn cells from that came from donors with different skin tones, cells purchased from Fischer Scientific were first cultured in 2D before use in the 3D models. The resulting cells were fixed and imaged through light microscopy and fluorescence microscopy. Figure 14 shows a side-by-side comparison of HEMn cells from light and dark pigmented donors. The most distinct feature was the level of pigmentation that is observable even under the light microscope at 20x magnification. The HEMn cells from the dark pigmented donors had a significantly darker colour than the light pigmented HEMn cells. The outline of the dark skinned HEMn cells is more distinguished from the background, unlike the light pigmented HEMn cells, which are less defined against the backdrop. Furthermore, the dark skinned HEMn cells have increased dendricity compared to light pigmented donor cells. Both images were of HEMn cells grown for 7 days. The confluency of the light pigmented HEMn cells were closer to 100% than that of the dark pigmented donor cells. This suggests that the light pigmented cells grow quicker in culture than dark skin donor.

The immunofluorescence in Figure 15 and 16 looks at the response of HEMn cells in 2D culture to pigment altering agents. The primary antibody was against GP100, a marker of early melanosomes, usually localised around the endoplasmic reticulum. Figure 15, shows the response of these cells to a-MSH at 0.5ug/ml for 48hrs compared to the control. The dark skinned HEMn cells have a significantly stronger signal than light pigmented HEMn cells. The fluorescents in both cell types showed an increase when compared to the control images.
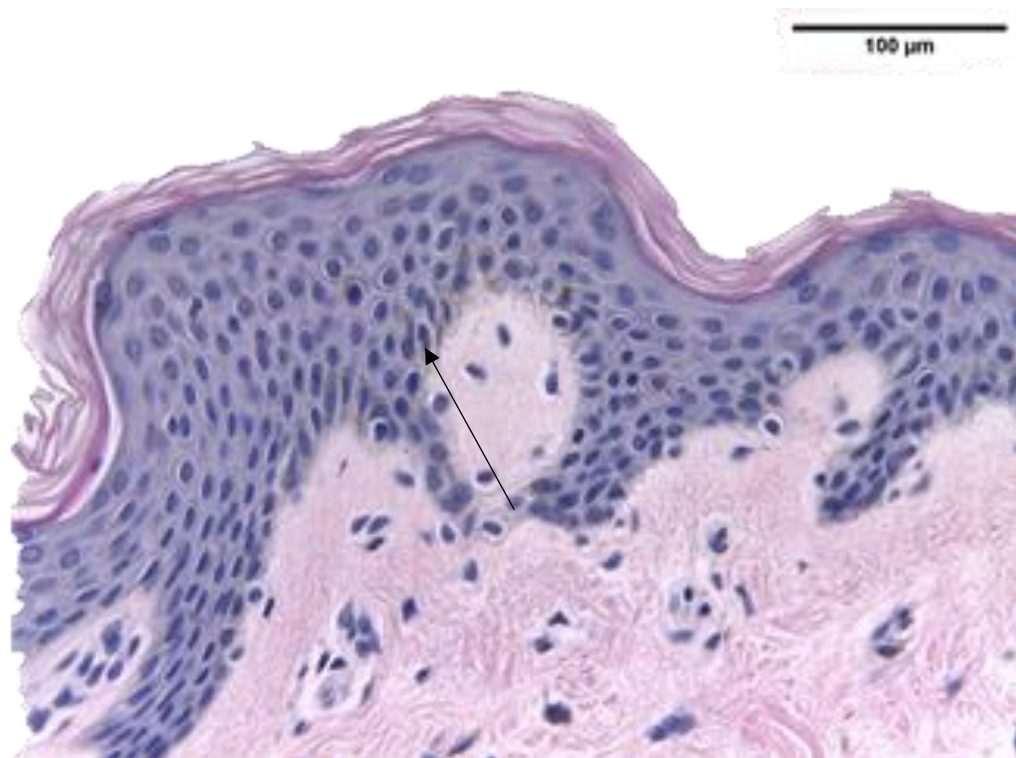

Figure 17. Histological analysis of human skin.

Punch biopsies from human skin were taken and stained with H&E stain. This stain shows the general structure of tissue. It highlights the four different layers seen in the epidermis, with columnar cells seen in the basal layer of the epidermis. As the cells move up through the layers the become flatter and become corneocytes, seen by the outer layers which stain pink at the top of the epidermis. There is evidence of melanin highlighted by the arrow. This is seen by patches of darker staining inside keratinocytes residing in the Stratum *Basale*. The underlying dermal layer, seen at the dermal-epidermal junction. This section is packed full of proteins seen by the pink area with nuclei of the dermal fibroblasts seen in blue.

Epidermal equivalent
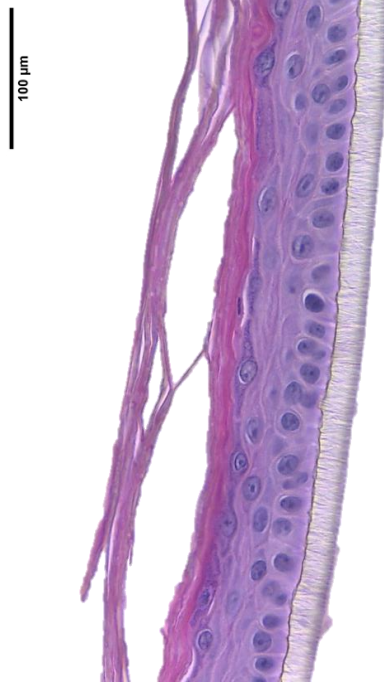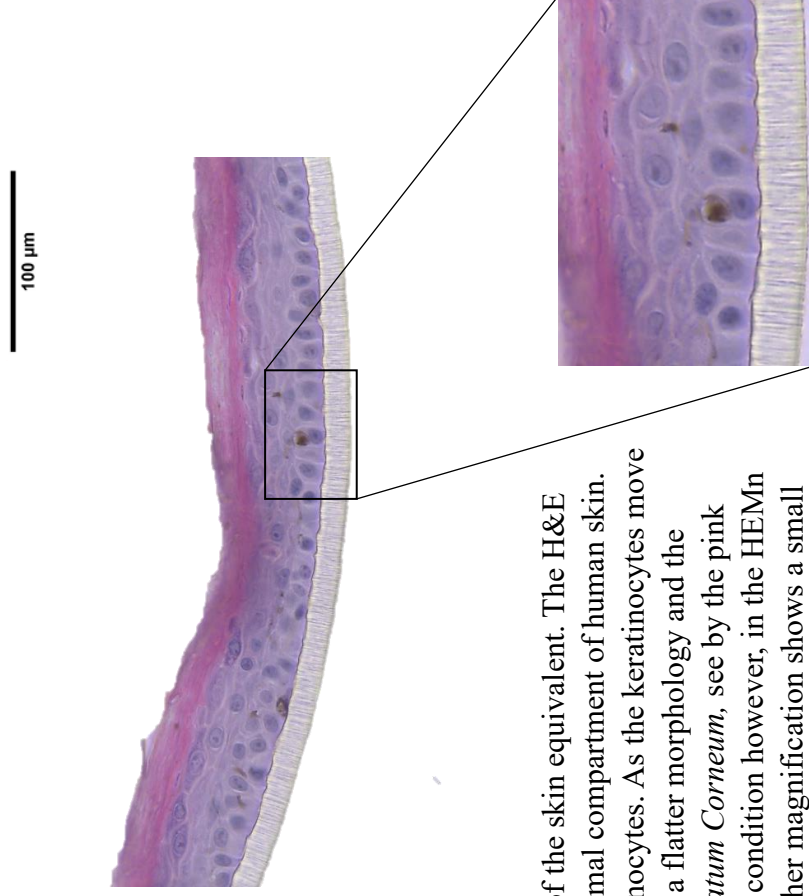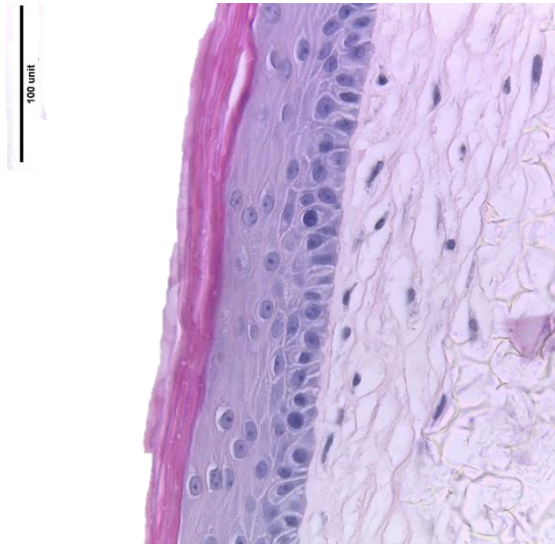
Epidermal equivalent HEMn

Figure 18. H&E analysis of the epidermal model.

Sections of epidermal model were H&E stained to show the general structure of the skin equivalent. The H&E analysis highlights the similarities between the epidermal model and the epidermal compartment of human skin. We see 4 distinct layers in the model and columnar morphology of basal keratinocytes. As the keratinocytes move up through the four layers, they begin to specialise into corneocytes, they have a flatter morphology and the number nuclei seen in these upper layers starts to reduce and they form the *Stratum Corneum*, see by the pink layers of corneocytes. These features are visible in both the control and HEMn condition however, in the HEMn condition we can see evidence of melanocytes. The area highlighted with a higher magnification shows a small patch of brown colouration that isn't attributable to the H&E stain but is likely a section of a melanocyte packed with melanin.

Full thickness HEMn

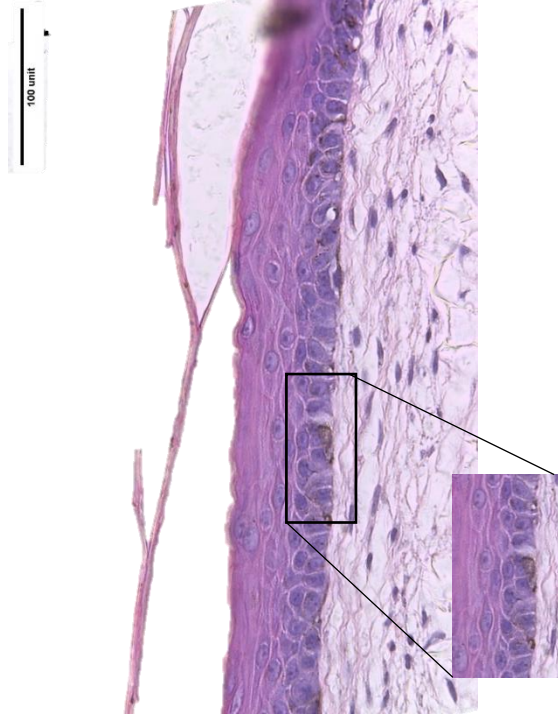Full thickness control

100 unit

100 unit

Figure 19. H&E analysis of the full thickness model.

Sections of epidermal model were H&E stained to show the general structure of the skin equivalent. This image shows the similarities between the full thickness model and human skin. We see an established dermis at the bottom with HDFn producing ECM that stain pink with a purple nucleus. These HDFn cells have populated the Alvetex polystyrene insert and produced ECM proteins. The epidermis shows four distinct layers, as seen in human skin. There are columnar cells in the *Stratum Basale* with cells specialising into corneocytes that make up the outer cornified top layer that is stained pink at the top of the model. At a higher magnification we can see the highlighted area shows a cell that is stained darker likely due to a concentration of melanin pigment in what is potentially a HEMn cell.

Furthermore, Figure 15 shows HEMn cells after 48hr incubation with kojic acid at 50mg/ml in 2D culture. From the images, it shows a decrease in fluorescence in the both cell types,
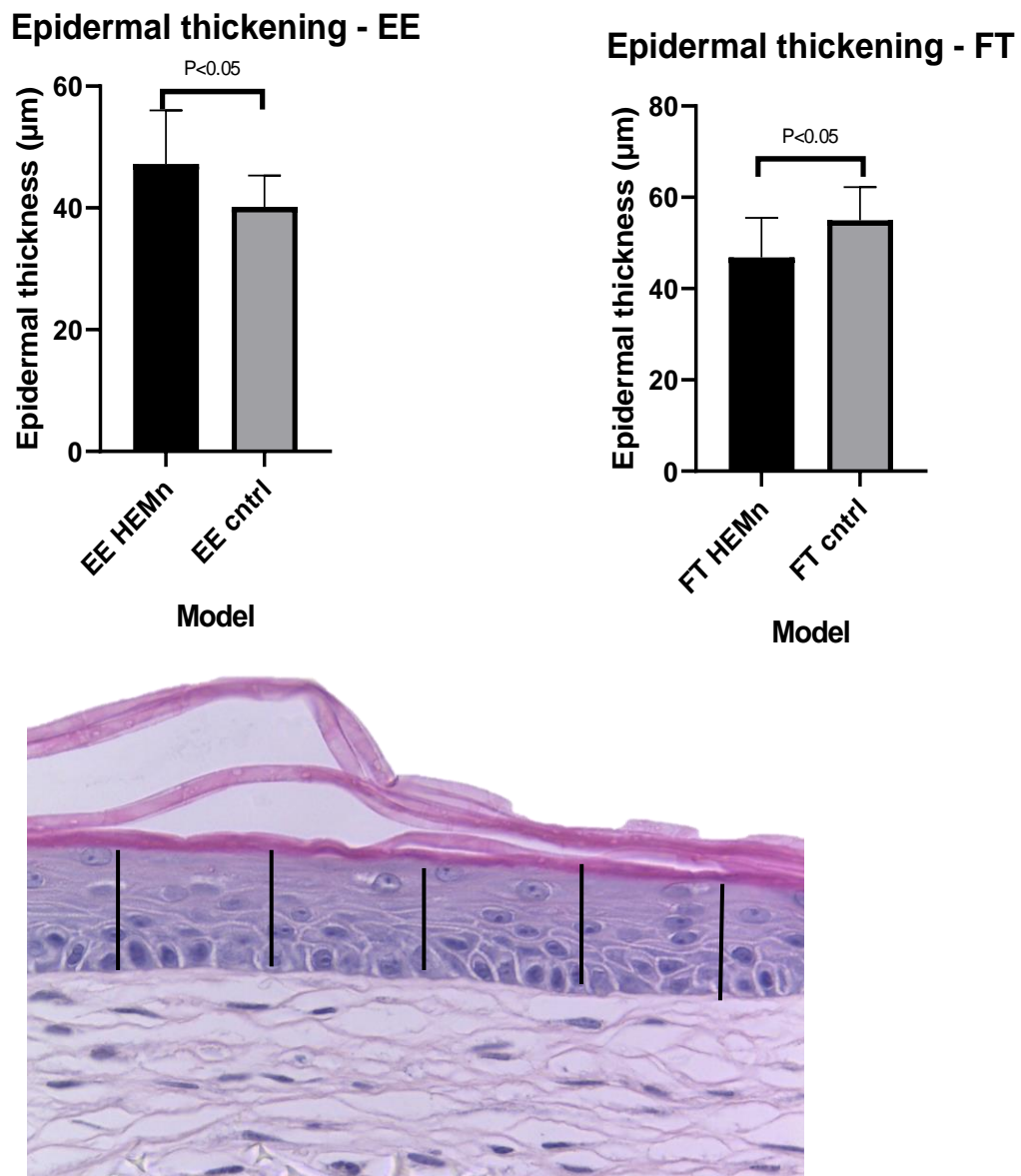

Figure 20. Quantification of epidermal thickness before and after the addition of melanocytes.

The thickness of the epidermis minus the *Stratum Corneum* was measured in ImageJ by analysing the thickness of the living section of the epidermis. Five points along a 40x magnification image of H&E stain skin were taken at random. The average of the measurements was taken across a range of images. In both the epidermal equivalent and full thickness model, there is a significant difference between the HEMn when compared to the control. However, this result, whilst statistically significant, offers a confusing look at the epidermal thickness in epidermal and full thickness models. There is epidermal thickening in the case of the epidermal equivalent, however, the full thickness model shows epidermal thinning when HEMn cells are introduced. Therefore, further repeats of this are required to for further clarification.

compared to their respective controls. Further to this, dark skinned donor HEMn cells show an even greater reduction in fluorescent signal when the two cell types were compared. Both the a-MSH and Kojic acid conditions suggest that HEMn cells form dark skinned donors had a greater propensity to respond to pigment altering compounds.
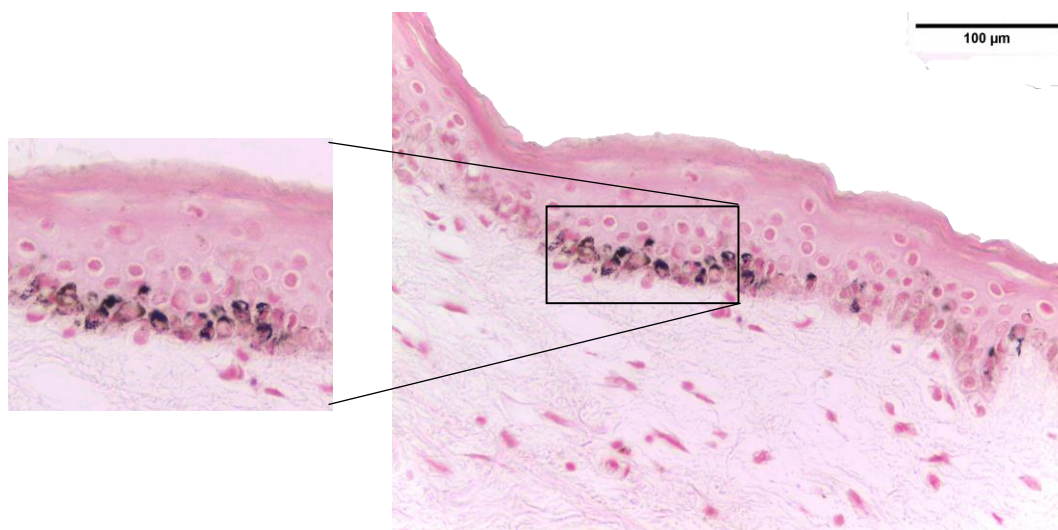

Figure 21. Observation of melanin content in human skin by Fontana Masson stain.

Punch biopsies of human skin were stained following the Fontana Masson protocol in section 3.4. This specific melanin stain shows the high level of melanin content found in melanocytes and keratinocytes in the *Stratum Basal* of human skin. The melanin can also be seen forming supranuclear caps, intended to protect the nucleus against UVR. The melanin is localised to the *Stratum Basal* with minimal black/brown staining seen in the next epidermal layer with no visible staining in the top layers of the epidermis.

4.2 Incorporation of Melanocytes into the epidermal equivalent

The first step for developing the pigmented skin equivalent was to introduce melanocytes into the epidermal model. This was achieved by including HEMn cells into the HEKn cell suspension at a ratio of 1:10 (Cichorek et al 2013). These models were grown submerged for two days then raised to the ALI for two weeks. The histology was performed on these models to examine the general structure of the model, this can see in Figure 18. The H&E analysis revealed that the melanocytes have organised themselves into the basement, highlighted by the higher magnification section of the image, with two visible melanocytes with a darker cell body than the surrounding keratinocytes. There are also visible dendrites extending through the keratinocytes either side of these HEMn cells which can be seen as thin dark   projections   around

Epidermal equivalent control

Epidermal equivalent HEMn
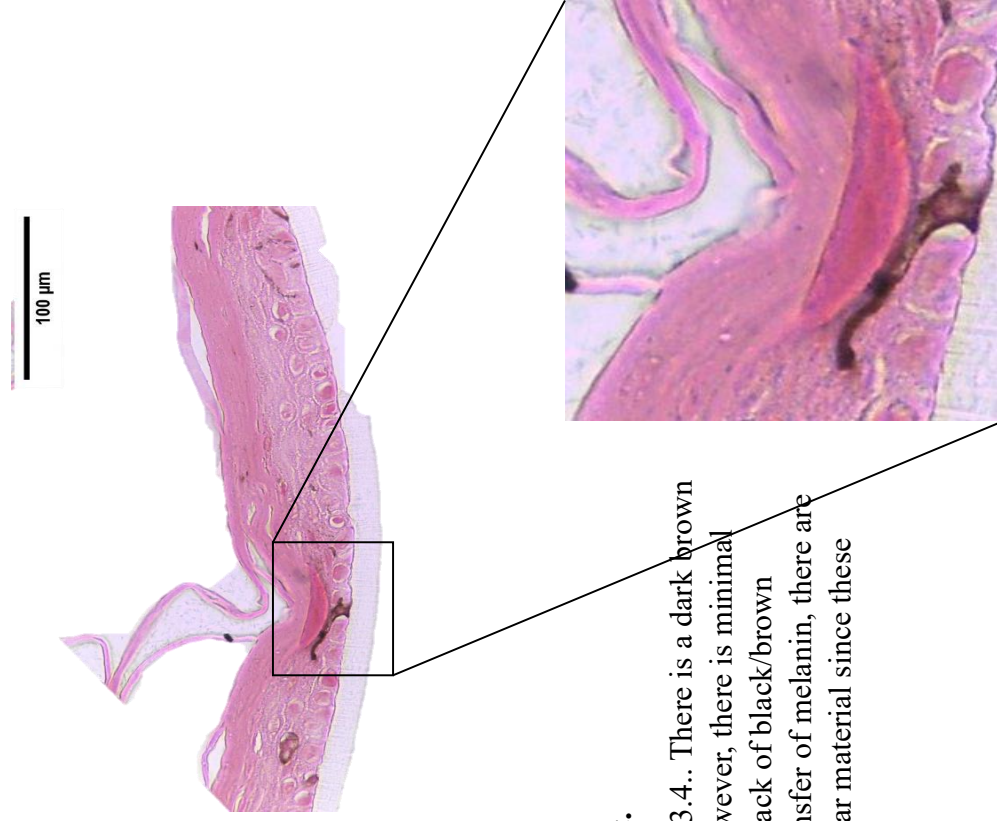
Figure 22. Melanin specific Fontana Masson stain of the epidermal equivalent.

Epidermal models were stained following the Fontana Masson protocol in section 3.4.. There is a dark brown staining of melanin in the HEMn cell found in the condition with HEMn cells. However, there is minimal melanin transfer in the epidermal model when compared to human skin seen by a lack of black/brown staining in the HEKn cells in the *Stratum Basal*. Furthermore, since there is no transfer of melanin, there are no distinct supranuclear caps. This is a crucial function of melanin to protect nuclear material since these aren't forming, the pigmentation functioning properly in the epidermal model.

Full thickness HEMn
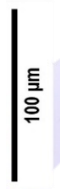
Full thickness control
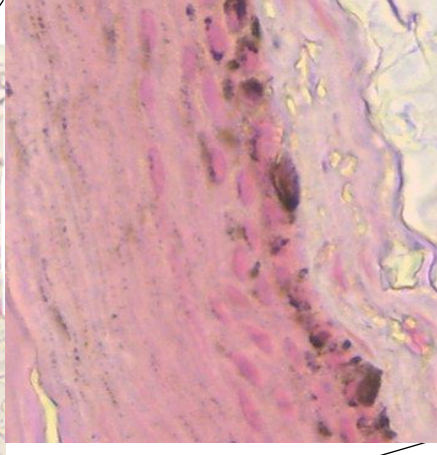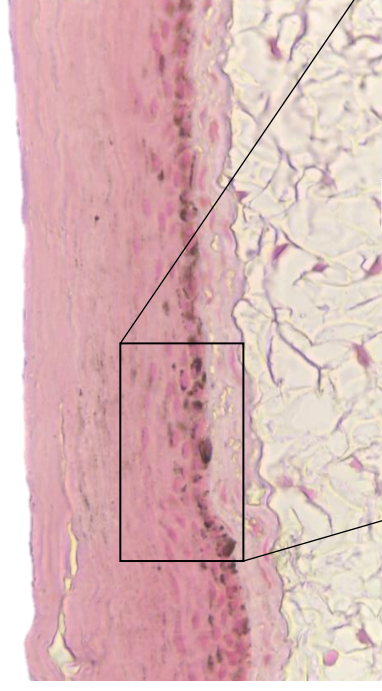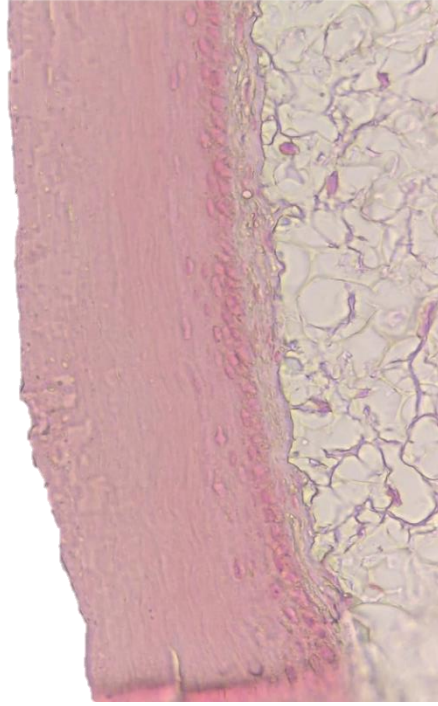
Figure 23. Fontana Masson staining of the full thickness model with and without HEMn cells.

Full thickness models were stained following the fontana Masson protocol in section 3.4. The control model has no black/brown staining in any area of the epidermal model. The full thickness model shows the expected staining pattern. Black/brown patches of melanin can be seen throughout the *Stratum Basal*, with some staining continuing into the next layer of the epidermis. An important aspect of melanosomes is to form a supranuclear cap, this is clearly visible in the higher magnification section of the *Stratum Basal*. This melanin localisation exists in the majority of HEKn cells in the models.

the HEKn cells. In the H&E stain it was difficult to see any evidence of the melanin transfer to the keratinocytes in the basal layer. The general structure of the model had not changed in comparison with the control model. There is clear specialisation of the keratinocytes as they move through the four layers of the epidermis and become a stratified outer layer. In the epidermal model, there was a visible change in the thickness of the epidermis, whilst the *Stratum Corneum* looks to be of similar thickness, the previous layers, minus the *Stratum Basale,* seem to have more layers of cells residing in them.
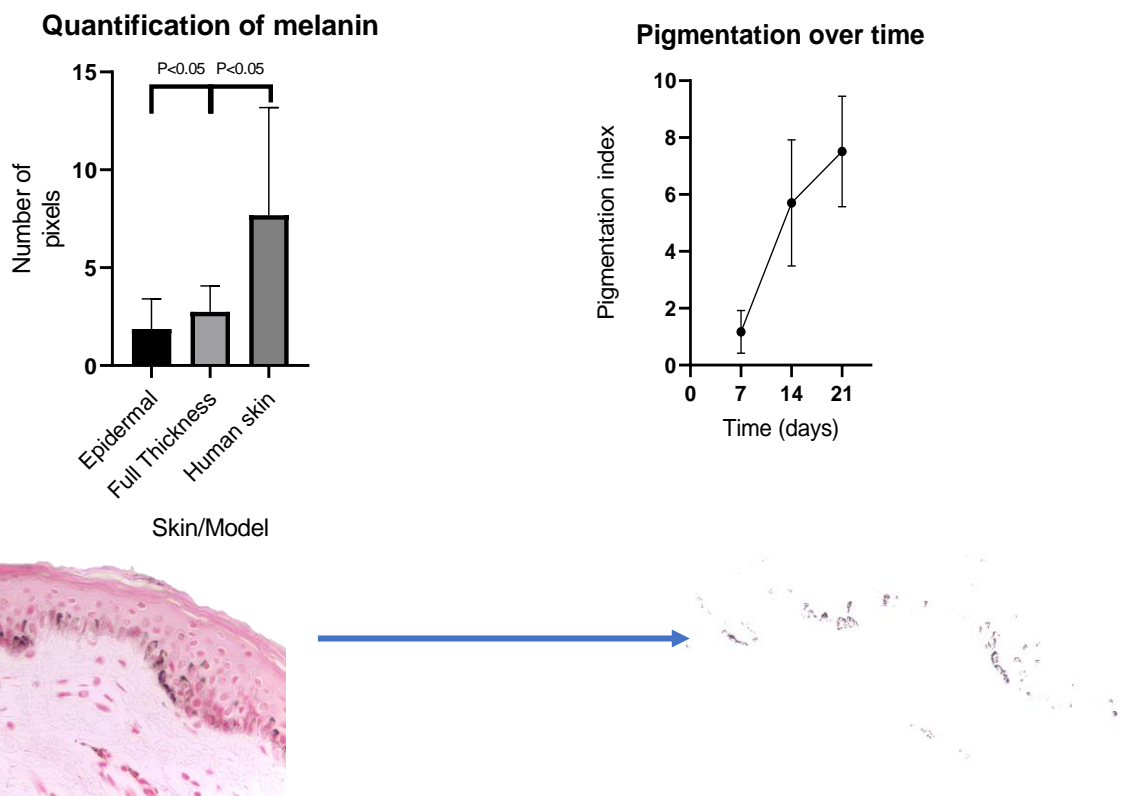
Figure 24. Quantification of melanin content by pixel count shows more melanin in the full thickness than the epidermal model.

To quantify the observations seen in the sections of the models, two melanin specific bioanalytic's were performed. Pixels corresponding to melanin stain were isolated and analysed with ImageJ's histogram tool. Quantification of total melanin content per section shows the highest level of pigmentation in human skin samples. However, the full thickness model performs favourably when compared to the epidermal model. When pigmentation was tracked over time, it is clear at 7 days that pigmentation is still developing in the models. However, once the models reach 14 days there is a significant increase in melanin content per section compared to 7 days. There is slight increase between 14 and 21 days but melanin production levels out after 14 days.

4.3 Incorporation of HEMn cells into a more complex full thickness model

After the melanocytes were incorporated into the epidermal model and observed them functioning inside the model, the focus was shifted towards incorporating HEMn cells into the full thickness model seen in Figure 19. This was achieved again by adding HEMn cells into the HEKn cell suspension and seeding them onto the dermal compartments. Again, the HEMn cells organised themselves to the basal layer and were producing a visible amount of melanin, seen by the darker staining of the HEMn cell body compared to the surrounding HEKn cells. The dendrites can be seen extending out of the body along the dermal-epidermal junction. Interestingly there are visible small areas of dark brown staining that can attributed to melanin content in the HEKn cells. The general structure of the epidermis in the full thickness model looks good, with the four distinct layers and a stratified outer layer. The epidermis looks to be thicker than the epidermal equivalents, however, the thickness of the epidermis of HEMn
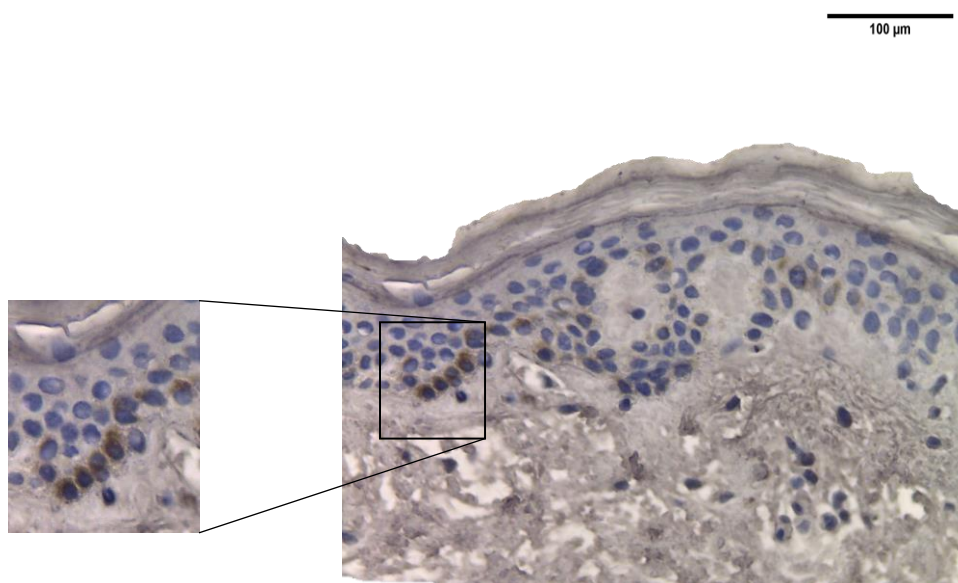
Figure 25. S100 staining of human skin highlighting the location of melanocytes in the *Stratum Basal*.

Human tissue was stained against S100 melanocyte marker by following immunohistochemistry protocol found in section with a 1:1000 primary antibody dilution. This is a neural crest marker which binds to melanocytes and langerhan cells in skin, the former residing in the *Stratum Basal*. The brown staining seen in the higher magnification points to the location of HEMn cells in the epidermis, which is the most obvious staining of a melanocyte in this image. There are a number of other faintly stained areas along the *Stratum Basal.*

conditions appears thinner than the control. There is a visible layer of HDFn cells below the epidermis and there are signs they have invaded into the Alvetex®.

Figure 17 shows a H&E analysis of human skin, taken from donor punch biopsies. This was used as a comparison for the models to try and replicate this as closely as possible. Both models show a strong resemblance to human skin, with the clear four layers of the epidermis visible and for the full thickness model, visible HDFn cells residing underneath the epidermis. Furthermore, the pigmentation is visible in the *Stratum* Basale of human skin, which can also be seen in the full thickness model, to a lesser extent. However, there are visible differences between the models and human skin. There is variation in the thickness of the epidermis along the image of human skin with visible rete ridges.

To quantify the observations about thickness and potentially health of the epidermis in both models, an average measurement of the epidermal thickness was taken. In Figure 19, an average measurements per image is shown in the graphs. When comparing the effects of HEMs cells on the epidermal thickness there are not any significant difference between the control and HEMn condition. In the full thickness model, slight epidermal thinning with HEMn cells was observed, whereas, in the epidermal model a slight epidermal thickening was observed. When

Epidermal equivalent control

Epidermal equivalent HEMn

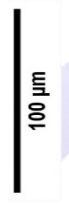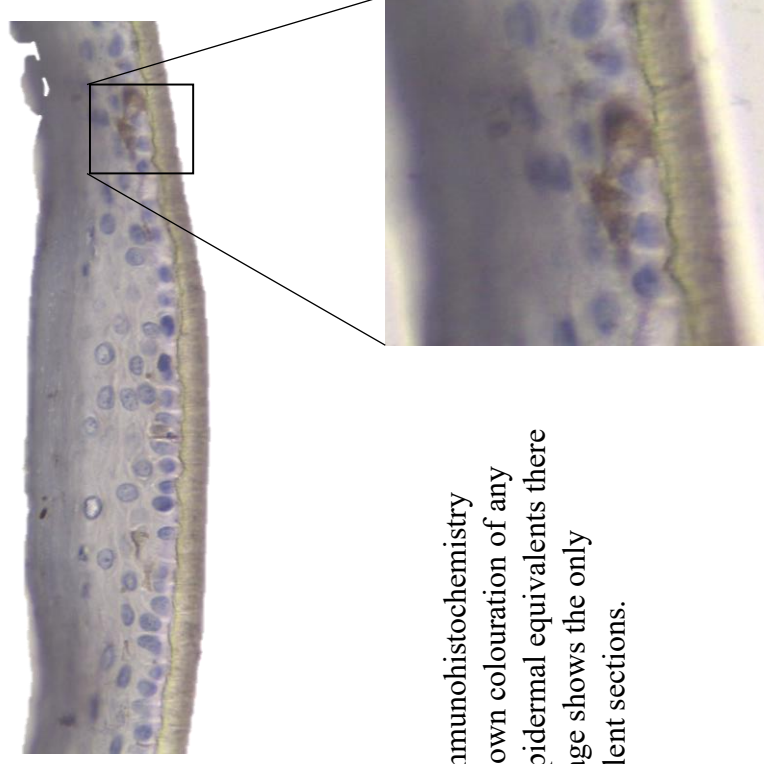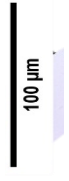**Figure 26. staining for S100 melanocyte marker in the epidermal model.**

The epidermal model was stained against S100 melanocyte marker by following immunohistochemistry protocol found in section with a 1:1000 primary antibody dilution… There is no brown colouration of any cells in the *Stratum Basal* of the control condition. In the HEMn condition of the epidermal equivalents there is some minor staining of HEMn cells. The higher magnification section of the image shows the only obvious staining in this image. This was indicative of the stained epidermal equivalent sections.

Full thickness control
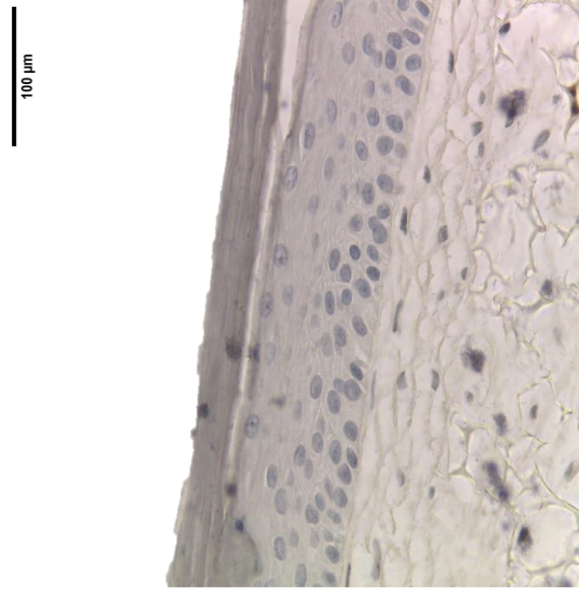
Full thickness HEMn
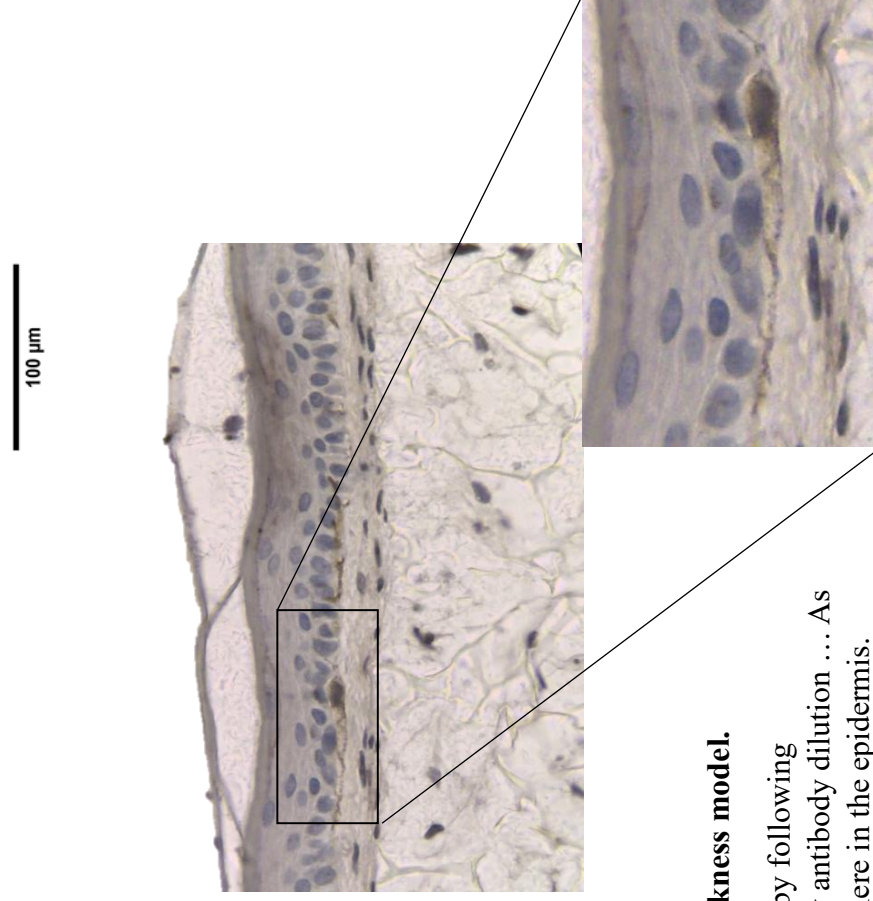
Figure 27. Staining against S100 melanocyte marker in the full thickness model.

The full thickness model was stained against S100 melanocyte marker by following immunohistochemistry protocol found in section with a 1:1000 primary antibody dilution …. As expected, the full thickness control model has no brown staining anywhere in the epidermis. However, The HEMn condition there is one distinct HEMn cell with the dendrites visible in the model. The HEMn cell in the magnified section shows its location in the *Stratum Basal* with the dendrites extending out of both sides of cell, reaching halfway across the model and able to interact with the HDFn dermal cells.

No. of Keratinocytes

(bar chart: y-axis 0, 50, 100, 150; categories: Epidermal, Full thickness, Human skin)

No. of Melanocytes

(bar chart: y-axis 0, 5, 10, 15; categories: Epidermal, Full thickness, Human skin)

HEKn:HEMn ratio

(bar chart: y-axis "Ratio of HEKn:HEMn" 0, 5, 10, 15, 20, 25; categories: Epidermal, Full thickness, Human skin; P<0.05 P<0.05)
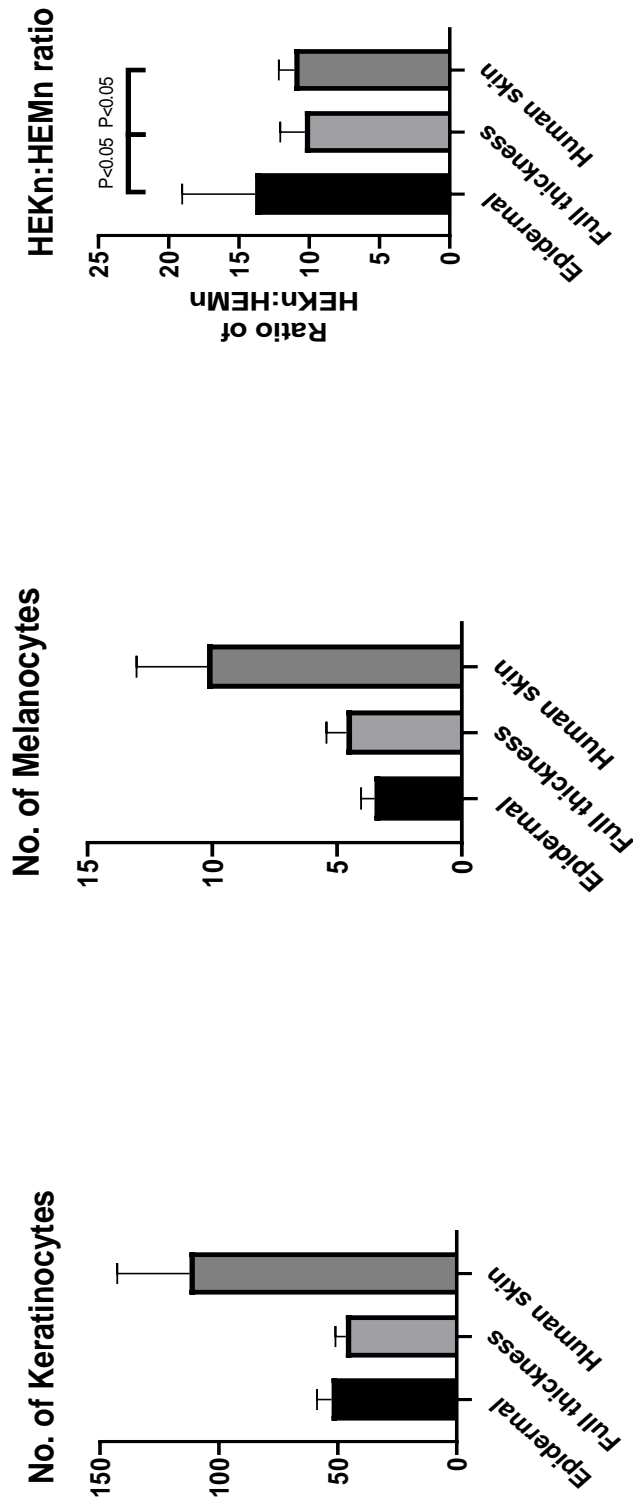
Figure 28. A quantificational analysis of the cell populations in the epidermal model, full thickness model and human skin.

Slides were stained against S100 antibody using immunohistochemical analysis. There was no significant difference on a unpaired t-test at p value 0.05. A) Shows the average number of keratinocytes to show that a change in ratio was due to a change in melanocyte number. B) shows the average number of melanocytes C) shows the ratio of melanocytes to keratinocytes when the average number of melanocytes was divided by average number of keratinocytes. D) A section of a full thickness equivalent with immunohistochemistry S100 primary antibody stain at a 1:1000 dilution concentration with haemotoxylin counter stain. There is a slight increase in the ratio of HEKn:HEMn cells. This suggests that there is a reduction in the number of melanocytes in the model compared to the seeding density.
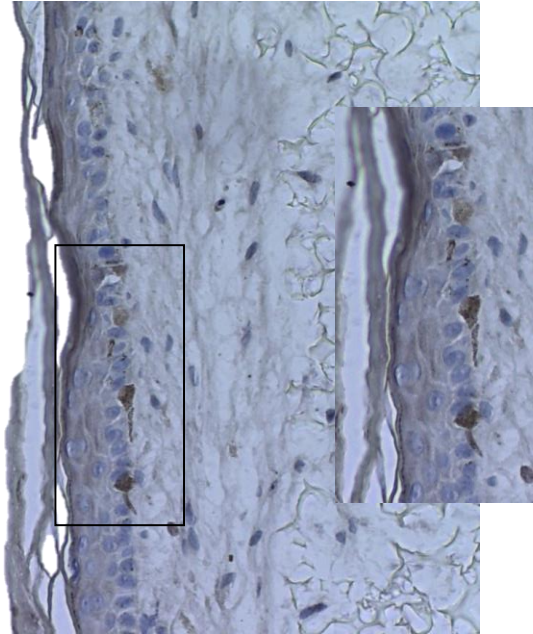
comparing the epidermal thickness across the two model types, it is worth noting that the condition with the HEMn cells were fairly close in thickness. However, the control condition in the full thickness model was much thicker than the epidermal model. The HEMn conditions have a thickness of roughly 40um whereas, the epidermal control was just below at 38-39um. The full thickness control is much larger, this condition has an epidermal thickness around 55um.

4.4 The full thickness model shows higher HEKn melanin content than the epidermal model

Once the HEMn cells were successfully introduced into both of the skin models and the structure was verified, the next step was to observe the functionality of the HEMn cells and melanin production. In order to visualise the melanin inside the models, wax sections were stained using the Fontana Masson protocol, which stains melanosomes brown/black.

The epidermal models show that there is limited melanin transfer occurring inside these models. The images in Figure 21 show that there was melanin being produced inside the HEMn cells. The section of the image in higher magnification shows a HEMn cell packed melanin and had stained dark brown throughout the cell. There were some small patches of brown staining along the *Stratum Basale,* however, this is minimal and there was no observable supranuclear caps. There was no visible black or brown staining in the control model. The full thickness model had a visibly different staining pattern to the epidermal models seen in Figure 22. Throughout the *Stratum Basale* there was dark brown and black staining in the packed inside HEKn cells. The melanosomes have also formed supranuclear caps, a crucial aspect to the function of melanosomes. There is no visible black or brown staining in the control model without HEMn cells.

Figure 20, shows the Fontana Masson staining of human skin. This image is included as a comparison and the desired aim for the melanin content and melanosome location in the skin equivalent models. There are clear examples of HEKn cells packed with melanin forming supranuclear caps in the *Stratum Basale*. Clearly the epidermal model did not match this staining pattern, however, the full thickness model seemed to show melanin content much closer to that of human skin.

To quantify these observations, the number of pixels per 40x magnification image were quantified in ImageJ. Figure 23, showed the number of pixels that fall within in the colour range attributable to melanin when highlighted using GIMP image manipulation software. The epidermal models showed the least melanin per 40x magnification image. Whereas the full

64

thickness model and human skin showing a statistically significant increase in the amount of melanin in a 40x image.

Human Tissue   Full Thickness Model
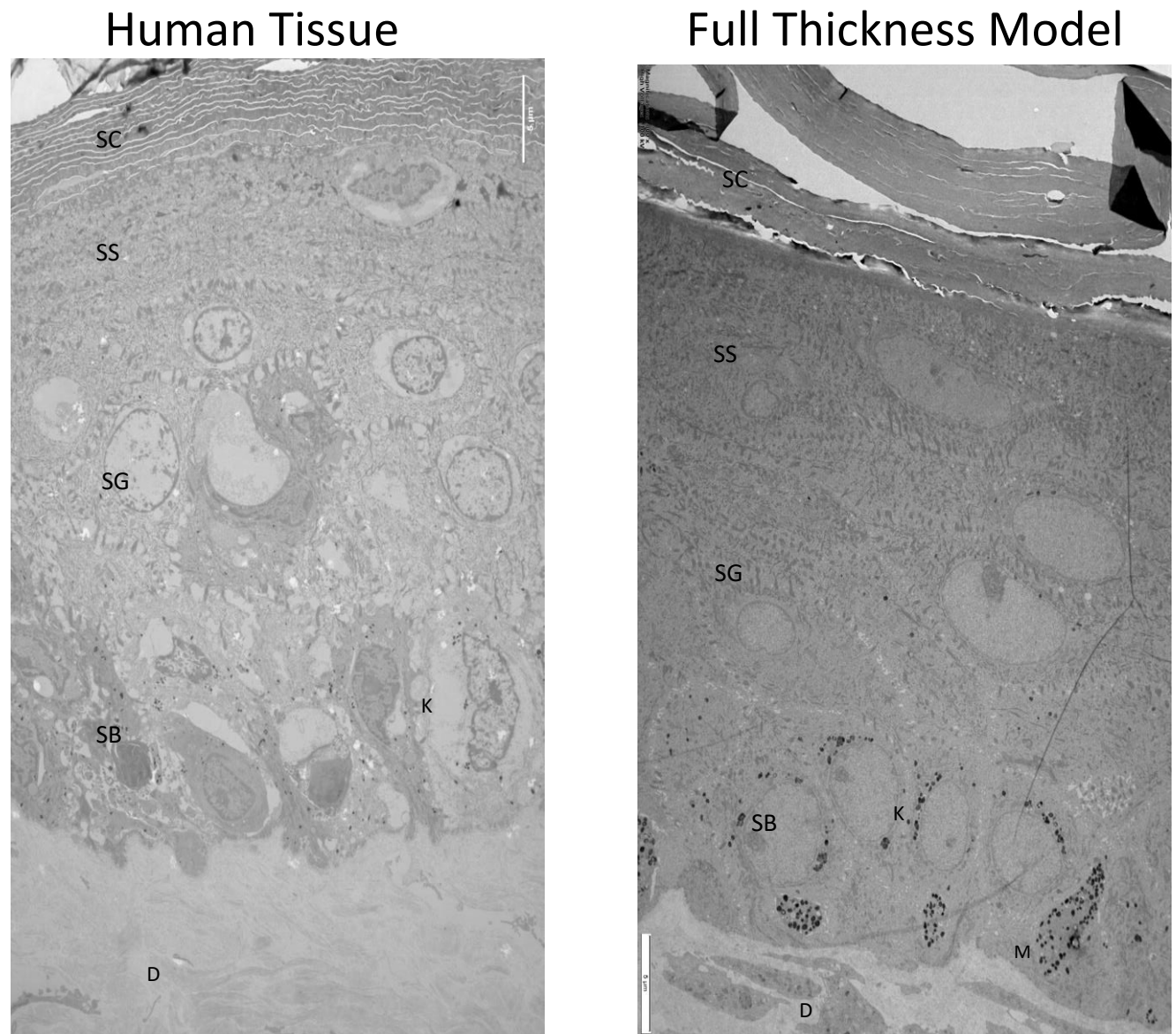
Figure 29. A comparison of human tissue and full thickness model under the transmission electron microscope.

Human Tissue was taken as a punch biopsy from human donors. Samples were fixed in Karnovsky's fixative immediately upon arrival. At a cellular level we can see the similarities between human skin and the full thickness model. There are four distinct layers in the epidermis and at the top, there is noteable layers of cornified cells acting as a protective barrier. In the full thickness model, there are a number of keratinocytes with melanosomes in forming the ypical supranuclear cap. There is also a visible melanocyte dendrite projection, highlighted by the M in the bottom right of the image. In the human skin, there are signs of tissue degradation with membrane shrinkage and breakdown of nucleus.

Legend: D – Dermis, E – Epidermis, M – Melanocyte, K – Keratinocyte
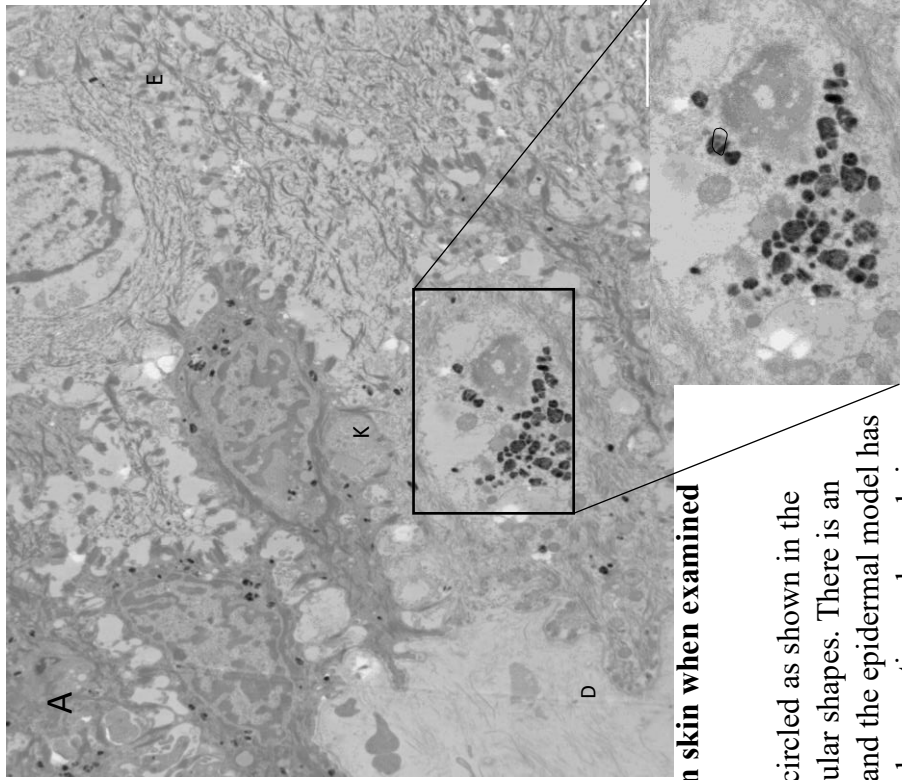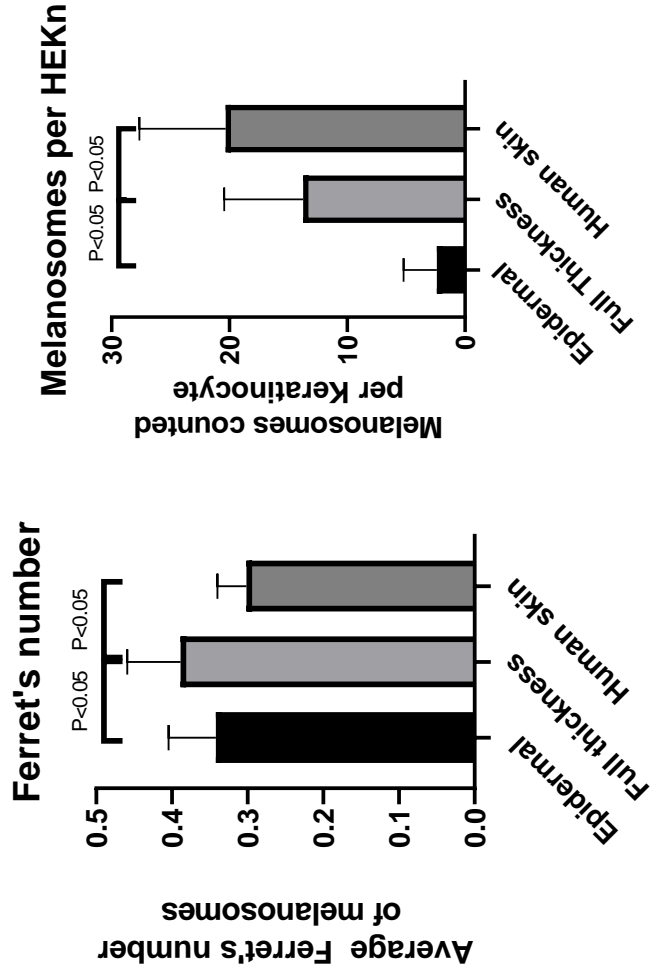
Figure 30. A quantification of epidermal model, full thickness model and human skin when examined under the transmission electron microscope.

Ferrets number was calculated using imageJ measurement tool. Melanosomes were circled as shown in the higher magnification image, then ferrets number was calculated to measure non-circular shapes. There is an increase in melanosomes size in the full thickness model compared to human tissue and the epidermal model has a larger melanosomes size than human skin which is an unexpected result. However, human tissue showed signs of degradation before fixation and could of affected the results. The melanosomes per keratinocyte shows more expected results. The human skin out performed both the models but full thickness is still producing significantly more melanosomes than the epidermal model A) a high magnification image of human skin showing a keratinocyte with a high density of melanosomes.

Legend: D – Dermis, K – Keratinocyte, E - Epidermis

4.5 Mature epidermal models have fewer melanocytes than full thickness model

To further understand the differences between the epidermal and full thickness model, the ratio of HEMn to HEKn cells was examined in the basal layer. In human skin the ratio for keratinocytes to melanocytes is roughly 10:1 (Cichorek et al 2013), and to replicate this, the models were seeded at the same ratio. Therefore, the expectation is that this ratio is maintained for cells in the basal layer. To examine the ratio, sections were stained for S100 and any brown/black staining indicates the location of HEMn cells. The blue nuclei were counted as keratinocytes. In Figures. 25 – 27, are examples of the models and human skin stained for S100 immunohistochemistry. Whilst the models still showed good morphology compared to human skin, there was a reduced number of visible melanocytes in the sections after staining.

In Figure 25, which showed S100 stain of human skin, there were a number of patches of dark brown staining, indicating a number of melanocytes residing in the field of view. However, in Figure 26, the only visible melanocytes in the image were highlighted in a higher magnification. Comparing the control against the HEMn condition, there was no staining in the control. In Figure 27, the full thickness model stained for S100 highlights a number of HEMn cells residing in the basal layer. When compared to the control, there was no visible brown staining. The higher magnification of the full thickness model in Figure 26 showed a HEMn cell with the dendritic projections into the neighbouring keratinocytes.

To quantify the observations seen in Figures 25-27, cell types in the basal layer were counted and a ratio was produced of HEMn to HEKn cells. As previously mentioned, the models are seeded at a 1:10 ratio to imitate the ratio of these cells in human skin. Therefore, the hypothesis was to see a stable ratio across throughout the models. Figure 28 shows the final ratio averaged across a number of 20x magnification images. The ratio for the full thickness model had stayed consistent at 1:10 through the incubation process. Whereas, the ratio of HEMn to HEKn cells in the epidermal model sits around 1:14. The average number of each cell type was counted and included in graphs in the Figure. There was a drop in the of HEMn cells per image and an increase in the number of keratinocytes counted.

4.6 The full thickness model and human skin show a similar structure at a cellular level

To characterise the full thickness model at a cellular level and compare it against human skin, both were examined under the TEM. The epidermal model was excluded from this due to problems ultra-sectioning the millicell insert that the model was grown on. Figure 29 shows a side-by-side comparison of the full thickness model and human skin. The similarities between

the two skin types are very clear. The four layers of the epidermis were clearly distinguishable in the full thickness model.

One major difference that very quickly becomes apparent from these images was the amount of pigmentation that can be seen in human skin. The full thickness model shows a high density of melanosomes in the *Basale Stratum*, with supranuclear caps forming around HEKn cells. Further to this, there were visible dendrites between the HEKn cells that were packed with melanosomes. The *Stratum Corneum* was visible in both samples and had a similar structure in both. In the full thickness model, the specialisation of HEKn cells can be seen as they move through the four layers. In the *Basale Stratum* they have a columnar morphology and as they moved towards the *Stratum Corneum* they flatten and lose their nucleus. HDFn cells were visible at the bottom of the image of the full thickness, providing support for the epidermis.

In human skin, there are fewer melanosomes and no visible melanocytes in this image. However, this image was chosen to show the structure of skin and is not representative of the number of melanosomes seen in the human skin samples. Furthermore, there are signs of cell death and tissue degradation in the human skin sample. This arose from the time the sample spent in transit after the biopsy was taken. The membrane of the cells is starting to breakdown and pull away from neighbouring cells and degradation of the nuclei is visible in a number of cells in the *Basale Stratum*. The epidermal model was excluded from this due to problems ultra-sectioning the millicell insert that the model is grown on.

4.7 Dimensions of melanosomes in the full thickness model exceed epidermal and human skin

In order to examine the size of melanosomes within the models, samples were prepared for TEM outlined in section 3.6. The sections were imaged and in ImageJ Ferrets diameter was measured. Feret's number is used to measure irregularly shaped particles under the microscope, providing a way to accurately compare dimensions of particles (Walton et al 1948). This method was used because melanosomes are rarely circular and therefore, of irregular shape shown in Figure 30.

The most interesting part of this analysis were the results from measuring melanosomes in human skin. The results show that the melanosomes in human skin are the smallest when compared to both model types, with an average melanosome size of 300nm. This was compared to the full thickness model that had an average melanosome size of 400nm and the epidermal model which sat around 330nm. In Figure 29, the image of human skin under the electron

microscope shows a number of signs of tissue degradation. Furthermore, the images taken from human were from a donor with Fitzpatrick scale III. The models had melanocytes from donors with different skin tones, which might explain the variations in melanosomes that were seen in this quantification.

4.8 Number of melanosomes per HEKn is closer to that of human skin than the epidermal model.

To support the evidence seen in Figure 29, the number of melanosomes per HEKn cell was counted at a molecular level with images from the TEM. Figure 28 shows the number of Melanosomes per HEKn. The graph shows that the observations seen in the Figure 28 with the Fontana Mason stain are supported. In the epidermal model, there were on average 5 melanosomes visible per keratinocyte. Furthermore, we see the full thickness model exceeds 10 melanosomes per keratinocyte, averaging about 12-13. This is a significant improvement on the epidermal model and supports other observations about the strength of the full thickness model compared to the epidermal.

4.9 Pigmentation levels remain constant in a fully formed epidermis

To understand how the pigmentation develops in these the full thickness skin equivalents and to determine if the pigmentation remains constant over time, the models were harvested at three different time points and examined with H&E and Fontana Masson. The images of the H&E analysis in Figure 31 shows that the models harvested at the 7-day time point are underdeveloped. Interestingly, the HEMn condition have a better structure at this early time point than the control. Once they reach 14 days, both models have developed into a recognisable skin equivalent, with the four distinct layers and a stratified outer layer. The biggest change occurs between the 7- and 14-day time points with a clear difference in skin
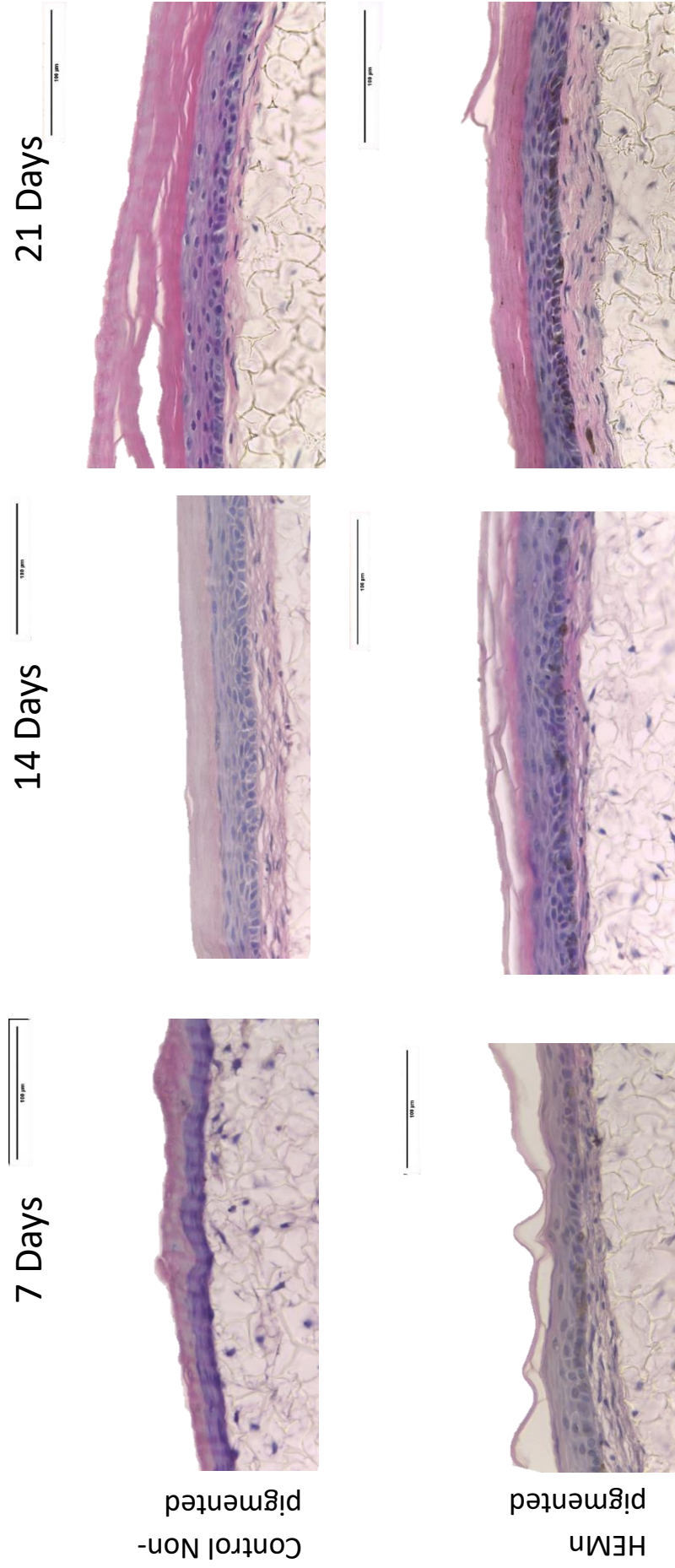
Figure 31. H&E staining shows a stratified epidermis at 7 days but the epidermal layers continues to develop until 14 days.

The models in this experiment were harvested at three different time points: 7, 14 and 21 days and stained here for H&E to examine the general structure of the models. At the 7 day time point, the epidermal section of the full thickness model has developed and a cornified layer has emerged. However, at 7 days the layers of the epidermis still looks under-developed compared to the other time points. At 14 and 21 days the four layers of the epidermis are more distinct and larger in size. This can be seen in both the control and HEMn condition which suggests that the full thickness model is still developing up to 14 days. At day 7 there is almost no sign of melanin in the *Stratum Basal.* in the later two time points, there are signs of dark brown pigmentation along the bottom layer of the epidermis.

Figure 32. Fontana masson staining shows increasing pigmentation throughout the time frame, with the biggest change from 7 to 14 days
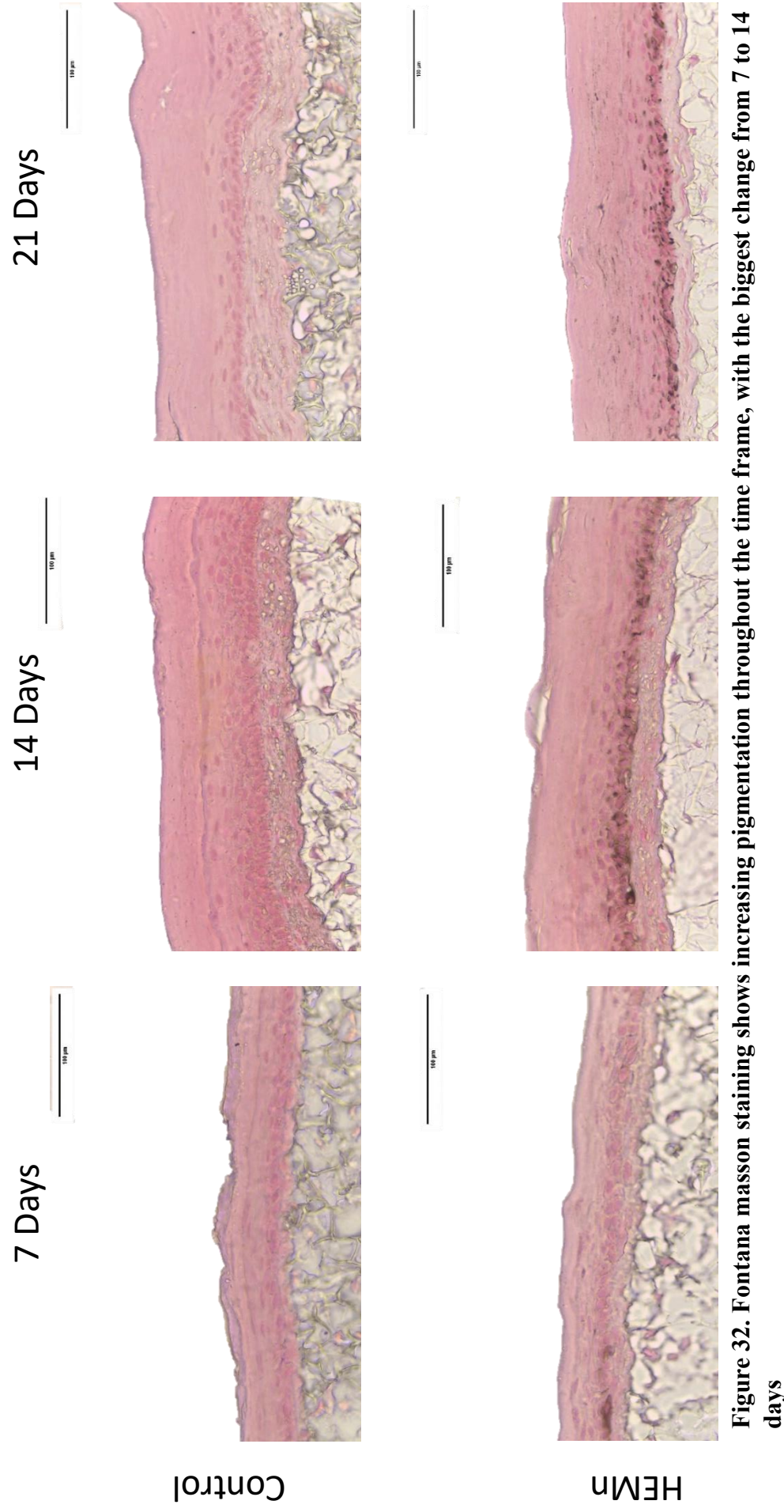
The pigmentation over time experiment was stained in this figure following the Fontana Masson protocol outlined in section (). At 7 days post-ALI, the model shows minimal black/brown staining. On the left side of the image, there is a patch of brown staining which appears to be a HEMn cell. However, melanin is restricted to the melanocyte and no melanin transfer can be seen. at 14 and 21 days, there is the classic melanin staining pattern across the *Stratum Basal* with supranuclear caps forming clearly in the 21 day condition. In the control models without HEMn cells, there is not observable black/brown staining at any time point.

structure. The biggest change from 14 to 21 days is a thickening of the *Stratum Corneum.* The Fontana Masson staining in Figure 32 shows similar results. There was no brown or black staining in the control condition at any time points. At the 7-day mark in the HEMn condition there is no visible staining of melanin inside the keratinocytes, however, there was a visible melanocyte, which contains brown staining of the melanin. The models that were stopped at 14 days show clear signs of brown staining through the *Stratum Basale,* with signs of supranuclear caps forming. Again, the biggest change occurs between these 7 and 14 day time points, with melanin transfer beginning at some point in this 7 days. By 21 days, the model had a slightly darker concentration of staining, with clear supranuclear caps in the *Stratum Basale.*

Figure 33. Imaging of the full thickness model at a macro level with colour changing compounds.

Models were grown in the presence of known pigment altering compounds, three conditions were used in this experiment: control(Left), Kojic acid (Centre) and a-MSH (Right). Kojic acid and a-MSH was used at a concentration of 50ug/ml and 0/5ug/ml respectively. A high concentration of both compounds were used as these are known lightening and tanning agents. Therefore, the expectation is to see changes in pigmentation in both conditions. The Kojic acid condition shows signs of lightening compared to the control suggesting the kojic acid is influencing the level of pigmentation. However, the a-MSH condition shows minimal darkening of the model compared to the control. In addition to colour changes, there are areas where melanocytes have aggregated together creating a freckled appearance in all the models.

In Figure 32, the same experiment was stained against Fontana Masson, designed to highlight areas of pigmentation. The images collected support similar conclusions to the H&E analysis of the models. At 7 days, the full thickness model shows minimal signs of pigmentation. The only visible melanin staining is found localised to a HEMn cells on the left

side of the 7-day image. Once the models reach 14 days, the model has started to represent human skin more closely. The *Stratum Corneum* has thickened and more importantly melanin production and transfer are underway by 14 days. There is an increase in the amount of melanin observed in the stained sections by 21 days.

In Figure 23, the amount of Fontana Masson staining was quantified using the method outlined in section 3.9. The line graph shows a clear a significant increase from 7 to 14 day. Whilst there is an increase in staining between 14 and 21 days, the difference is not as big but it is still statistically significant at p value 0.05. (Billings et al 2015). The pigmentation index was calculated by dividing the total number of pixels at the melanin peak by 10^{-3}. It also supports the notion that the biggest increase occurs between 7 and 14 days with a change from 1 to 6 on the pigmentation index.

4.10 The full thickness model responds appropriately to tanning and lightening agents

To understand how known tanning or lightening agents affect pigmentation in the 3D model, the full thickness model was incubated with Kojic acid or a-MSH after raising the models to the ALI. Concentrations of the agents were based on the literature and the 2D culture observations. Figure 33 showed a macro perspective of the models prior to fixation with formaldehyde. The first feature that stood out was the freckled appearance of the pigmentation within the model. It is unlikely that this was caused by the inclusion of a-MSH or Kojic acid since it was ubiquitous across the conditions including the control. It was potentially due to aggregating of HEMn cells in culture prior to incorporation in the full thickness model. Furthermore, the frequency and density of pigmentation in the patches did not change across the three conditions. Even though there was not a difference in the freckled pigmentation, the surrounding skin in the model appears to respond to the pigment altering agents. The Kojic acid condition had the clearest change in skin tone compared to the control. In the a-MSH condition   the   skin
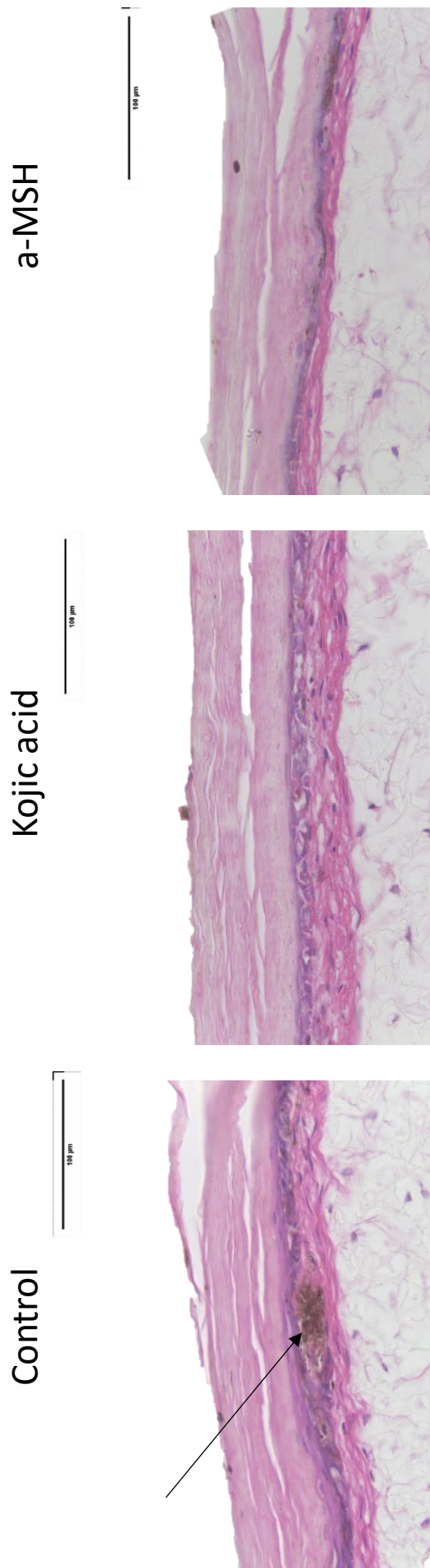
Figure 34. H&E comparison of full thickness models grown with pigmentation altering compounds.

Full thickness models were grown for 28 days after raising the models to the air-liquid interface. The compounds were added to the media at 50ug/ml and 0.5ug/ml for kojic acid and a-MSH respectively at day 1 at the air-liquid interace. The *Basal Stratum* of these models shows poorer organisation compared to other models, this may be due to the age of the model or the batch of keratinocytes used. The model shows clear differentiation of keratinocytes into corneocytes that form a stratified outer layer. Without Desquamation occurring this layer has thickened substantially compared to younger models. The layer of HDFn cells is visible under the epidermis, providing nutrients and structural support along with the Alvetex polystyrene insert. There are signs of less pigmentation in the Kojic acid condition and minor increases in a-MSH condition. However, with it being a non-specific stain, it is hard to determine this.

tone
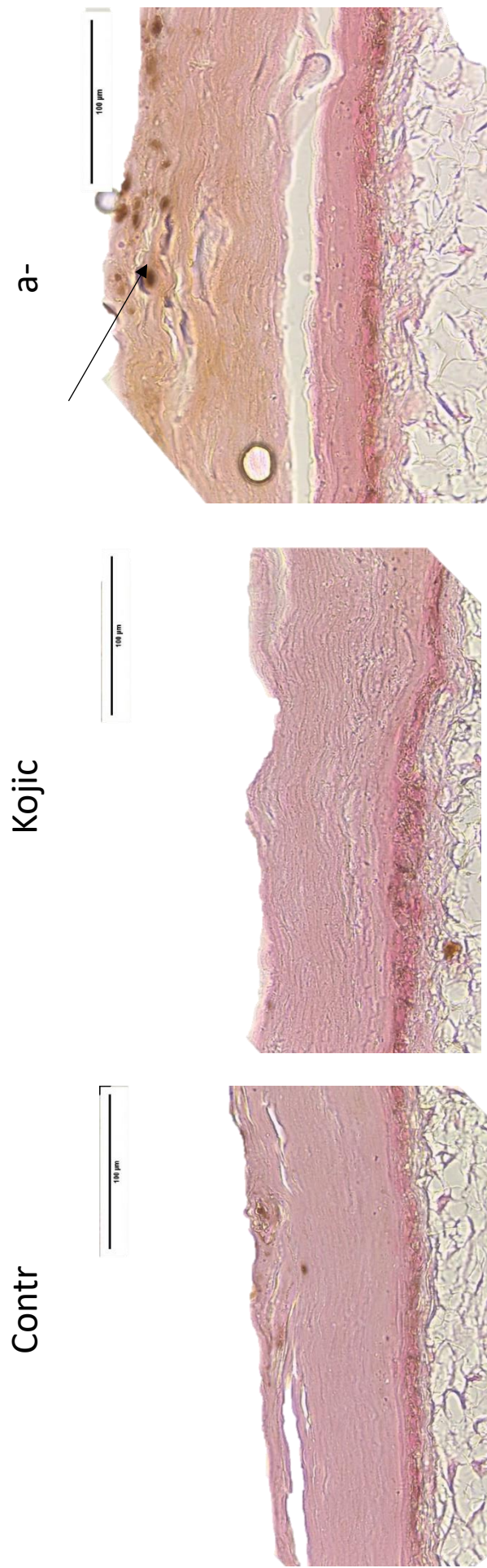
Figure 35. Fontana Mason comparison of full thickness models grown with pigmentation altering compounds.

Models were grown to a 28 day time point and incubated with either a-MSH (centre), Kojic acid (left) or the control (right). The pigmentation changing compounds were added to the media at 50ug/ml and 0.5ug/ml for kojic acid and a-MSH respectively at day 1 at the air-liquid interface. There is a slight difference in the levels of pigmentation across the three conditions, however, it is difficult to see the levels of pigmentation due to the disorder *Basal Stratum*. In the a-MSH condition there does seem to be an increase in the levels of pigmentation. In addition to this, there is a large amount of melanin in the upper layers of the *Stratum Corneum* which isn't seen in the other conditions. There seems to be a fall in pigmentation in the Kojic acid condtion as there is less visible brown staining in the *Stratum Basal* and no staining in the upper layers of the model. All the conditions show good specialisation of HEKn into corneocytes, however, the lower three layers of the epidermis are a lot less well defined.

between this and the control looks similar. Therefore, the full thickness did not show any changes at a macro-level to the compound compared to the control condition.

The H&E analysis in Figure 34 of the models used in the pigmentation altering experiment showed interesting physiological features. The organisation of the epidermal layers in these models was less well defined and less organised. There seems to be a layer of HEKn cells at the dermal-epidermal junction. This is acting as the *Stratum Basale,* however, there doesn't seem to be distinct *Stratum Spinosum* or *Stratum Granulosum*. The HEKn cells seem to quickly move through and specialise into corneocytes. As expected of models after this length of time, the *Stratum Corneum* has continued to thickened without the process of desquamation occurring.

Down at the cellular level there are differences between the levels of pigmentation. Figure 35 is the Fontana Mason stain of these models and show the level of pigmentation in the model. The images from this stain show consistent observations with the macro images, the Kojic acid condition shows a reduction in pigmentation and a-MSH shows an increase in pigmentation in the basal layer compared to the control. What was interesting in these models there is evidence of melanin in the upper layers of the epidermis. In the a-MSH image, there was brown staining in the *Stratum Corneum.* Whilst this staining might be down to abnormal models, the presence of it in a-MSH conditions and, to a lesser extent, in the control suggests the pigment altering agents were having an effect.

The results from the experiment carried out for the purpose of this thesis highlight the role of the dermis in the control of pigmentation in skin equivalents. This interaction between the dermis and epidermis is well understood in human skin and to understand how these fit with skin equivalents, it is important to discuss these results as part of the literature as a whole.

5. Discussion

To understand the relationship between different cell types and how pigmentation is affected in a 3D skin model, it was important to first characterise the HEMn cells. This provides a foundation to build upon our understanding of how the dermal compartment influences pigmentation and what other factors influences the development pigmentation in a skin equivalent.

5.1 Characterisation of HEMn cells

The first challenged faced in creating the pigmented model was determine what ethnicity of donor that HEMn cells were taken from. All cells used with in the models were purchased from Fischer scientific. Therefore, it was important to characterise the cells before seeding them into the model because cells from different donors will showcase different characteristics. Alaluf (2001) showed through high-performance liquid chromatography (HPLC) that epidermal melanin content in people with a Fitzpatrick skin type V and VI was significantly increased and there was a significantly higher level of eumelanin compared to pheomelanin. In addition, in 2002 Alaluf further showed how pigmentation in skin from European, Chinese and Mexican donors had approximately half as much epidermal melanin as darker ethnic backgrounds such as African and Indian skin types.

Figures 1-5 show the results of these characterisation experiments. What becomes clear quickly from culturing the cells in 2D is the propensity for DP HEMn cells to produce melanin. The light microscope images in Figure 1 show a distinctly darker colour for the cells compared to LP HEMn cells. The light is unable to penetrate as effectively through the melanin packed cells and a white outline forms around the cell. This is not visible in the LP HEMn cells due to less melanin content. This is further backed up by two stains performed on these cells following seven days of culture. The Fontana Mason stain, whilst giving better results on 3D cultures, it showed a difference in the amount of melanin found in two donor ethnicities of the HEMn cells. The DP HEMn cells are packed with melanin, unlike LP HEMn cells which had very little visible melanin. Improving on this stain, the immunofluorescence of these two cells types, stained using GP100 antibody – an early melanosome marker (Adema et al 1994). Both cell types expressed this protein at similar levels seen by the fluorescent signal in the control images in Figures 3 and 4. Whilst this characterisation supports the notion that the cells come from different donors, which likely have a different skin tones, it is not enough to show that they are from different ethnic backgrounds entirely.

Further to this, we examined how this marker in these cells responded to a-MSH and Kojic acid. HEMn cells were incubated for 24 hours with either a-MSH or Kojic acid. The images show a strong response to both compounds from both cell types. Unsurprisingly, ##650 HEMn cells had a stronger response to a-MSH, with a significant increase in signal strength. However, these cells also responded stronger than ##107 to Kojic acid. It seems that cells from a dark pigmented donor have a higher sensitivity to either form of pigment alteration. Therefore, this led to favouring the ##650 for use in the pigmented skin model. It also showed

that the concentrations of the compounds used were effective and showed a good result on both cell types.

Interestingly, the ##107 HEMn cells were often seen to have fewer dendrites than ##650. It is clear in Figures 1-5 that ##107 HEMn cells showed fewer dendrites across all the stains. This might be a result of culturing HEMn cells in 2D. It has been shown that cells have a different morphology when cultured in 3D. Therefore, this might be a temporary phenotype that is reverted when seeded into 3D models. Furthermore, it could be due to only receiving a select number of growth factors and other paracrine signals found in the media. Whereas, once HEMn cells are used in the model, especially the full thickness model, a wider array of signals are received from HEKn cells, HDFn cells and the ECM.

Whilst it was important to use HEMn cells that cultured the best, a long-term goal for this model was to develop models of different ethnicities. Therefore, where possible, ##650 HEMn cells were used to develop the model early. It will be interesting to see how the lighter pigmented HEMn cells perform within the 3D models and whether the level of pigmentation is altered and to what extent the HEMn cells influence the final.

5.2 The importance of fibroblasts inclusion for pigmentation in skin equivalents

Once the HEMn cells were characterised and ##650 were incorporated into the model, the first step was to compare how the models performed at against human skin. In the case of tissue, the structure of the organs is often linked to its function. Therefore, we hypothesised that the closer the structure of our model came to that of human skin, the more favourably the model would perform when comparing the two. Therefore, the first step was to generate models and through a number of stains, compare them to human skin.

Firstly, we used H&E analysis to observe the structure of skin. This is a non-specific stain aimed to highlight structural similarities or differences between the models and human skin. At this stage, there were no notable differences were observed between the full thickness and epidermal model. Both model types showed the four layers of the epidermis with appropriate cornification of HEKn cells to form an outer layer that acts as a barrier. The cells in the *Stratum Basale* showed columnar morphology that flattened and lost their nucleus as they moved up through the epidermis. Even though this is not a melanin or HEMn specific stain, the melanin was often visible, causing the HEKn cells in the *Stratum Basale* to stain darker than other cells.

The first marker of skin model health we looked at was epidermal thickness in the full thickness and epidermal model (Figure 17-20). H&E images were taken of the models and an average of five measures were taken along the epidermis in ImageJ. The results were inconsistent between the two model types. It seems that the inclusions of HEMn cells into both skin equivalent models gives different results for the thickness of the epidermis, neither of which are significant differences. Therefore, it seems the incorporation of HEMn cells into the full thickness model has minimal affect on the thickness of the epidermis.

Once the models were stained for melanocyte markers and melanin specific stains such as Fontana Masson (figure 21-24), there were significant differences between the epidermal and full thickness model. The Fontana Masson stain in Figure 20-22 and the S100 stain in Figure 23-25 showed that the full thickness model, with a structure that more closely resemble human skin with the addition of the dermis, had increased levels of melanin production and transfer. The images showed the *Stratum Basale* of the full thickness model had HEKn cells containing melanin whereas often the epidermal model had minimal to no staining of these cells.

Next, the final ratio of HEMn to HEKn cells in the *Stratum Basale* compared to the original seeding density. The ratio of keratinocytes to melanocytes in human skin is roughly 1:10 (Cichorek et al 2013) and the data from the experiment supports that, with the ratio at between 1:10 and 1:11. This was the basis for the seeding density of cells when setting up the models. The results from counting cells in the skin equivalents showed was an interesting outcome (figure 25-28). The full thickness model maintained a ratio of 1:10, the same as the seeding density, however, the epidermal model saw a decrease in the number melanocytes in the *Stratum Basale*. This led to the final ratio being 1:14 in the epidermal model. This seems to suggests that either the melanocytes and being out proliferated or the chance of these cells surviving through the incubation period is reduced without the dermal compartment.

Dermal fibroblasts have a crucial role to play in the skin and it seems this is supported by the work in these models. The fibroblasts produce a number of factors to support the epidermis with growth factors and nutrients. It has been shown that fibroblasts are able to both promote and inhibit melanogenesis and the data from our results suggests the dermis is influencing the full thickness model. Literature has shown that fibroblasts inhibit melanogenesis through the WNT signalling pathway (Kim et al 2013) to prevent pigmentation from developing on the soles of feet and palms of the hands. KGF produced from both

fibroblasts has shown to have an activatory effect on melanogenesis and melanin transfer (Cardinali et al 2007). Since fibroblasts can have dual mechanism of action, there is not a clear-cut link. To understand this further and develop on Kim's research, dermal fibroblasts from different areas of the body may have different effects on the pigmentation in models.

There was very similar research into the effects of a dermal compartment on the function of melanocytes in skin equivalent models done by the Duval lab (Duval et al 2014). This paper specifically focuses on the role of the dermal compartment within skin equivalents. Interestingly, Duval found that when models were grown with adult fibroblasts, a significant drop in the amount of pigmentation. However, when the models were grown with foetal fibroblast, they showed far greater pigmentation in the skin equivalents than that of adult fibroblast cells. Aged cells often have different morphology and produce models which appear to function in culture poorer than neonatal cells. It is possible the expression of genes to do with melanin production might cause a reduced amount of melanin. It would be interesting to recreate this full thickness model with adult fibroblasts and examine whether the same changes occur in this model. This may directly explain the link that is seen in the data here. Since neonatal fibroblasts were used throughout the experiments in this thesis, the results from Duval support the observations seen here. Furthermore, using different types of fibroblasts might produce different responses in an Alvetex® based system.

In addition to paracrine signalling, contact with an ECM that is similar to human tissue might be positively influencing the model. Ransom et al (1998) grew melanocytes on plastic with and without ECM coating. When melanocytes were in the presence of the ECM, they had larger cell bodies and produced more melanin. In melanoma cells, this ability to respond to the ECM was lost, which is a strong indicator of the important role the ECM plays in melanocyte regulation.

There might be a role for indirect upregulation of melanogenesis by the dermis via keratinocytes. Chung et al 2014 showed that keratinocyte produced Laminins upregulate melanogenesis by promoting the uptake of tyrosine into melanoma cells. Furthermore, Cardinali also showed that keratinocytes were also producing KGF and to promote melanogenesis and melanin transfer (Cardinali et al 2008).   Therefore, there is the possibility that HEMn function is being indirectly improved by the presence of HDFn cells and endogenous ECM. It give strength to the argument that structure relates to function. Achieving

a model that is as close to the native tissue as possible may inadvertently improve other aspects of the model.

However, this is only speculation as to the method of action and even though the literature supports the link between the dermal compartment and improved melanocyte function, it would be interesting to further explore this area of research. In order to do this, media from HDFn 2D cultures could be harvested and grow epidermal models with melanocytes in. This would indicate if either a paracrine factor or direct contact with ECM had a bigger influence on the models. However, due to time restrictions this experiment was not carried out.

After observing an improvement in the behaviour of melanocytes in the full thickness model. The focus shifted towards further characterisation of the full thickness model. Figure 31 and 32 are examining how the model and HEMn cells develop at different points along 21 days after raising the model, to the ALI. The hypothesis was the pigmentation in the model would develop early and remained partially correct. At 21 days the amount of observable pigmentation in sections stained with Fontana Masson was consistent compared to 14 days. However, at 7 days the sections had minimal black staining. It would be interesting to have a shorter experiment with more time intervals between 0-14 days to gain further understanding how the melanin production changes each day. In addition, PCR could be performed to examine how gene expression changes in these early days of the model.

What is important to note from this experiment is to ensure models are grown to at least 14 days before being used to test compounds. Even though the general structure of the HEKn cells and skin as a whole is established before this point. Any pigmentation experiments should use the model at the later stages of development. This will ensure accurate and consistent results from using the model each time. There is likely to also be an upper limit on the model's viability. The models lack the ability to carry out desquamation and as the model ages, the *Stratum Corneum* will thicken. The upper limit should also be investigated to observe what happens to pigmentation in skin equivalents if left for an extended length of time.

It was important to be able to quantify the amount of melanin within our models to support the observations drawn from images of the models. What became clear after we quantified the images is that the conclusions that were drawn from the images were relevant. The images and quantification showed that the inclusion of a dermis grown on the Alvetex® polystyrene insert led to an increase in the amount of observable melanin. Further to this,

melanin content increased over time with the biggest change occurring between 7 and 14 days. For the quantification of melanin to support so clearly what was seen in the images, shows the strength of the full thickness model. However, going forward, it is important to use a different method of quantification. Due to time restrictions, the melanin quantification assay outline in Fernandes et al 2016 is a better method to quantify total melanin within a model. However, the method used here better suited the available models and was chosen due to the ease of the methodology.

5.3 The model is a dynamic environment with malleable pigmentation

After observing that the full thickness models showed better structure and function our focus shifted towards gaining a better understanding of this model. In order to develop a better understanding, two experiments were performed on the full thickness model.

The first experiment was designed to observe how the pigmentation changes over the course of the incubation period. Previous iterations of the models were grown to 14 days, however, it was suspected that after this point pigmentation may continue to change. This thinking was based upon advertising done by a company producing an epidermal equivalent (Melanoderm) that showed the model continuing to darken over time. This product shows the model continuing to change pigmentation significantly across all time points. Whilst there was an expectation that the model would darken, the hypothesis was that there would be an initially spike at some point before 14 days, then it would gradually increase after this time point.

Figure 31 and 32 show the H&E and Fontana Masson staining respectively. The H&E stain didn't show anything particularly interesting across the three time points. There is a change in the general structure of the model from 7- to 14-days. This was expected as the model takes up to 14 days to reach maturation. However, when the Fontana Masson images were examined, there were clear differences between 7- and 14-day time points. At 7-days, it is clear that melanin content is localised to the HEMn cells and there are no supranuclear caps forming in the HEKn cells. This changes at 14 days and the HEKn cells have melanosomes around the nucleus.

The process of human skin changing pigmentation over time in response to external stimuli such as UV is well documented. However, understanding how pigmentation within skin equivalent changes without any external intervention is poorly understood. This experiment shows that within skin equivalents, there is a gestation period for melanin production and transfer. Further experimentation is required to understand how this process actually begins

and changes over time. However, here we have shown that the optimal time to use this full thickness model is after 14 days.

The second experiment, the skin models were incubated with either tanning or lightening agents which gave interesting results. The change in pigmentation in the models was minimal at a macroscopic level (Figure 33). Once the models were stained and the structure examined, the difference in amount of melanin produced was still fairly minimal. There is evidence in the a-MSH condition of increased melanin content in the upper layers of the epidermis. However, the lacking of structure in the epidermis may explain this. The HEKn cells within the model did not properly form an epidermal layer (figure 34 and 35). There is a clear cornified outer layer, however, the other layers of the epidermis are not defined at all. This is likely due to poor growing conditions or HEKn cells with poor viability. It is well documented in the literature that a-MSH and Kojic acid alter the pigmentation in skin and skin equivalents (Zurina et al 2020, Zöller et al 2019, La Pape et al 2008) Therefore, the insignificant change in pigmentation in these models is likely down to something within these models. hopefully if repeated and an epidermis formed correctly, we would expect to see more modulation in response to the compounds

5.4 Supranuclear caps were observed in full thickness but not epidermal-only skin equivalents

Crucial to melanin's function is its ability to form supranuclear caps within keratinocytes. It is important to be able to recreate this formation within both the epidermal and full thickness model. Without supranuclear caps, it is hard to be sure if the melanin is functioning correctly. To be sure the models were producing melanin and transferring it to HEKn cells in a pattern that is similar to endogenous melanin, the comparison with human skin was crucial. It is uncommon in the literature to have a comparison with human skin; however, we feel it is critical to show the strength of these models. Furthermore, it shows confidence in the model that is produced here.

Following this comparison, it was obvious that the model was producing supranuclear caps with a similar formation to that of human skin. Whilst there was some formation of supranuclear caps in the epidermal only model, the best defined supranuclear cap formation was seen in the full thickness model. from the literature, there is not much information about the mechanisms which cause supranuclear caps to form and it doesn't seem like any one factor will contribute to the results seen. What is likely is the supranuclear caps are forming in response to a well-built model. With the HDFn cells populating the Alvetex® and producing

endogenous ECM, the structure is similar to that of human skin and allows the HEMn and HEKn cells to be supported and carry out their functions. It may be hard to isolate a single cause for the supranuclear caps seen in the full thickness model because of the multiple factors that contribute to the microenvironment of cells within a tissue.

5.5 The strength of Alvetex®

The full thickness model outlined in this paper is an important step forward for pigmented skin equivalents. In the last 5 years, the models have become increasingly complex, with a method of generating a full thickness model without Alvetex® becoming fairly simple and easy to produce. However, these models rely on the use of endogenous collagen gels, with HDFn cells seeded in the gel. This potentially goes some way to fixing the issues that were seen in the epidermal model. It would require further study to compare these full thickness models with epidermal models. Furthermore, in this paper, there is no evidence to suggest that the incorporation of HDFn cells alone makes up the differences seen between the model types. In addition, there are drawbacks to using collagen gels, especially ones that use animal collagen, which is fairly common practice.

Compared to other full thickness model methodologies currently in the literature, Alvetex® allows for a fairly simple process, the model only uses media 106 with LSGS, TGF-B and ascorbic acid during the dermal growth phase. Once the HEKn cells are seeded the model uses epilife with HKGS, KGF and ascorbic acid. These consumables are simple and readily available, making the model easy to reproduce. Furthermore, the strength of Alvetex® shows that it requires minimal labour input to generate. Apart from seeding cells into the model, which requires no more labour than seeding HDFn's into collagen gels, the process only requires two media changes per week.

It is difficult to draw comparisons between the Alvetex® full thickness model and ones using collagen gels without experimental data to support any conclusions. However, what Alvetex® does provide, which these models do not, is a scaffold for HDFn cells to produce their own ECM and remodel it to closely match that of human skin (Hill et al 2015). This shows the range of ECM proteins that are produced within the model. As previously mentioned, it is difficult to draw any comparisons between these full thickness models without experimental data. However, it is unlikely that a model that closely resembles human skin in both the structure of the cellular environment and the ECM, will negatively affect the function of the model. What is likely is that this dermal compartment is positively affecting the model and

specifically pigmentation. Therefore, this research shows that it is not only important to continue to strive to generate a model that matches human skin as closely as possible. It also sheds light on the drawbacks of relying solely on any single model system to test these drugs on as they may produce unreliable results.

5.6 Problems encountered and experimental improvements

One of the major issues encountered during this project was around the HEKn cells that were available for use. The images of the models shown in Figure 17-19 highlight well the potential issues that poor HEKn cell batches caused. Fortunately, these HEKn cells only affected the final experiment and the data was still usable to show that the model responds to lightening and tanning agents. However, HEKn cells form possible the most crucial component of the skin equivalent and repeating this experiment with HEKn cells with improved viability will strength the validity of the findings.

One of the other improvements that could be made to the data is how the melanin was quantified. This process was done on models that were previously fixed in wax, which meant there were fewer options for quantifying melanin. This process allowed us to quantify melanin on old blocks but it seemed to be less reliable because it was quantifying the amount of staining not directly the amount of melanin. There is a protocol for quantifying melanin using its inherent ability to fluoresce and can therefore be quantified using a spectrophotometer (Fernandes et al 2016). This would give more accurate results that can be compared across experiments.

Finally, if given more time, a priority would be to repeat the experiments which would increase the validity of the findings seen in this thesis. In particular, it is important to have repeats of the experiments focusing on the characterisation of the full thickness model. The full thickness model shows great promise from the preliminary data seen here, however, without further repeats it is hard to know the validity of the results. Furthermore, extra time to complete further characterisation of the models would increase the depth of understanding on this topic. In order to understand the role of the dermis, an experimental procedure to incubate media with HDFn cells then grow epidermal models with melanocytes in this media. To summarise the main points of this discussion:

- Characterisation of HEMn cells shows #650 have a greater concentration of melanin in 2D culture than #106.

- Pigmented versions of the full thickness and epidermal model were successfully created.
- The melanocytes in both models showed the correct location and produced melanin.
- The full thickness model had more visible melanin and the generation of supranuclear caps.
- Alvetex$^©$ is a viable technology for the production of pigmented skin models.
- Pigmentation increases gradually over time but plateaus in later time points.
- The model responds appropriately to tanning and lightening agents.

5.7 future directions

The full thickness model now has the foundations required for a pigmented skin equivalent. The final aim for this research is to generate a model that can be used for cosmetic and pharmaceutical testing. Whilst the results in this paper show that the potential for this technology to develop into a product available for research there is still work to be done. Some experiments that would answer some inaccuracies in the data have been outlined in the discussion there are still some areas to further explore.

Firstly, melanocytes play an incredibly important role in the protection of skin from UVR. To see if this research is viable in our models and to ensure melanocytes are performing their function in the model this aspect needs to be investigated. A comparison with a non-pigmented full thickness model would show how the HEMn cells are influencing the model. It would also be prudent to examine how the pigmented full thickness model performs against human skin and the epidermal equivalents to understand if the dermis influences this process. The use of a UV irradiating machine to dose the models at different strengths and observe how the model recovers over the period of 24hrs.

To further expand on the 2D characterisation of HEMn cells, an important step would be to try and alter the skin tone of the model. Due to how the HEMn cells are sourced, this area might be difficult to keep consistent as different HEMn and HEKn donors might produce varying skin tones. However, developing models with differing skin tones will be an important step in bringing this model to market. The pigmented model is likely to be heavily used in the cosmetic research and it is important to be able to represent and test the compounds on a variety of skin tones.

It would be interesting to observe the role of aging upon pigmentation and this model could be altered to incorporate cells from donors of different ages. Duval et al 2014

incorporated HDFs from adult and neonatal donors and observed the effects on pigmentation within a full thickness model. They showed that in models built with HDFs from adult donors the amount of pigmentation in the model was significantly less. Not only does this show how ageing affects pigmentation but it also supports the conclusions previously drawn and suggests an important role for HDFn cells in helping pigmentation develop in the model. The next step for this model would be to include adult HDF cells and observe how this model responds. There might be a potential to generate a model with classic signs of aging in pigmentation such as liver spots on the skin.

Finally, there is the potential to develop the pigmented skin equivalent into a model for disease. The introduction to this paper briefly touches on pigmentation disorders and the epidemiology and causes of the disease. Whilst the genetic disorder such as Albinism is well understood, disease such as vitiligo and melanoma still require further understanding. The technology outlined here provides a basis to continue to develop models using cells from donors with these disorders.

The model developed in this thesis shows when trying to replicate tissue and organs, the closer in structure the model is the better the function. The epidermal equivalents, whilst a good starting point for a test model, show a noticeable difference between it and a full thickness model. That is not to say that the epidermal models have no place as a test system for drugs and cosmetics. What is important to state is that each system has its strength and weaknesses. The epidermal model is quick to produce and easy to replicate. Therefore, it could be used as a model system, however, it could be argued that it shouldn't be used alone and instead used as part of a number of checks done for testing a compound. The full thickness model may be more costly to produce however, the data shown here highlight why it is important to develop these technologies.

In conclusion, the data gathered for the purpose of this thesis form a good starting point, highlighting the importance of developing tissue equivalents that resemble the desired tissue as closely as possible. However, there is still a way to go to characterise this particular skin equivalent before it is ready for use commercially and in academic research.

Reference

Abdel-Naser MB, Liakou AI, Elewa R, Hippe S, Knolle J, Zouboulis CC. Increased Activity and Number of Epidermal Melanocytes in Lesional Psoriatic Skin. Dermatology. 2016;232(4):425-30.

Adema GJ, de Boer AJ, Vogel AM, Loenen WA, Figdor CG. Molecular characterization of the melanocyte lineage-specific antigen gp100. J Biol Chem. 1994 Aug 5;269(31):20126-33.

Akay BN, Bozkir M, Anadolu Y, Gullu S. Epidemiology of vitiligo, associated autoimmune diseases and audiological abnormalities: Ankara study of 80 patients in Turkey. J Eur Acad Dermatol Venereol. 2010 Oct;24(10):1144-50.

Alaluf S, Atkins D, Barrett K, Blount M, Carter N, Heath A. Ethnic variation in melanin content and composition in photoexposed and photoprotected human skin. Pigment Cell Res. 2002 Apr;15(2):112-8.

Alaluf S, Heath A, Carter N, Atkins D, Mahalingam H, Barrett K, Kolb R, Smit N. Variation in melanin content and composition in type V and VI photoexposed and photoprotected human skin: the dominant role of DHI. Pigment Cell Res. 2001 Oct;14(5):337-47.

Alkhateeb A, Fain PR, Thody A, Bennett DC, Spritz RA. Epidemiology of vitiligo and associated autoimmune diseases in Caucasian probands and their families. Pigment Cell Res. 2003 Jun;16(3):208-14.

Bao M, Xie J, Huck WTS. Recent Advances in Engineering the Stem Cell Microniche in 3D. Adv Sci (Weinh). 2018 Jun 13;5(8):1800448.

Billings PC, Sanzari JK, Kennedy AR, Cengel KA, Seykora JT. Comparative analysis of colorimetric staining in skin using open-source software. Exp Dermatol. 2015 Feb;24(2):157-9.

Brancato V, Ventre M, Imparato G, Urciuolo F, Meo C, Netti PA. A straightforward method to produce decellularized dermis-based matrices for tumour cell cultures. J Tissue Eng Regen Med. 2018 Jan;12(1):e71-e81.

Brenner M, Hearing VJ. The protective role of melanin against UV damage in human skin. Photochem Photobiol. 2008 May-Jun;84(3):539-49.

Breslin S, O'Driscoll L. Three-dimensional cell culture: the missing link in drug discovery. Drug Discov Today. 2013 Mar;18(5-6):240-9.

Buscà R, Ballotti R. Cyclic AMP a key messenger in the regulation of skin pigmentation. Pigment Cell Res. 2000 Apr;13(2):60-9.

Byers HR, Maheshwary S, Amodeo DM, Dykstra SG. Role of cytoplasmic dynein in perinuclear aggregation of phagocytosed melanosomes and supranuclear melanin cap formation in human keratinocytes. J Invest Dermatol. 2003 Oct;121(4):813-20.

Calautti E, Li J, Saoncella S, Brissette JL, Goetinck PF. Phosphoinositide 3-kinase signaling to Akt promotes keratinocyte differentiation versus death. J Biol Chem. 2005 Sep 23;280(38):32856-65.

Calautti E, Grossi M, Mammucari C, et al. Fyn tyrosine kinase is a downstream mediator of Rho/PRK2 function in keratinocyte cell-cell adhesion. *J Cell Biol*. 2002;156(1):137-148.

Cardinali G, Bolasco G, Aspite N, Lucania G, Lotti LV, Torrisi MR, Picardo M. J Invest Dermatol. 2008 Mar;128(3):558-67.

Chen N, Hu Y, Li WH, Eisinger M, Seiberg M, Lin CB. The role of keratinocyte growth factor in melanogenesis: a possible mechanism for the initiation of solar lentigines. Exp Dermatol. 2010 Oct;19(10):865-72.

Choi W, Yin L, Smuda C, Batzer J, Hearing VJ, Kolbe L. Molecular and histological characterization of age spots. *Exp Dermatol*. 2017;26(3):242-248.

Chung H, Jung H, Lee JH, et al. Keratinocyte-derived laminin-332 protein promotes melanin synthesis via regulation of tyrosine uptake. *J Biol Chem*. 2014;289(31)

Cichorek M, Wachulska M, Stasiewicz A, Tymińska A. Skin melanocytes: biology and development. Postepy Dermatol Alergol. 2013;30(1):30-41.

Celli A, Sanchez S, Behne M, Hazlett T, Gratton E, Mauro T. The epidermal Ca(2+) gradient: Measurement using the phasor representation of fluorescent lifetime imaging. *Biophys J*. 2010;98(5):911-921.

Commandeur S, Sparks SJ, Chan HL, Gao L, Out JJ, Gruis NA, van Doorn R, El Ghalbzouri A. In-vitro melanoma models: invasive growth is determined by dermal matrix and basement membrane. Melanoma Res. 2014 Aug;24(4):305-14.

Cooke MS, Podmore ID, Mistry N, Evans MD, Herbert KE, Griffiths HR, Lunec J. Immunochemical detection of UV-induced DNA damage and repair. J Immunol Methods. 2003 Sep;280(1-2):125-33.

Cooper KL, Liu KJ, Hudson LG. Enhanced ROS production and redox signaling with combined arsenite and UVA exposure: contribution of NADPH oxidase. *Free Radic Biol Med*. 2009;47(4):381-388.

Corre S, Primot A, Sviderskaya E, Bennett DC, Vaulont S, Goding CR, Galibert MD. UV-induced expression of key component of the tanning process, the POMC and MC1R genes, is dependent on the p-38-activated upstream stimulating factor-1 (USF-1). J Biol Chem. 2004 Dec 3;279(49):51226-33.

Correia MS, Moreiras H, Pereira FJC, Neto MV, Festas TC, Tarafder AK, Ramalho JS, Seabra MC, Barral DC. Melanin Transferred to Keratinocytes Resides in Nondegradative Endocytic Compartments. J Invest Dermatol. 2018 Mar;138(3):637-646.

Creel D, O'Donnell FE Jr, Witkop CJ Jr. Visual system anomalies in human ocular albinos. Science. 1978 Sep 8;201(4359):931-3.

Crumrine D, Khnykin D, Krieg P, Man MQ, Celli A, Mauro TM, Wakefield JS, Menon G, Mauldin E, Miner JH, Lin MH, Brash AR, Sprecher E, Radner FPW, Choate K, Roop D, Uchida Y, Gruber R,

Cui R, Widlund HR, Feige E, Lin JY, Wilensky DL, Igras VE, D'Orazio J, Fung CY, Schanbacher CF, Granter SR, Fisher DE. Central role of p53 in the suntan response and pathologic hyperpigmentation. Cell. 2007 Mar 9;128(5):853-64.

Cui J, Arita Y, Bystryn JC. Characterization of vitiligo antigens. Pigment Cell Res. 1995 Feb;8(1):53-9.

El Ghalbzouri A, Hensbergen P, Gibbs S, Kempenaar J, van der Schors R, Ponec M. Fibroblasts facilitate re-epithelialization in wounded human skin equivalents. Lab Invest. 2004 Jan;84(1):102-12.

Englaro W, Rezzonico R, Durand-Clément M, Lallemand D, Ortonne JP, Ballotti R. Mitogen-activated protein kinase pathway and AP-1 are activated during cAMP-induced melanogenesis in B-16 melanoma cells. J Biol Chem. 1995 Oct 13;270(41):24315-20.

Evans RD, Robinson C, Briggs DA, et al. Myosin-Va and dynamic actin oppose microtubules to drive long-range organelle transport. *Curr Biol*. 2014;24(15):1743-1750.

Fassihi H, Eady RA, Mellerio JE, Ashton GH, Dopping-Hepenstal PJ, Denyer JE, Nicolaides KH, Rodeck CH, McGrath JA. Prenatal diagnosis for severe inherited skin disorders: 25 years' experience. Br J Dermatol. 2006 Jan;154(1):106-13.

Faustin B, Reed JC. Sunburned skin activates inflammasomes. Trends Cell Biol. 2008 Jan;18(1):4-8.

Feldmeyer L, Keller M, Niklaus G, Hohl D, Werner S, Beer HD. The inflammasome mediates UVB-induced activation and secretion of interleukin-1beta by keratinocytes. Curr Biol. 2007 Jul 3;17(13):1140-5.

Fernandes B, Matamá T, Guimarães D, Gomes A, Cavaco-Paulo A. Fluorescent quantification of melanin. Pigment Cell Melanoma Res. 2016 Nov;29(6):707-712.

Fischer H, Szabo S, Scherz J, Jaeger K, Rossiter H, Buchberger M, Ghannadan M, Hermann M, Theussl HC, Tobin DJ, Wagner EF, Tschachler E, Eckhart L. Essential role of the keratinocyte-specific endonuclease DNase1L2 in the removal of nuclear DNA from hair and nails. J Invest Dermatol. 2011 Jun;131(6):1208-15.

Friedman RC, Farh KK, Burge CB, Bartel DP. Most mammalian mRNAs are conserved targets of microRNAs. *Genome Res*. 2009;19(1):92-105.

Galibert MD, Carreira S, Goding CR. The Usf-1 transcription factor is a novel target for the stress-responsive p38 kinase and mediates UV-induced Tyrosinase expression. *EMBO J*. 2001;20(17):5022-5031.

Ghosh MM, Boyce S, Layton C, Freedlander E, Mac Neil S. A comparison of methodologies for the preparation of human epidermal-dermal composites. Ann Plast Surg. 1997 Oct;39(4):390-404.

Gibbs S, Corsini E, Spiekstra SW, Galbiati V, Fuchs HW, Degeorge G, Troese M, Hayden P, Deng W, Roggen E. An epidermal equivalent assay for identification and ranking potency of contact sensitizers. Toxicol Appl Pharmacol. 2013 Oct 15;272(2):529-41.

Gibbs S, Murli S, De Boer G, Mulder A, Mommaas AM, Ponec M. Melanosome capping of keratinocytes in pigmented reconstructed epidermis--effect of ultraviolet radiation and 3-isobutyl-1-methyl-xanthine on melanogenesis. Pigment Cell Res. 2000 Dec;13(6):458-66.

Gledhill K, Guo Z, Umegaki-Arao N, Higgins CA, Itoh M, Christiano AM. Melanin Transfer in Human 3D Skin Equivalents Generated Exclusively from Induced Pluripotent Stem Cells. PLoS One. 2015 Aug 26;10(8)

Godar DE. Preprogrammed and programmed cell death mechanisms of apoptosis: UV-induced immediate and delayed apoptosis. Photochem Photobiol. 1996 Jun;63(6):825-30.

Goyarts E, Muizzuddin N, Maes D, Giacomoni PU. Morphological changes associated with aging: age spots and the microinflammatory model of skin aging. Ann N Y Acad Sci. 2007 Nov;1119:32-9.

Graier T, Hofer A, Wolf P. Digital ultraviolet B phototherapy in vitiligo: proof of concept. Br J Dermatol. 2020;182(5):1293-1294.

Guy GP Jr, Thomas CC, Thompson T, Watson M, Massetti GM, Richardson LC. Vital signs: melanoma incidence and mortality trends and projections - United States, 1982-2030. MMWR Morb Mortal Wkly Rep. 2015 Jun 5;64(21):591-6.

Han J, Chang H, Giricz O, Lee GY, Baehner FL, Gray JW, Bissell MJ, Kenny PA, Parvin B. Molecular predictors of 3D morphogenesis by breast cancer cell lines in 3D culture. PLoS Comput Biol. 2010 Feb 26;6(2).

Haridas P, McGovern JA, McElwain SDL, Simpson MJ. Quantitative comparison of the spreading and invasion of radial growth phase and metastatic melanoma cells in a three-dimensional human skin equivalent model. PeerJ. 2017;5:e3754.

Hennessy A, Oh C, Diffey B, Wakamatsu K, Ito S, Rees J. Eumelanin and pheomelanin concentrations in human epidermis before and after UVB irradiation. Pigment Cell Res. 2005 Jun;18(3):220-3.

Hennings H, Holbrook KA. Calcium regulation of cell-cell contact and differentiation of epidermal cells in culture. An ultrastructural study. Exp Cell Res. 1983 Jan;143(1):127-42.

Hill DS, Robinson ND, Caley MP, et al. A Novel Fully Humanized 3D Skin Equivalent to Model Early Melanoma Invasion. Mol Cancer Ther. 2015;14(11):2665-2673.

Huh D, Hamilton GA, Ingber DE. From 3D cell culture to organs-on-chips. Trends Cell Biol. 2011 Dec;21(12):745-54.

Inman JL, Bissell MJ. Apical polarity in three-dimensional culture systems: where to now? J Biol. 2010;9(1):2.

Jaeger K, Sukseree S, Zhong S, et al. Cornification of nail keratinocytes requires autophagy for bulk degradation of intracellular proteins while sparing components of the cytoskeleton. *Apoptosis*. 2019;24(1-2):62-73.

Jung JY, Oh JH, Kim YK, Shin MH, Lee D, Chung JH. Acute UV irradiation increases heparan sulfate proteoglycan levels in human skin. J Korean Med Sci. 2012 Mar;27(3):300-6.

Katagiri C, Iida T, Nakanishi J, Ozawa M, Aiba S, Hibino T. Up-regulation of serpin SCCA1 is associated with epidermal barrier disruption. J Dermatol Sci. 2010 Feb;57(2):95-101.

Katz MH, Alvarez AF, Kirsner RS, Eaglstein WH, Falanga V. Human wound fluid from acute wounds stimulates fibroblast and endothelial cell growth. J Am Acad Dermatol. 1991 Dec;25(6 Pt 1):1054-8.

Kim JY, Lee TR, Lee AY. Reduced WIF-1 expression stimulates skin hyperpigmentation in patients with melasma. J Invest Dermatol. 2013 Jan;133(1):191-200.

Kim SM, Chung HS, Hann SK. The genetics of vitiligo in Korean patients. Int J Dermatol. 1998 Dec;37(12):908-10.

Kleinman HK, Martin GR. Matrigel: basement membrane matrix with biological activity. Semin Cancer Biol. 2005 Oct;15(5):378-86.

Kovacs D, Cardinali G, Aspite N, Cota C, Luzi F, Bellei B, Briganti S, Amantea A, Torrisi MR, Picardo M. Role of fibroblast-derived growth factors in regulating hyperpigmentation of solar lentigo. Br J Dermatol. 2010 Nov;163(5):1020-7.

Krude H, Biebermann H, Luck W, Horn R, Brabant G, & Grüters A (1998). Severe early-onset obesity, adrenal insufficiency and red hair pigmentation caused by POMC mutations in humans. Nature Genetics, 19, 155.

Lassalle MW, Igarashi S, Sasaki M, Wakamatsu K, Ito S, Horikoshi T. Effects of melanogenesis-inducing nitric oxide and histamine on the production of eumelanin and pheomelanin in cultured human melanocytes. Pigment Cell Res. 2003 Feb;16(1):81-4.

Le Pape E, Wakamatsu K, Ito S, Wolber R, Hearing VJ. Regulation of eumelanin/pheomelanin synthesis and visible pigmentation in melanocytes by ligands of the melanocortin 1 receptor. *Pigment Cell Melanoma Res*. 2008;21(4):477-486.

Lee DJ, Rosenfeldt H, Grinnell F. Activation of ERK and p38 MAP kinases in human fibroblasts during collagen matrix contraction. Exp Cell Res. 2000 May 25;257(1):190-7.

Lewis BP, Burge CB, Bartel DP. Conserved seed pairing, often flanked by adenosines, indicates that thousands of human genes are microRNA targets. Cell. 2005 Jan 14;120(1):15-20.

Li L, Fukunaga-Kalabis M, Herlyn M. The three-dimensional human skin reconstruct model: a tool to study normal skin and melanoma progression. *J Vis Exp*. 2011;(54):2937. Published 2011 Aug 3.

Liu Y, Xue L, Gao H, Chang L, Yu X, Zhu Z, He X, Geng J, Dong Y, Li H, Zhang L, Wang H. Exosomal miRNA derived from keratinocytes regulates pigmentation in melanocytes. J Dermatol Sci. 2019 Mar;93(3):159-167.

Lo Cicero A, Delevoye C, Gilles-Marsens F, Loew D, Dingli F, Guéré C, André N, Vié K, van Niel G, Raposo G. Exosomes released by keratinocytes modulate melanocyte pigmentation. Nat Commun. 2015 Jun 24;6:7506.

Matsuki M, Yamashita F, Ishida-Yamamoto A, Yamada K, Kinoshita C, Fushiki S, Ueda E, Morishima Y, Tabata K, Yasuno H, Hashida M, Iizuka H, Ikawa M, Okabe M, Kondoh G, Kinoshita T, Takeda J, Yamanishi K. Defective stratum corneum and early neonatal death in mice lacking the gene for transglutaminase 1 (keratinocyte transglutaminase). Proc Natl Acad Sci U S A. 1998 Feb 3;95(3):1044-9.

Matei AE, Chen CW, Kiesewetter L, Györfi AH, Li YN, Trinh-Minh T, Xu X, Tran Manh C, van Kuppevelt T, Hansmann J, Jüngel A, Schett G, Groeber-Becker F, Distler

JHW. Vascularised human skin equivalents as a novel *in vitro* model of skin fibrosis and platform for testing of antifibrotic drugs. Ann Rheum Dis. 2019 Dec;78(12):1686-1692.

Migliorini E, Thakar D, Kühnle J, Sadir R, Dyer DP, Li Y, Sun C, Volkman BF, Handel TM, Coche-Guerente L, Fernig DG, Lortat-Jacob H, Richter RP. Cytokines and growth factors cross-link heparan sulfate. Open Biol. 2015 Aug;5(8).

Minwalla L, Zhao Y, Le Poole IC, Wickett RR, Boissy RE. Keratinocytes play a role in regulating distribution patterns of recipient melanosomes *in vitro*. J Invest Dermatol. 2001 Aug;117(2):341-7.

Moreiras H, Pereira FJC, Neto MV, Bento-Lopes L, Festas TC, Seabra MC, Barral DC. The exocyst is required for melanin exocytosis from melanocytes and transfer to keratinocytes. Pigment Cell Melanoma Res. 2020 Mar;33(2):366-371.

Muthusamy V, Piva TJ. UVB-stimulated TNFα release from human melanocyte and melanoma cells is mediated by p38 MAPK. *Int J Mol Sci*. 2013;14(8):17029-17054. Published 2013 Aug 19.

Nakazawa K, Nakazawa H, Collombel C, Damour O. Keratinocyte extracellular matrix-mediated regulation of normal human melanocyte functions. Pigment Cell Res. 1995 Feb;8(1):10-8.

Nordlund JJ, Collins CE, Rheins LA. Prostaglandin E2 and D2 but not MSH stimulate the proliferation of pigment cells in the pinnal epidermis of the DBA/2 mouse. J Invest Dermatol. 1986 Apr;86(4):433-7.

Nyström A, Bernasconi R, Bornert O. Therapies for genetic extracellular matrix diseases of the skin. Matrix Biol. 2018 Oct;71-72:330-347.

Oda Y, Tu CL, Pillai S, Bikle DD. The calcium sensing receptor and its alternatively spliced form in keratinocyte differentiation. J Biol Chem. 1998 Sep 4;273(36):23344-52.

Ongenae K, Dierckxsens L, Brochez L, van Geel N, Naeyaert JM. Quality of life and stigmatization profile in a cohort of vitiligo patients and effect of the use of camouflage. Dermatology. 2005;210(4):279-85.

Patel S, Rauf A, Khan H, Meher BR, Hassan SSU. A holistic review on the autoimmune disease vitiligo with emphasis on the causal factors. Biomed Pharmacother. 2017 Aug;92:501-508.

Pillai S, Bikle DD. Adenosine triphosphate stimulates phosphoinositide metabolism, mobilizes intracellular calcium, and inhibits terminal differentiation of human epidermal keratinocytes. J Clin Invest. 1992 Jul;90(1):42-51.

Plonka PM, Passeron T, Brenner M, Tobin DJ, Shibahara S, Thomas A, Slominski A, Kadekaro AL, Hershkovitz D, Peters E, Nordlund JJ, Abdel-Malek Z, Takeda K, Paus R, Ortonne JP, Hearing VJ, Schallreuter KU. What are melanocytes really doing all day long...?. Exp Dermatol. 2009 Sep;18(9):799-819.

Ranson M, Posen S, Mason RS. Extracellular matrix modulates the function of human melanocytes but not melanoma cells. J Cell Physiol. 1988 Aug;136(2):281-8

Robinson CL, Evans RD, Briggs DA, Ramalho JS, Hume AN. Inefficient recruitment of kinesin-1 to melanosomes precludes it from facilitating their transport. *J Cell Sci*. 2017;130(12):2056-2065.

Roger M, Fullard N, Costello L, Bradbury S, Markiewicz E, O'Reilly S, Darling N, Ritchie P, Määttä A, Karakesisoglou I, Nelson G, von Zglinicki T, Dicolandrea T, Isfort R, Bascom C, Przyborski S. Bioengineering the microanatomy of human skin. J Anat. 2019 Apr;234(4):438-455.

Schmuth M, Gruber R, Elias PM, Williams ML. Ichthyosis update: towards a function-driven model of pathogenesis of the disorders of cornification and the role of corneocyte proteins in these disorders. *Adv Dermatol*. 2007;23:231-256.

Schmuth M, Elias PM.Mutations in Recessive Congenital Ichthyoses Illuminate the Origin and Functions of the Corneocyte Lipid Envelope. J Invest Dermatol. 2019 Apr;139(4):760-768.

Seiji M, Fitzpatrick TB. The reciprocal relationship between melanization and tyrosinase activity in melanosomes (melanin granules). J Biochem. 1961 Jun;49:700-6.

Serre C, Busuttil V, Botto JM. Intrinsic and extrinsic regulation of human skin melanogenesis and pigmentation. Int J Cosmet Sci. 2018 Aug;40(4):328-347.

Shi Y, Vesely I. Fabrication of mitral valve chordae by directed collagen gel shrinkage. Tissue Eng. 2003 Dec;9(6):1233-42.

Silva de Castro CC, do Nascimento LM, Walker G, Werneck RI, Nogoceke E, Mira MT. Genetic variants of the DDR1 gene are associated with vitiligo in two independent Brazilian population samples. J Invest Dermatol. 2010 Jul;130(7):1813-8.

Szymański Ł, Jęderka K, Cios A, et al. A Simple Method for the Production of Human Skin Equivalent in 3D, Multi-Cell Culture. *Int J Mol Sci*. 2020;21(13):4644. Published 2020 Jun 30.

Takeda K, Yasumoto K, Takada R, Takada S, Watanabe K, Udono T, Saito H, Takahashi K, Shibahara S. Induction of melanocyte-specific microphthalmia-associated transcription factor by Wnt-3a. J Biol Chem. 2000 May 12;275(19):14013-6.

Tarafder AK, Bolasco G, Correia MS, Pereira FJC, Iannone L, Hume AN, Kirkpatrick N, Picardo M, Torrisi MR, Rodrigues IP, Ramalho JS, Futter CE, Barral DC, Seabra MC. Rab11b mediates melanin transfer between donor melanocytes and acceptor keratinocytes via coupled exo/endocytosis. J Invest Dermatol. 2014 Apr;134(4):1056-1066.

Thingnes J, Lavelle TJ, Hovig E, Omholt SW. Understanding the melanocyte distribution in human epidermis: an agent-based computational model approach. PLoS One. 2012;7(7):e40377.

Theocharis AD, Skandalis SS, Gialeli C, Karamanos NK. Extracellular matrix structure. Adv Drug Deliv Rev. 2016 Feb 1;97:4-27.

Tinkle CL, Lechler T, Pasolli HA, Fuchs E. Conditional targeting of E-cadherin in skin: insights into hyperproliferative and degenerative responses. *Proc Natl Acad Sci U S A*. 2004;101(2):552-557.

Tu CL, Chang W, Bikle DD. Phospholipase cgamma1 is required for activation of store-operated channels in human keratinocytes. J Invest Dermatol. 2005 Jan;124(1):187-97.

Tu CL, Chang W, Bikle DD. The calcium-sensing receptor-dependent regulation of cell-cell adhesion and keratinocyte differentiation requires Rho and filamin A. *J Invest Dermatol*. 2011;131(5):1119-1128.

Tu CL, Crumrine DA, Man MQ, et al. Ablation of the calcium-sensing receptor in keratinocytes impairs epidermal differentiation and barrier function. *J Invest Dermatol*. 2012;132(10):2350-2359.

Tu CL, Bikle DD. Role of the calcium-sensing receptor in calcium regulation of epidermal differentiation and function. *Best Pract Res Clin Endocrinol Metab*. 2013;27(3):415-427.

Uzawa K, Marshall MK, Katz EP, Tanzawa H, Yeowell HN, Yamauchi M. Altered posttranslational modifications of collagen in keloid. Biochem Biophys Res Commun. 1998 Aug 28;249(3):652-5.

Videira IF, Moura DF, Magina S. Mechanisms regulating melanogenesis. *An Bras Dermatol*. 2013;88(1):76-83.

Wäster P, Eriksson I, Vainikka L, Rosdahl I, Öllinger K. Extracellular vesicles are transferred from melanocytes to keratinocytes after UVA irradiation. Sci Rep. 2016 Jun 13;6:27890.

Walton, W. Feret's Statistical Diameter as a Measure of Particle Size. *Nature* **162,** 329–330 (1948).

Watson RE, Gibbs NK, Griffiths CE, Sherratt MJ. Damage to skin extracellular matrix induced by UV exposure. Antioxid Redox Signal. 2014 Sep 1;21(7):1063-77.

Whiteman DC, Green AC, Olsen CM. The Growing Burden of Invasive Melanoma: Projections of Incidence Rates and Numbers of New Cases in Six Susceptible Populations through 2031. J Invest Dermatol. 2016 Jun;136(6):1161-1171.

Won JY, Lee MH, Kim MJ, Min KH, Ahn G, Han JS, Jin S, Yun WS, Shim JH. A potential dermal substitute using decellularized dermis extracellular matrix derived bio-ink. Artif Cells Nanomed Biotechnol. 2019 Dec;47(1):644-649.

Wu X, Bowers B, Rao K, Wei Q, Hammer JA. Visualization of melanosome dynamics within wild-type and dilute melanocytes suggests a paradigm for myosin V function *In vivo*. *J Cell Biol*. 1998;143(7):1899-1918.

Wu XS, Masedunskas A, Weigert R, Copeland NG, Jenkins NA, Hammer JA. Melanoregulin regulates a shedding mechanism that drives melanosome transfer from melanocytes to keratinocytes. Proc Natl Acad Sci U S A. 2012 Jul 31;109(31):E2101-9.

Xie Z, Bikle DD. Phospholipase C-gamma1 is required for calcium-induced keratinocyte differentiation. J Biol Chem. 1999 Jul 16;274(29):20421-4.

Yamaguchi Y, Itami S, Watabe H, et al. Mesenchymal-epithelial interactions in the skin: increased expression of dickkopf1 by palmoplantar fibroblasts inhibits melanocyte growth and differentiation. *J Cell Biol*. 2004;165(2):275-285.

Yamamoto-Tanaka M, Makino T, Motoyama A, Miyai M, Tsuboi R, Hibino T. Multiple pathways are involved in DNA degradation during keratinocyte terminal differentiation. *Cell Death Dis*. 2014;5(4):e1181. Published 2014 Apr 17.

Yoon TJ, Lei TC, Yamaguchi Y, Batzer J, Wolber R, Hearing VJ. Reconstituted 3-dimensional human skin of various ethnic origins as an *in vitro* model for studies of pigmentation. Anal Biochem. 2003 Jul 15;318(2):260-9.

Zhang Y, Cai Y, Shi M, Jiang S, Cui S, Wu Y, Gao XH, Chen HD. The Prevalence of Vitiligo: A Meta-Analysis. PLoS One. 2016 Sep 27;11(9)

Zurina IM, Gorkun AA, Dzhussoeva EV, et al. Human Melanocyte-Derived Spheroids: A Precise Test System for Drug Screening and a Multicellular Unit for Tissue Engineering. *Front Bioeng Biotechnol*. 2020;8:540. Published 2020 Jun 4.